University of Alberta

Insights into the Role of CTP:phosphocholine Cytidylyltransferase-α in Hepatic Lipid Metabolism and Cellular Integrity

by

Lorissa Niebergall

A thesis submitted to the Faculty of Graduate Studies and Research
in partial fulfillment of the requirements for the degree of

Doctor of Philosophy

Biochemistry

Fall 2011
Edmonton, Alberta

Examining Committee

Dennis E. Vance, Department of Biochemistry

Charles Holmes, Department of Biochemistry

Ing Swie Goping, Department of Biochemistry

Andrew Mason, Department of Medicine

Rama Mallampalli, University of Pittsburgh

To my husband Ryan

Thank you for your encouragement throughout the many years of school.

Abstract

Lower levels of hepatic phosphatidylcholine (PC) are suggested to play a role in the pathogenesis of non-alcoholic steatohepatitis (NASH). Mice lacking hepatic CTP:phosphocholine cytidylyltransferase-α (LCTα$^{-/-}$), the regulatory enzyme in the CDP-choline pathway for PC biosynthesis, were fed a high fat diet to investigate the role of impaired PC biosynthesis in the pathogenesis of NASH. CTα-deficient livers developed moderate NASH within one week of high fat feeding. In addition, LCTα deficiency caused a 2-fold increase in hepatic levels of ceramide, and a 20% decrease in hepatic PC mass. Although stimulation of PC biosynthesis prevented hepatic steatosis, normalization of hepatic PC did not prevent either hepatic ceramide accumulation, or the development of NASH. These data indicate that impaired PC biosynthesis does not play a direct role in the transition from steatosis to NASH. Although reduced cellular PC induces apoptosis, a lower PC to phosphatidylethanolamine (PE) ratio has been demonstrated to influence membrane integrity, causing NASH. To investigate whether a reduced PC:PE ratio, rather than reduced cellular PC, influences membrane integrity, we utilized mutant 58 (MT58) Chinese hamster ovary cells. After incubation at the restrictive temperature, MT58 cells showed a 2-fold reduction in cellular PC and in the PC:PE ratio, leading to cellular death. In an attempt to normalize the PC:PE ratio and stabilize cellular membranes, MT58 cells were treated with silencing RNA to inhibit PE biosynthesis. However, inhibition of PE biosynthesis caused

a 30% reduction in cellular PE and PC masses, and therefore, did not normalize the PC:PE ratio. Moreover, MT58 cells showed a further loss of membrane integrity after knockdown of PE biosynthesis. Treatment of MT58 cells with lysophosphatidylcholine normalized cellular PC mass and prevented cellular death. However, lysophosphatidylcholine treatment caused an increase in PE mass, and therefore, did not normalize the PC:PE ratio. These data show that manipulation of the PC:PE ratio will not rescue MT58 cells from cell death since cellular growth and integrity are influenced by the total amount of cellular PC and PE, and not by the PC:PE ratio. In summary, these studies outline the importance of CTα in maintaining cellular integrity and hepatic lipid metabolism.

Acknowledgements

First, I must thank my supervisor, Dr. Dennis Vance. Thank you, Dennis, for welcoming me into your lab, and providing me with the resources, and support to complete my challenging and rewarding projects. Through your mentorship, I have realized that I absolutely love research and that I have the capabilities to succeed with any future scientific endeavours.

Second, I owe a huge debt to Dr. René Jacobs. Thank you, René, without your constructive criticisms, and insightful discussions, much of this work would not be possible. Furthermore, thank you, René, for making me laugh on several occasions (even when it was at my own expense).

Thank you to my supervisory and examination committee members for advice, comments and review of this work.

Thank you to Susanne Lingrell for spending many hours generating adenoviruses, teaching proper cell culture techniques, and for excellent assistance throughout the many years of school. Thank you to Randy Nelson for the excellent assistance with molecular biology, and to Audric Moses excellent assistance and for solving many computer issues. Thank you to Dr. Todd Chaba for clinically analyzing several histology slides.

I would like to thank everyone who has passed through the DEV lab and to all past and present members of the MCBL. Each person has given valuable advice, and has made graduate studies enjoyable. To Dr. Laura Cole, and Dr. Jelske van der Veen, thank you for been great colleagues and amazing friends. Thank you for all laughs and the fun that we have shared over the past years.

To my family and Ryan's family, thank you for your constant love and for believing in me. Thank you to all of my close friends for making graduate studies an unforgettable experience.

Table of Contents

CHAPTER 1: Introduction

List of Tables

List of Figures

Abbreviations

ABCA1	ATP-binding cassette, sub-family A , member 1
ACC	acetyl-CoA carboxylase
p-ACC	phosphorylated acetyl-CoA carboxylase
Ad. CTα	adenoviruses expressing CTα
Ad. GFP	adenoviruses expressing GFP
AdoHcy	*S*-adenosylhomocysteine
AdoMet	*S*-adenosylmethionine
AHCY	adenosylhomocysteine hydrolase
ALT	alanine aminotransferase
ApoA-1	apolipoprotein A-1
ApoB-100	apolipoprotein B-100
ATGL	adipose triglyceride lipase
BADH	betaine aldehyde dehydrogenase
BHMT	betaine:homocysteine methyltransferase
b.w.	body weight
CBS	cystathionine β-synthase
CBL	cystathionine γ-lyase
CDP-choline	cytidine 5’-diphosphocholine
CEPT	choline/ethanolamine phosphotransferase
ChAT	choline acetyltransferase

CHDH	choline dehydrogenase
ChoK1	Chinese hamster ovary
CHOP	CCAAT/-enhancer-binding protein homologous protein
CH_3THF	5-methyltetrahydrofolate
CK	choline kinase
CM	chylomicron
CPT	CDP-choline:1,2-diacylglycerol cholinephosphotransferase
CT	CTP:phosphocholine cytidylyltransferase
Cyp2E1	cytochrome P450 2E1
DAG	Diacylglycerol
ER	endoplasmic reticulum
ET	CTP:phosphoethanolamine cytidylyltransferase
FA	fatty acid
FAS	fatty acid synthase
GAPDH	glyceraldehyde 3-phosphate dehydrogenase
GFP	green fluorescent protein
GRP78	glucose regulated/immunoglobulin protein 78
GSH	reduced glutathione
GTT	glucose tolerance test
H & E	hematoxylin and eosin
HA	hemagglutinin

Hcy	homocysteine
HDL	high-density lipoprotein
HF	high fat
HF/HC	high fat/high cholesterol
HSL	hormone sensitive lipase
ITT	insulin tolerance test
LDH	lactate dehydrogenase
LDL	low-density lipoprotein
LPC	lysophosphatidylcholine
MAT	methionine adenosyltransferase
Met	methionine
MCD	methionine and choline deficient diet
MS	methionine synthase
MT58	mutant 58 Chinese hamster ovary
NADPHox	nicotinamide adenine dinucleotide phosphate oxidase
NAFLD	non-alcoholic fatty liver disease
NASH	non-alcoholic steatohepatitis
NEFA	non-esterified fatty acids
PC	phosphatidylcholine
PC:PE	phosphatidylcholine to phosphatidylethanolamine
PDI	protein disulfide isomerase

PDME	phosphatidyldimethylethanolamine
PE	phosphatidyethanolamine
PEMT	phosphatidylethanolamine *N*-methyltransferase
PLA_1	phospholipase A_1
PLA_2	phospholipase A_2
PLC	phospholipase C
PLD	phospholipase D
PMME	phosphatidylmonomethylethanolamine
PPAR	peroxisome proliferator activated receptor
PS	phosphatidylserine
PSD	phosphatidylserine decarboxylase
PTT	pyruvate tolerance test
qPCR	quantitative PCR
S.E.	standard error of the mean
siPSD/ET	silencing RNA targeting either PSD or ET
siScrambled	scrambled silencing RNA
TBARS	thiobarbituric acid reactive substances
TG	triacylglycerol
THF	tetrahydrofolate
UCP2	uncoupling protein 2
VLDL	very-low-density lipoprotein

CHAPTER 1

Introduction

1.1 Phosphatidylcholine

Phosphatidylcholine (PC) is the most abundant phospholipid within mammalian membranes, comprising of approximately 50% of the total phospholipid content (1). PC is composed of two fatty acid (FA) hydrocarbon chains attached to a glycerol backbone, and a choline head group attached via a phosphodiester linkage to the third hydroxyl group of the glycerol backbone (Figure 1.1) (2). The choline head group specifies the phospholipid class and adds a level of diversity among lipids. However, the molecular species of the two FA hydrocarbon chains which are esterified to the *sn*-1 and *sn*-2 positions of the glycerol backbone provide the diversity between PC molecules (Fig. 1.1) (2). PC plays many biological roles as it is a vital phospholipid within mammalian membranes, is an essential structural component of circulating lipoproteins, and is important in both bile and pulmonary lung surfactant (3). Furthermore, PC serves as a precursor for second messengers (4,5).

1.2 Biological Roles of Phosphatidylcholine

1.2.1 Phosphatidylcholine as a component of lipoproteins

Lipoproteins are a complex of apolipoproteins and lipids which function to transport the lipids throughout the circulation (6). All lipoproteins consist of a monolayer of apolipoproteins and amphipathic lipids (phospholipids and a small portion of unesterified cholesterol) which form a spherical shell enclosing a core of neutral lipids (mostly triacylglycerols (TG) and cholesteryl esters) (6). Classification of lipoproteins is based on their relative content of protein and lipids. The lipoprotein classes include: chylomicrons (CM), very low-density (VLDL), low-density (LDL), and high-density (HDL) lipoproteins. CM particles are the largest particles in diameter with lower density, whereas HDL particles

are smallest in diameter with a higher density (6). The apolipoprotein component is characteristic for each lipoprotein class. For instance, apolipoprotein B-100 (apoB-100) is characteristic of VLDL and LDL particles, whereas apolipoprotein A-1 (apoA-1) is characteristic of HDL particles (6). The phospholipid component of lipoproteins is directly proportional to the surface area of the lipoprotein particle. PC is the predominant phospholipid subclass in all plasma lipoproteins, and accounts for 75% in VLDL, 50% in LDL and 60% in HDL of total phospholipids (7).

1.2.2 Phosphatidylcholine as a component of bile

Biliary secretion of lipids (bile acids, phospholipids and cholesterol) is critical for cholesterol homeostasis and dietary fat absorption. The liver not only secretes a significant portion of PC into plasma on the surface of lipoproteins, but also secretes a significant portion of PC across the apical membrane into bile. PC consists of ~90% of total bile phospholipids (8,9). Moreover, the molecular species of biliary PC is predominantly C16:0 fatty acid esterified in the *sn*-1 position, and C18:1 or C18:2 fatty acids esterified in the *sn*-2 position (8,9). In mice, the daily secretion of hepatic PC into bile predominantly originates from a pre-existing pool of hepatic PC, and the amount secreted is equivalent to the total content of hepatic PC (10,11). The multiple drug-resistant 2 (MDR2) is a PC-specific flippase which translocates PC from the inner to the outer leaflet of the canalicular membrane (12). Mice which lack the *mdr2* gene develop liver disease due to impaired PC secretion into bile which highlights the importance of biliary PC secretion (12).

1.2.3 Phosphatidylcholine is an important component of pulmonary surfactant

Pulmonary surfactant, composed of a mixture of lipids and proteins, is produced by alveolar epithelial type II cells (reviewed in (13)). Pulmonary surfactant reduces the surface tension and stabilizes the alveoli during expiration (reviewed in (13)). In late gestation, alveolar type II cells increase both lipid and protein synthesis in order to generate sufficient pulmonary surfactant. PC is the most abundant lipid species of pulmonary surfactant with dipalmitoylphosphatidylcholine being the predominant molecular species of PC (reviewed in (13).

1.2.4 Phosphatidylcholine catabolism

Catabolism of PC is catalyzed by specific enzymes known as phospholipases (PL). The classification of PLs is based on their site of attack (14). As depicted in Figure 1.1, hydrolysis of PC by PLA_1 liberates the fatty acid (FA) from the *sn*-1 position, whereas hydrolysis of PC by PLA_2 liberates the FA from the *sn*-2 position. Both PLA_1 and A_2 generate lysophosphatidylcholine (LPC) via hydrolysis of PC. Catabolism of PC by PC-specific PLC generates phosphocholine and 1,2-*sn*-diacylglycerol (DAG) (Figure 1.1) while PLD-mediated degradation of PC generates phosphatidic acid and choline (Figure 1.1). Degradation of PC is important as it provides important signalling molecules which include LPC, DAG, free FAs, phosphatidic acid, and phosphocholine (4,5,15). Aside from providing signalling molecules, constant turnover of PC, together with PC biosynthesis, is essential for maintaining cellular PC homeostasis. Previous studies have shown that PLA_2 is involved in maintaining PC homeostasis (16-18). Additionally, recent studies have illustrated PC-specific PLC is involved in the conversion LDL-PC and HDL-PC to TG (19,20). The liberated DAG from the PLC reaction is subsequently

converted into TG via diacylglycerol acyltransferase (19,20). Clearly, PC catabolism is highly important to maintain cellular PC homeostasis, and to generate cellular TG and intracellular signalling molecules.

1.2.5 Phosphatidylcholine biosynthesis

In all nucleated cells, the Kennedy (CDP-choline) pathway, elucidated by Eugene Kennedy and colleagues in the 1950s, is responsible for the biosynthesis of PC (21,22). This pathway is responsible for the conversion of choline into PC which occurs through three enzymes: choline kinase (CK), CTP:phosphocholine cytidylyltransferase (CT), and CDP-choline:1,2-diacylglycerol cholinephosphotransferase (CPT) (Figure 1.2). The phosphatidylethanolamine *N*-methyltransferase (PEMT) pathway, which was first described by Bremer and Greenberg in 1961, is a second pathway for generating PC (Figure 1.2) (23). PEMT, quantitatively significant only in the liver, catalyzes the conversion of phosphatidylethanolamine (PE) to PC via three sequential methylation reactions (24). The PEMT pathway produces ~30% of hepatic PC, while the remaining 70% is produced via the CDP-choline pathway (25,26). The molecular species of PC generated by CDP-choline pathway differs from that produced by the PEMT pathway (27). The molecular species of PC produced by the CDP-choline pathway is mainly comprised of medium chain, saturated fatty acid species (27), while the molecular species of PC produced by the PEMT pathway is comprised primarily of long chain, polyunsaturated fatty acid species (27).

1.3 The CDP-choline Pathway

1.3.1 The transport and metabolic fates of Choline

The CDP-choline pathway uses choline as the substrate for the biosynthesis of PC. Choline is either acquired from the diet, or is generated from *de novo* biosynthesis. *De novo* biosynthesis of choline includes the coupling of PE methylation and PC catabolism (reviewed in (28). Choline is first internalized before metabolized into its various metabolic fates. Three types of choline transport systems have been identified: facilitated diffusion; high-affinity choline transport; and low affinity choline transport (29-31). Facilitated diffusion of choline is driven by a choline concentration gradient, and was identified as an important choline transporter in erythrocytes (29). The high-affinity choline transport system is a Na^+- and energy-dependent choline transport system. Neuronal cells use this transport system to couple choline transport with acetylcholine production (30). Finally, the low-affinity choline transport system is found in most cells as it is a means for internalization of choline for subsequent PC synthesis (31). Once internalized, choline is metabolized into a number of metabolites. Choline-containing metabolites include: choline, phosphocholine, PC, LPC, sphingomyelin, lysosphingomyelin, platelet-activating factor, glycerophosphocholine, acetylcholine, and betaine. The majority of choline is incorporated into PC via the CDP-choline pathway (Figure 1.2). However, choline (via its oxidation into betaine) is a donor of labile methyl groups (Figure 1.3) (32). The liver and kidney are the major sites of choline oxidation. In the process of choline oxidation, choline is first converted into betaine aldehyde via the action of choline dehydrogenase. This reaction occurs in the mitochondria (32). Betaine aldehyde is converted into betaine via betaine aldehyde dehydrogenase (32). As outlined in Figure 1.3, betaine is utilized as a methyl donor in the methionine cycle as betaine donates its methyl group to homocysteine to produce methionine. This reaction is

catalyzed by betaine:homocysteine methyltransferase (33). Methionine is subsequently adenylated to form *S*-adenosylmethionine (AdoMet), which is the methyl donor for most biological methylation reactions, including the PEMT pathway (Figure 1.2 and 1.3) (33). *S*-adenosylhomocysteine (AdoHcy) is produced from all methylation reactions and is subsequently hydrolyzed to form homocysteine. Homocysteine is either catabolised to cysteine via the transsulfuration pathway, or is converted into methionine for re-entry into the methionine cycle (Figure 1.3) (33). Thus, choline is not only an important precursor for PC biosynthesis, but is also highly important to maintain labile methyl balance.

The physiological importance of choline was first demonstrated in 1932 when Charles Best discovered that animals had a dietary requirement for choline (34). Later studies have clearly demonstrated that choline is also an essential dietary requirement for humans. After three weeks of consuming a choline-deficient diet, humans developed incipient liver dysfunction as indicated by a steady increase in serum alanine aminotransferase (ALT) activity (35). In addition, choline may play a role in the function of brain development. Since choline is a precursor for acetylcholine production (Figure 1.3), choline-deficiency may alter normal brain development due to impaired acetylcholine production (reviewed in (36)). As normal diets contain sufficient choline, choline-deficiency is rare. However, choline-deficiency has manifested during pregnancy, lactation and during periods of starvation (37).

1.3.2 Choline kinase

The first reaction in the CDP-choline pathway is catalyzed by CK, which was first described by Wittenberg and Kornberg in 1953 (38). CK catalyzes the phosphorylation of choline to phosphocholine in the presence of ATP (Figure 1.2). Three isoforms of CK have been identified, CKα-1, CKα-2, and CKβ (39). Alternative splicing of the *Chka* gene, located on chromosome 19, results in CKα-1 and CKα-2 (40,41). CKβ is encoded by the *Chkb* gene, located on chromosome 15 (42). CKα-1 contains 455 amino acids, while CKα-2 is identical to CKα-1 except for an additional 18 amino acids inserted after methionine-150. CKβ contains 394 amino acids, and is 60% similar to CKα (reviewed in (43)). CKα and CKβ are cytosolic proteins and are active in either homo- or hetero-dimer form, but are inactive in their monomeric form (44). Although both CK isoforms are ubiquitously expressed, CKα expression is exceptionally high in testis and liver, while high expression of CKβ has been observed in heart and liver (43,44). There is limited research regarding the regulation of CK expression in mammalian cells. Earlier studies have shown that CK activity in rat liver is induced by polycyclic aromatic hydrocarbons which can be prevented by cycloheximide or actinomycin D (45-47). In addition, CCl_4 has previously been shown to induce CK activity in rat liver, which can also be blocked by the use of cycloheximide (48). More recently, CCl_4 has been shown to induce mouse liver CKα, but not CKβ activity (44). The induction of CKα by CCl_4 was demonstrated to result from increased binding of the transcription factor c-jun to a distal Activating Protein-1 element on the CKα promoter resulting in increased gene expression (49). Clearly, more research is required for further characterization of CK regulation.

Elevated levels of CKα expression and activity, along with elevated concentration of phosphocholine have been associated with tumor growth in human cancers such as ovarian cancer (50), breast cancer (51), and

bladder carcinomas (52). The role of CKα in tumour growth is likely a consequence of the putative role of phosphocholine as a signalling molecule for cellular growth (15). To evaluate the physiological importance of CKα, mice lacking *Chka* have been generated. CKα activity contributes to 80% of total CK activity in mouse embryonic fibroblasts (53). Hence, deletion of *Chka* in mice is embryonic lethal around day 3.5 demonstrating that CKα is vital for early embryogenesis (53). However, *Chka*$^{+/-}$ mice had normal embryonic development, and were fertile. Furthermore, despite a 30% decrease of total choline kinase activity, the amount of PC in liver and testis was comparable to *Chka*$^{+/+}$ mice (53). These results suggested that adult mice do not require full expression of *Chka* to maintain PC homeostasis in liver and testis.

CKβ$^{-/-}$ mice naturally developed from a molecular defect within *ChkB* resulting in mice lacking CKβ. CKβ has been shown to be important in maintaining skeletal muscle integrity and bone formation as mice which lack *ChkB* develop hindlimb rostrocaudal muscular dystrophy and neonatal forelimb bone deformity (54). While it is unclear why *CKβ*$^{-/-}$ mice develop neonatal bone deformity, extensive studies have occurred to elucidate the mechanism of hindlimb muscular dystrophy. The hindlimbs of *CKβ*$^{-/-}$ mice showed impaired PC biosynthesis resulting in 20% less PC within hindlimb skeletal muscle compared to *CKβ*$^{+/+}$ mice (55). Furthermore, PC catabolism was increased within the hindlimbs of *CKβ*$^{-/-}$ mice (55). Therefore, the development of hindlimb muscular dystrophy in *CKβ*$^{-/-}$mice was due to an imbalance of PC metabolism, leading to loss of membrane integrity. The forelimbs of *CKβ*$^{-/-}$ mice do not develop muscular dystrophy due to a compensatory increase in PC biosynthesis, without a significant change in PC catabolism (56). Therefore, forelimbs of *CKβ*$^{-/-}$ mice have the capacity to maintain normal PC composition to maintain the integrity of skeletal muscle.

1.3.3 CTP:phosphocholine cytidylyltransferase

The second step of the CDP-choline pathway, the conversion of phosphocholine to cytidine 5'-diphosphocholine (CDP-choline), is catalyzed by CT and is the rate-limiting reaction for PC biosynthesis (Figure 1.2) (3). CT is an amphitropic enzyme which exists as a homodimer in either a soluble, inactive form, or an active, membrane-bound form (57). Membrane-binding of CT is a key regulatory event for PC biosynthesis via the CDP-choline pathway (58-63). There are two isoforms of CT, CTα and CTβ, each encoded by separate genes (64). *Pcyt1a*, located on chromosome 16, encodes for CTα, while *Pcyt1b*, located on the x-chromosome, encodes for CTβ (64). *Pcyt1a* encodes two CTα isoforms, CTα1 and CTα2, which differ in their initiating exons (64). Furthermore, while CTα1 mRNA is detected in all tissues, CTα2 mRNA has been detected only in testis (64). The CTα transcript is 5 kb, consists of 9 exons, and translates into a 42 kDa protein (64). *Pcyt1b* encodes three isoforms of CTβ (CTβ1, CTβ2 and CTβ3). CTβ1, CTβ2 isoforms are present in humans and CTβ2 and CTβ3 isoforms have been identified in mice (64,65). Although mRNA of both CTβ2 and CTβ3 are abundant in the brain, CTβ2 has been detected in the embryonic brain, while CTβ3 transcript levels are not evident until 5 weeks after birth (64). The CTβ2 transcript is 5.2 kb, and translates into a 41 kDa protein, while CTβ3 cDNA is 3.7 kb and translates into a 39 kDa protein (64).

As depicted in Figure 1.4A, CTα consists of an N-terminal nuclear localization signal, a catalytic domain, a lipid-binding domain, and a phosphorylation domain. CTβ is similar to CTα in the domain structures, however, it lacks the nuclear localization signal (64-67). The first crystal structure of the soluble rat CTα containing the N-terminal and catalytic domains in complex with CDP-choline has been solved by x-ray crystallography at 2.2Å resolution (Figure 1.4B) (68). Although the fold of the catalytic domain shows similarities between other proteins within the

cytidylyltransferase superfamily, two residues (histidine-168 and tyrosine-173) are novel to the active site of CTα (68). Furthermore, histidine-168 and tyrosine-173 are important for phosphocholine binding as they form hydrogen bonds with the choline-phosphate which is necessary for binding and catalysis to form CDP-choline (68).

1.3.4 CDP-choline:1,2-diacylglycerol cholinephosphotransferase

The final step of the CDP-choline pathway, the reaction of CDP-choline with DAG to generate PC, is catalyzed by CPT (Figure 1.2), and was first identified by Kennedy and coworkers (22). Although the protein has yet to be purified, yeast genetics have allowed for the cloning of both human CPT and choline/ethanolamine phosphotransferase (CEPT) which have 60% sequence identity (69,70). CDP-choline is the only substrate used by CPT, and this enzyme is specific for PC biosynthesis, while CEPT uses either CDP-choline or CDP-ethanolamine as substrates for either PC or PE biosynthesis (69,70). Both CEPT and CPT are integral membrane proteins with an estimated seven membrane-spanning helices (69). As CPT and CEPT catalyze the final step of the CDP-choline pathway, the site of PC biosynthesis is determined by the subcellular location of the enzymes. Coimmunofluorescence and subcellular fractionation experiments with Chinese hamster ovary cells (Cho) revealed that CPT1 was found in the Golgi apparatus, while CEPT was found in both the endoplasmic reticulum (ER) and nuclear membranes (71). One transcript of 2.3 kb was detected for CEPT and was ubiquitously expressed among various tissues (70). One transcript of 1.6 kb was detected for CPT, and was detected between various tissues with various expression patterns. The highest expression of CPT was detected in testis, colon, intestine, and heart (69). CPT is regulated by levels of its substrates, DAG and CDP-choline (72).

1.4 The Phosphatidylethanolamine *N*-Methyltransferase Pathway

1.4.1 Biochemical characterization of phosphatidylethanolamine *N*-methyltransferase

The PEMT pathway is the second pathway for synthesizing PC, and is quantitatively significant only in the liver (24). PEMT catalyzes the conversion of PE to PC via three sequential methylation reactions (Figure 1.2) (24). PEMT is localized at the ER and at the mitochondria-associated-membrane (a subfraction of the ER), and contains 4 membrane-spanning sequences (73,74). PEMT uses three AdoMet molecules for the methylation of PE and generates three AdoHcy molecules from each methylation reaction (75). PEMT contains two putative AdoMet-binding motifs, located in close proximity to the cytosolic side of the ER membrane, which are responsible for substrate binding during methylation-dependent PC biosynthesis (76). The activity of PEMT is dependent on the supply of its substrates, PE and AdoMet. On top of this, PEMT is inhibited by high concentrations of AdoHcy (75).

1.4.2 Molecular characterization of phosphatidylethanolamine *N*-methyltransferase

Despite being an intrinsic membrane protein, Ridgeway and Vance were successful in purifying PEMT from rat liver microsomes (77). The purification of PEMT made it possible for cloning and characterization of the PEMT gene. In mice, the PEMT gene is located on chromosome 11 (chromosome 17 in humans), and spans 35 kb containing seven exons and six introns (78). The gene encodes for a single mRNA transcript of 1 kb, which translates into the PEMT protein with a molecular weight of 22.5 kDa (78). Previous studies demonstrated that PEMT expression, both

protein and mRNA, are detectable from birth onwards, demonstrating that expression of the PEMT gene begins during the perinatal period (79,80). Stimulation of liver growth, either by partial hepatectomy or by injection with lead nitrate, has demonstrated that PEMT activity, protein and mRNA decreases during liver growth and regeneration (81,82). CT activity, on the other hand, is elevated during liver growth (79), indicating an inverse regulation between the two PC biosynthetic enzymes. A recent study has suggested that transcriptional regulation of CT and PEMT may indeed be inversely regulated via the action of Sp1 (83). In this study, PEMT mRNA and protein was shown to be increased in 3T3-L1 cells during differentiation to adipocytes. Sp1 protein decreased prior to PEMT activation suggesting that Sp1 suppresses PEMT gene expression (83). Tamoxifen, a common drug for the treatment of breast cancer, inhibits expression of PEMT by promoting Sp1 binding to the PEMT gene promoter showing that under physiological conditions, Sp1 represses PEMT mRNA expression (83). Interestingly, CTα gene expression is activated by Sp1 during the S-phase of the cell cycle (84). Taken together, these studies demonstrate an inverse relationship occurs in the regulation of the two PC biosynthetic enzymes (CTα and PEMT), which may be achieved through Sp1.

1.4.3 Evolutionary significance of phosphatidylethanolamine *N*-methyltransferase

The PEMT pathway is responsible for producing one-third of hepatic PC, while the CDP-choline pathway produces the remainder (25,26). Therefore, as there is sufficient PC biosynthetic capacity via the CDP-choline pathway, it was curious why PEMT survived during evolution. Insights into the physiological importance of PEMT were highlighted with the generation of mice which lacked the PEMT gene (85). Deletion of PEMT had little effect on hepatic levels of either PC or PE, which could be

explained by a compensatory increase in hepatic CT activity. Moreover, *Pemt*$^{-/-}$ mice did not show any obvious phenotype as hepatocyte morphology, plasma lipid levels, and bile composition were comparable to that seen in *Pemt*$^{+/+}$ mice (85). Therefore, these initial experiments did not clarify the physiological importance of the PEMT pathway. However, the significance of PEMT in the liver was underscored when *Pemt*$^{-/-}$ mice were fed a choline-deficient diet which attenuated the CDP-choline pathway. Within 3 days of the choline-deficient diet, *Pemt*$^{-/-}$ mice rapidly developed severe liver failure, while *Pemt*$^{+/+}$ mice fed the choline-deficient diet did not show obvious liver pathology (86). Choline-deficient livers of *Pemt*$^{-/-}$ mice showed a 50% decrease in hepatic PC compared with the choline-deficient livers from *Pemt*$^{+/+}$ mice. Furthermore, plasma TG and cholesterol were also reduced by > 90% in *Pemt*$^{-/-}$ mice compared with *Pemt*$^{+/+}$ mice (86). Further studies revealed that liver damage could be reversed with the addition of dietary choline (87). Interestingly, neither dimethylethanolamine nor propanolamine could substitute for dietary choline when fed to *Pemt*$^{-/-}$ mice, indicating specificity for PC in liver function (88,89). Therefore, the PEMT gene is believed to be maintained during evolution to provide PC and/or choline when dietary choline is insufficient, such as during pregnancy and lactation (37).

1.4.4 Phosphatiylethanolamine *N*-methyltransferase and lipoprotein metabolism

Although *Pemt*$^{-/-}$ mice fed a chow diet appear outwardly normal, *Pemt*$^{-/-}$ mice fed a high fat/high cholesterol (HF/HC) diet show a striking phenotype, and have demonstrated that PEMT is important for VLDL secretion (90,91). When challenged with a HF/HC diet, male *Pemt*$^{-/-}$ mice have 50% less plasma TG, along with 40% less plasma PC and cholesterol compared to *Pemt*$^{+/+}$ mice. Furthermore, apoB100 secretion also was 50% decreased indicating VLDL section is impaired in *Pemt*$^{-/-}$

mice fed the HF/HC diet (90). In agreement with altered plasma lipids in male *Pemt*$^{-/-}$ mice, hepatocytes prepared from *Pemt*$^{-/-}$ mice showed a 50-70% decrease in secreted apopB100, PC and TG compared with hepatocytes from *Pemt*$^{+/+}$ mice (91). Along with impaired VLDL secretion, a significant reduction of plasma HDL was also observed in *Pemt*$^{-/-}$ mice fed either the chow diet, or the HF/HC diet (90,92). Enhanced hepatic uptake of HDL by scavenger-receptor class B1 proved to be the reason for decreased plasma HDL in *Pemt*$^{-/-}$ mice compared to *Pemt*$^{+/+}$ mice (92).

As elevated levels of circulating VLDL and LDL are risk factors for cardiovascular disease (93), Vance and coworkers (94) proposed that the hypolipidemic effect of PEMT may attenuate the development of atherosclerosis and cardiovascular disease. This hypothesis was confirmed when mice, which lack the LDL receptor, were crossed with *Pemt*$^{-/-}$ mice (94). LDL receptor (*LDLr*$^{-/-}$) knockout mice develop atherosclerosis when fed a HF/HC diet (95). However, *LDLr*$^{-/-}$ mice deficient in PEMT showed an 80% reduction in atherosclerotic lesion area, and a reduction of VLDL/LDL associated PC, TG, cholesterol and cholesteryl esters. Furthermore, PEMT deficiency in *LDLr*$^{-/-}$ mice resulted in decreased hepatic VLDL secretion and increased rate of VLDL clearance from plasma, while HDL was unaffected (94). This was the first report to show that impaired hepatic phospholipid biosynthesis may have a beneficial effect on the development of atherosclerosis. A second study has confirmed that impaired PC biosynthesis via the PEMT pathway has atheroprotective effects (96). In this study, ApoE deficient mice (*ApoE*$^{-/-}$) were crossed with mice lacking PEMT. *ApoE*$^{-/-}$ mice spontaneously develop atherosclerosis on a chow diet (97). After one year of the chow diet, the atherogenic plasma lipoprotein profile was improved in *ApoE*$^{-/-}$ /*Pemt*$^{-/-}$ mice as plasma TG was decreased by 45%, and cholesterol associated with the VLDL and LDL lipoprotein fraction was decreased by 25%. The changes in plasma lipids was associated with a 30% decrease in atherosclerotic lesion area (96). Additionally, *ApoE*$^{-/-}$/*Pemt*$^{-/-}$mice

showed decreased cardiac TG content attenuating cardiac dysfunction (96). Clearly, impaired PC biosynthesis via the PEMT pathway is beneficial for the prevention of atherosclerosis.

PEMT has also shown to be a potential therapeutic mechanism to target obesity as *Pemt*$^{-/-}$ mice are resistant to high fat diet-induced obesity compared to *Pemt*$^{+/+}$ mice (98). Furthermore, despite developing hepatomegly and steatosis, *Pemt*$^{-/-}$ mice have increased energy expenditure and maintain normal insulin sensitivity after 10 weeks of being fed the high fat diet. Surprisingly, this observed phenotype was not due to impaired PC biosynthesis, but instead resulted from insufficient choline as choline supplementation normalized energy expenditure, weight gain and insulin resistance in *Pemt*$^{-/-}$ mice (98). The above mentioned studies clearly outline the importance of both choline and PEMT as regulators of lipoprotein metabolism and whole-body energy metabolism.

1.5 Localization and Regulation of CTP:phosphocholine Cytidylyltransferase

1.5.1 Subcellular localization of CTP:phosphocholine cytidylyltransferase

As CTα contains the nuclear localization signal on the N-terminus, subcellular localization studies have identified CTα to be a nuclear protein which binds to the nuclear envelope and ER upon activation by lipids. Unlike CTα, CTβ lacks a nuclear localization signal, and is therefore, a cytosolic protein which binds to ER membranes upon lipid activation (99-101). Although the role of CTα in the nucleus is not entirely known, recent studies have shown that CTα, in coordination with lamin A and B, are required for proliferation of the nucleoplasmic reticulum indicating that CTα

is important for maintaining the membrane curvature of the nucleoplasmic reticulum (102-104).

The nuclear localization of CTα is not universal to all cells, and the enzyme has been identified as a cytosolic enzyme in cells where high rate of PC biosynthesis is required (105-107). For instance, CTα is localized in the cytosol of pulmonary lung epithelial cells which tend to show enhanced rates of PC formation to support the secretion of lung surfactant (105). Intriguingly, a recent study has demonstrated that CTα is transported into the nucleus in response to cellular stress (increased Ca^{2+} levels) in murine lung epithelial cells (108). Furthermore, the association of 14-3-3ζ protein with CTα was a key regulator for CTα trafficking into the nucleus (108). The transport of CTα to the nucleus in response to cellular stress suggests that the nuclear localization of CTα is a mechanism to preserve the enzyme for PC biosynthesis and prevent turnover. In fact, CTα is a target of degradation by calpain in response to oxidized lipoproteins (109), and is a target of caspase-mediated cleavage in response to apoptosis induced by farnesol (110,111). Interestingly, farnesol induced apoptosis of Cho cells promotes nuclear export of CTα before being targeted by caspase which further indicates that nuclear localization of CTα potentially acts as a protective mechanisms to prevent CTα degradation (110,111).

CTα has also been demonstrated to shuttle out of the nucleus and localize to the ER in response to re-entry into G_1 of the cell cycle, suggesting that the nucleus may serve as a "storage" reservoir for inactive, soluble CTα when cellular requirements for PC are low (101). Furthermore, nuclear export of CTα has been shown to be triggered by oleate in both mutant 58 (MT58) Chinese hamster ovary cells and *Drosophila* Schneider 2 (S2) cells (112,113). Interestingly, oleate activation of CTα resulted in the association of CTα with cytosolic lipid droplets. Subsequent experiments revealed that CTα localizes with lipid droplets as a mechanism to provide adequate PC to the phospholipid

monolayer of growing lipid droplets (113). CTα has also been reported to localize with the Golgi apparatus in macrophage cells (114). Interestingly, the secretion of vesicles from the Golgi apparatus is impaired in yeast, MT58 cells and macrophages which are deficient in CTα protein and enzyme activity suggesting that PC biosynthesis via the CDP-choline pathway is required for vesicular transport from the Golgi apparatus (114-116).

1.5.2 Translocation and lipid activation of CTP:phosphocholine cytidylyltransferase

FAs, such as oleate, stimulate PC biosynthesis via translocation of CT to biological membranes, which is a key event in the activation of CT and regulation of PC biosynthesis (Figure 1.2) (58-63). Deletion of the lipid-binding domain causes a constitutively active enzyme which is non-responsive towards lipids suggesting that the lipid-binding domain is inhibitory towards CT activity when CT is in its soluble, inactive form (117,118). Association of CT with biological membranes involves intercalation of the amphipathic helix of the lipid-binding domain into the polar head group of the phospholipids (57). Figure 1.5 depicts how reversible binding of CT with biological membranes may occur. The classical view of membrane binding involves both membrane-binding domains interacting with the same membrane (left panel, Figure 1.5) (119). Intriguingly, a recent study by Cornell and colleagues has provided evidence which suggests that the N-terminal nuclear localization signal of CTα may also be involved in membrane binding. The nuclear localization signal may be involved in the cross-bridging of CTα between membranes (right panel, Figure 1.5) (119). However, further research needs to be conducted to determine how the nuclear localization signal is involved in this process, and how this effects nuclear localization of CT.

As indicated by Figure 1.2, the association of CT to biological membranes is modulated by: alterations of membrane concentrations of PC, DAG, and by the degree of phosphorylation within the C-terminal domain of CT (3). Treatment of Cho cells with phospholipase C was the first to show the translocation of CT from its soluble form to its membrane bound form, and the translocation of CT likely resulted from the production of DAG (63,120). Further studies have verified that increased content of DAG within membranes enhances the binding of CT to biological membranes. However, along with modulating CT binding to membranes, DAG may also alter PC biosynthesis by providing substrate for the final step of the CDP-choline pathway (121-123). Feedback regulation of CT by membrane composition of PC has also been described (124-126). Rats fed a choline-deficient diet have a 70% reduction in hepatic PC biosynthesis which is associated with a reduction in membrane PC. However, a 2-fold increase in CT activity corresponding to increased binding of CT to membranes was observed in choline-deficient livers suggesting that CT activity and membrane binding was regulated by the loss of hepatic PC (126). Choline-deficient hepatocytes incubated with substrates for PC biosynthesis (choline, methionine, and LPC) showed increased PC biosynthesis which was associated with a translocation of CT from its soluble, inactive form to its membrane-bound, active form (125). These studies clearly show that the amount of membrane PC modulates membrane-binding of CT.

1.5.3 Phosphorylation of CTP:phosphocholine cytidylyltransferase

As shown in Figure 1.2, phosphorylation of CT adds another layer of regulation. The phosphorylation domain of CT is extensively phosphorylated as it contains 16 serine residues, all of which can be phosphorylated (127). Although deletion of the phosphorylation domain does not impair PC biosynthesis, previous studies have suggested that the

phosphorylation domain adds to the regulation of CT activity by interfering with the membrane-binding domain. Thus, increased phosphorylation of CT interferes with the enzyme's ability to bind to biological membranes. (128-130). Other studies have shown that the extent of phosphorylation of CT regulates its enzymatic activity (123,131,132). For instance, oxysterols inhibit PC biosynthesis in lung epithelial cells. This inhibitory mechanism was shown to be due to increased CT phosphorylation of serine 315 via p42 kinase (ERK) (133). In addition, free-cholesterol loading of macrophages results in an increase in the amount of CT found associated with membranes. Moreover, the CT which was bound to membranes showed a decreased state of phosphorylation (134). Therefore, although there is limited research on the mechanism involved in the phosphorylation of CT, it is clear that phosphorylation impedes membrane-binding of CT and adds an additional layer of regulation of PC biosynthesis.

1.5.4 Transcriptional regulation of CTP:phosphocholine cytidylyltransferase

Along with post-translational modifications of CT, several lines of evidence have suggested that CTα is regulated at the transcriptional level (79,82,135-137). To begin, CTα mRNA is up-regulated during the perinatal period of hepatic development (79). In addition, increased CT activity, protein and mRNA were observed in rat livers after partial hepatectomy. The increase in CT corresponded to enhanced PC biosynthesis (82,136,137). A murine macrophage cell line also showed a 4-fold increase of CTα mRNA after treatment with colony-stimulation factor 1. The increase in gene expression was accompanied by a 50% increase in CT activity (135). Furthermore, lipoprotein-deficient serum has been shown to stimulate CT activity by 150% in lung epithelial cells (138). Further analysis revealed that the induced expression of CTα was due to

an increase in CTα gene expression. Therefore these studies indicated that regulation of CTα at the transcriptional level may be an additional method of regulation for the biosynthesis of PC. Analysis of the proximal promoter region of the CTα gene revealed many potential regulatory elements (139). Further analysis revealed that CTα gene expression was regulated by Sp1 and Sp3 transcription factors (139,140). Along with the Sp family of transcription factors, ETS-1, Net and TEF-4 are other transcription factors which have been indicated to play a role in either activation or repression of CTα gene expression (141,142). Although there is little information regarding the transcriptional regulation of CTβ, the transcriptional start sites and promoter regions have been characterized for the two murine isoforms, CTβ2 and CTβ3 (143).

PC is an essential component of cell cycle progression as it is a vital component of mammalian membranes (144). PC biosynthesis is stimulated in rat liver after partial hepatectomy, and the increased PC biosynthesis correlated with increased CT mRNA (136). Therefore, to understand the role of transcriptional regulation of CTα in a physiological setting, Vance and coworkers (145) analyzed CTα expression in a murine fibroblast cell line as a function of cell cycle progression. Interestingly, while PC biosynthesis occurs during G0 to G1 phase of the cell cycle (131), transcription of CTα is enhanced during the S phase of the cell cycle. Furthermore, the transcription factors, Sp1 and E2F1, were shown to regulate CTα expression during the S phase of the cell cycle (84,145,146). Subsequent studies revealed that phosphorylation of Sp1 by cyclin A-CDK2 and cyclin E-CDK2 was required for enhanced expression of CTα (147). These studies indicated that increased PC biosynthesis during G0 to G1 phase is not due to transcriptional regulation of CTα. However, the increase of CTα expression during the S phase of the cell cycle may occur in preparation for cell division.

1.5.5 Physiological importance of CTP: phosphocholine cytidylyltransferase

To evaluate the physiological importance of both CTα and CTβ, targeted deletion of either isoform was performed in mice. Mouse embryos with a targeted deletion of CTα do not develop past day 3.5, and were unable to develop into the blastocyte stage of embryonic development (148). While targeted deletion of CTα is embryonic lethal, mice with a targeted deletion of CTβ2 live to be adults, and do not display delayed development (149). Interestingly, even though CTβ2 expression is most abundant in the brain, knockout of CTβ2 does not lead to brain abnormalities, but instead results in gonadal dysfunction (149). CTβ2 was shown to be essential for both ovary maturation and maintenance of sperm production (149). Although CTβ2 knockout mice do not develop brain abnormalities, CTβ2 does play a role in neuronal differentiation, as the expression of CTβ2 promotes the differentiation of neurons, neurite outgrowth and branching in PC12 cells (150,151).

As targeted deletion of CTα is embryonic lethal (148), to gain insight into the physiological importance of CTα, various groups have utilized the Cre-*loxP* genetic system to knockout CTα within various tissues in mice. Targeted deletion of CTα in lung epithelial cells results in respiratory failure after birth due to impaired synthesis and secretion of PC (152). This is not unexpected as PC is the most abundant phospholipid of pulmonary surfactant (reviewed in (13)). Deletion of CTα in B lymphocytes showed that CTα is responsible for ER membrane expansion (153). CTα-deficient mouse macrophages are highly susceptible to apoptosis upon cholesterol-loading indicating that impaired PC biosynthesis increases the sensitivity of macrophages towards external stress (154). Furthermore, macrophages deficient in CTα have dysfunctional Golgi secretion of cytokines, suggesting that PC biosynthesis is important for maintaining secretory function of the Golgi compartment (114).

To gain insight into the role of PC biosynthesis in lipoprotein metabolism, hepatic CTα knockout mice were generated (155). CTα-deficient livers show 25% reduction in PC content compared to control mice despite a compensatory increase of PEMT protein and specific activity (155). Furthermore, hepatic TG was 25-50% higher in liver-specific CTα ($LCT\alpha^{-/-}$) knockout mice fed a chow diet compared to the control mice. The accumulation of hepatic TG was attributed to decreased VLDL secretion since the $LCT\alpha^{-/-}$ mice had lower plasma TG and PC, and had impaired ApoB-100 secretion (155,156). Furthermore, reconstitution of CTα into CTα-deficient livers normalized both plasma TG and hepatic PC levels. These data demonstrate the importance of CTα in controlling hepatic VLDL secretion.

Along with changes in VLDL secretion, $LCT\alpha^{-/-}$ mice had lower levels of plasma HDL and 50% lower plasma concentration of ApoA-1, PC, and cholesterol compared to control mice (155). Hepatocytes cultured from CTα-deficient livers showed decreased protein expression of ATP-binding cassette, sub-family A, member 1 (ABCA1), which corresponded with decreased cholesterol and PC efflux to ApoA-1 (156). Reconstitution of CTα into CTα-deficient livers normalized plasma HDL levels and ABCA1 protein expression (156). This data illustrated that PC biosynthesis is also required for normal PC efflux to HDL. The reason for reduced ABCA1 expression remains unknown and will need to be explored in further studies.

1.6 Non-Alcoholic Fatty Liver Disease

1.6.1 Non-alcoholic steatohepatitis: definition and pathology

In 1980, Ludwig *et al*. (157) was the first to use the term non-alcoholic steatohepatitis (NASH) to differentiate patients who developed alcoholic steatohepatitis from those whom had steatohepatitis without alcohol consumption. Non-alcoholic fatty liver disease (NAFLD) is the preferential term to describe liver disease when liver histology has not been defined. NAFLD has become the most common form of chronic liver disease, and has been associated with the obesity epidemic which is on the rise in North America (158-162). Although the true prevalence of NAFLD remains unknown due to difficulties in diagnosing NAFLD in patients, the prevalence of NAFLD in the North American general population is 10-24%, and this raises to 25-75% in the obese and diabetic population (158,160,161). NAFLD encompasses a wide spectrum of disease ranging from hepatic steatosis, to NASH, fibrosis, and cirrhosis (158-162). The occurrence of NAFLD is strongly associated with obesity, type 2 diabetes, insulin resistance, and hyperglycaemia, and is considered to be the hepatic manifestation of the metabolic syndrome (158-162). Interestingly, some patients with NAFLD develop hepatic steatosis which does not progress to NASH, while other patients develop full-blown NASH, which may progress to fibrosis and cirrhosis. The molecular determinants defining the pathogenesis of NASH remain relatively unknown.

The hepatic lesions commonly associated with NASH include steatosis, hepatocyte ballooning degeneration (accumulation of intracellular, rarefied cytoplasm), and lobular and portal inflammation (163). Hepatocellular steatosis with or without inflammation is a benign condition which may not progress to NASH (Figure 1.6A). However, clinical diagnostics of NASH include all hepatic lesions (steatosis, inflammation, and hepatocyte ballooning) (Figure 1.6B-C) (164). Other hepatocellular injury which may be associated with NASH, but not

uniformly noted in pathology studies include: Mallory's hyaline (often associated with ballooned hepatocytes) (Figure 1.6 C), glycogenated nuclei, and megamitochondria (163). The patterns of fibrosis are also characteristic of NASH. During the initial stages of fibrosis, collagen deposition, produced by activated hepatic stellate cells, is observed in the perivenular and perisinusoidal spaces (Figure 1.6D). Progression of liver injury results in portal fibrosis, and further progresses to the development of cirrhosis (163). A grading system has been proposed which scores the level of lesions and stage of fibrosis observed in biopsies from patients with NASH (165). As outlined in Table 1.1, the grading criteria scores each of the lesions associated with NASH, and the grade of steatohepatitis present is defined by the total score for all lesions (165). Furthermore, the grading system also defines the stage of fibrosis present. The stage of fibrosis is defined by the extent of collagen deposition, and the location of fibrosis (Table 1.1) (165). The pathogenesis of NASH is not fully understood. However, the "two-hit" theory for the development of NASH has been proposed to explain why NASH development is inconsistent among individuals (166). The "first hit" constitutes hepatic TG accumulation and the "second hit" involves cellular stresses causing inflammation and apoptosis (166).

1.6.2 Possible mechanisms leading to the pathogenesis of hepatic steatosis (the "first hit")

Excessive accumulation of TG within hepatocytes is the hallmark of NAFLD. As depicted in Figure 1.7, hepatic TG homeostasis involves a balance between TG synthesis and TG disposal. Hepatic TG accumulation results from an imbalance between the availability of FA for storage in the form of TG, and the disposal of FAs from the liver (167). Sources of free FAs include: hepatic uptake from plasma non-esterified FA pool; hepatic uptake of FA from dietary TG within remnant lipoprotein

particles (CM and VLDL); or from increased *de novo* lipogenesis (Figure 1.7) (168). Recent studies have demonstrated that LDL- and HDL-associated PC also contributes to hepatic TG homeostasis (19,20). In human patients with NAFLD, 59% of hepatic FAs originate from the plasma non-esterified FA pool, 10-15% of hepatic FAs originate from dietary TG, and 26% of hepatic FA is produced from *de novo* lipogenesis (168). Defects in any of these processes are associated with the development of hepatic steatosis. For instance, increased hepatic FA uptake in animals correlates with the development of hepatic steatosis (169-171). In addition, silencing or deletion of genes involved in FA uptake is preventative towards the development of hepatic steatosis (172,173). Furthermore, increased hepatic expression of sterol regulatory element binding protein 1c, a key regulator in *de novo* lipogenesis, is observed in livers of obese animals (174-176).

Disposal of hepatic FAs include oxidation of FAs, or secretion of hepatic TG in VLDL particles (Figure 1.7). Defects in either FA oxidation or VLDL secretion have been implicated in the development of NASH. A recent study investigating the occurrence of NASH in a Japanese population showed that patients with NASH had impaired VLDL secretion (177). Compared to patients with simple steatosis, NASH patients showed a greater deficiency of VLDL synthesis and secretion showing that impediment of hepatic VLDL metabolism may be a key factor in the development of both hepatic steatosis and NASH (177). Moreover, mice which are deficient of peroxisome proliferator activated receptor-α (PPARα) gene develop severe steatohepatitis when fed a methionine and choline (MCD) diet compared to wild type mice (178). PPARα is a key regulator in genes of FA oxidation. Therefore, *PPARα*$^{-/-}$ mice develop NASH when fed the MCD diet due to impaired FA oxidation (178).

1.6.3 Possible mechanisms involved in the pathogenesis of non-alcoholic steatohepatitis ("the second hit")

The pathogenesis from hepatic steatosis to NASH includes a "second hit" which leads to hepatocyte injury and apoptosis. Excessive accumulation of hepatic TG increases the sensitivity of the liver to several types of injury, such as gut-derived endotoxins (179,180). Obese *fa/fa* rats show increased susceptibility to lipopolysaccharide induced liver injury compared to their lean littermate controls (179). Obese *fa/fa* rats exposed to lipopolysaccharide developed chronic hepatic inflammation as indicated by the induced expression of hepatic tumor necrosis factor-α (TNFα), and interferon γ (179). Furthermore, lipoplysaccharide augments liver injury in mice fed the MCD diet as indicated by increased serum ALT levels, inflammation and apoptosis (180). Chronic hepatic inflammation is a cellular insult which is associated with the pathogenesis of NASH. Chronic inflammation caused from cytokine overexpression, such as TNFα and interleukin-6, induces hepatocellular apoptosis resulting in NASH (181-185). Mice which are deficient in TNFα receptors do not manifest hepatic steatohepatitis when fed a high sucrose diet or the MCD diet (186,187). Furthermore, although interleukin-6 knockout mice are not protected from developing NASH when fed the MCD diet, these mice have reduced lobular inflammation, and reduced expression of inflammatory genes (188). These studies indicate a role of chronic inflammation in the induction of NASH.

Increased hepatocellular death associated with NASH also results from increased sensitivity to oxidative stress, as increased production of reactive oxygen species and lipid peroxides leading to mitochondrial dysfunction have been shown in animal models of NASH (189-192). Impaired mitochondrial function has been shown to cause a depletion of reduced glutathione, a known anti-oxidant (183,189,191). ER stress is linked to obesity, insulin resistance, type 2 diabetes and the induction of

hepatic lipogenesis via the action of sterol regulatory element binding protein 1c (193-195). As obesity, insulin resistance, type 2 diabetes and increased hepatic lipogenesis are associated with NASH, it is not surprising that ER stress has been linked with the pathogenesis of NASH (196-198). ER stress is induced in a steatotic liver in response to increased saturated FAs (197), and in response to increased delivery of FAs and the accumulation of hepatic TG (198). Taken together, the pathogenesis of NASH from simple steatosis is the result of a secondary cellular stress which includes chronic inflammation, oxidative stress and ER stress.

1.7 Phosphatidylcholine and Non-Alcoholic Fatty Liver Disease

1.7.1 Choline deficiency is a determinant of hepatic steatosis

It is well established that a diet deficient in choline causes hepatic steatosis. Humans fed a choline deficient diet for three weeks have increased plasma ALT levels, and develop incipient liver dysfunction (35). A choline-deficient diet also induces hepatic steatosis in animal models including rats and mice (199-201). Best and Huntsman were the first to describe that a massive accumulation of hepatic TG occurs when rats are fed a choline-deficient diet (34). Choline deprivation has been a widely utilized tool for inhibiting PC biosynthesis via the CDP-choline pathway in various cells lines including primary rat hepatocytes, and hepatoma cells (34,202,203). As PC is a major component of VLDL particles, comprising approximately 75% of total phospholipids, depriving cells and animals of choline was a suitable model to study the role of the CDP-choline pathway in VLDL secretion. Thus, it was proposed that choline-deficiency may impair secretion of lipoproteins from the liver, leading to the development of fatty liver (201). Indeed, rats fed a choline-deficient diet for 3 days

showed a 6.5-fold elevation in hepatic TG (201). Moreover, choline-deficient rats showed decreased levels of VLDL (and the associated lipids) along with a 73% reduction of plasma ApoB-100 suggesting that choline-deficiency impaired VLDL secretion in rat livers. In contrast, choline-deficiency had no effect on the concentrations of plasma HDL or ApoA-1 (201). The role of PC biosynthesis in VLDL secretion was confirmed as primary hepatocytes cultured from choline-deficient rats showed a 3-fold reduction of TG and PC secretion which was mainly due to impaired VLDL secretion, and not impaired HDL secretion. Furthermore, impaired VLDL secretion could be corrected by supplementation with choline, methionine, or betaine together with homocysteine (203,204). These results demonstrated that active PC biosynthesis is required for normal VLDL secretion from rat hepatocytes. On the other hand, the biosynthesis of sphingomyelin, a minor phospholipid of VLDLs comprising of 11% of total VLDL phospholipid content (7), is not required for normal VLDL secretion in rats (205). The generation of hepatic CTα knockout mice further supported the role of the CDP-choline pathway in controlling VLDL secretion (155). Clearly, choline-deficiency is an important predictor of hepatic steatosis. However, although choline-deficient humans have increased plasma ALT activity which is suggestive of increased liver injury (35), recent studies have suggested choline-deficiency results in hepatic steatosis without further progression to NASH (189,199,206). Choline-deficient rat livers show increased PEMT protein and specific enzyme activities compared to choline-supplemented livers (207). Therefore, if impaired PC biosynthesis is a determinant factor of NASH, choline-deficiency may not induce NASH due to a compensatory increase of PEMT.

1.7.2 Methionine and choline deficiency is a predictor of non-alcoholic steatohepatitis

The MCD diet has become a widely used nutritional model for NAFLD research, since along with hepatic steatosis, mice fed the MCD diet develop NASH (208). The accumulation of hepatic TG and elevated levels of serum ALT occur after 10 days of feeding C57BL6/J mice the MCD diet compared to a control diet (209). Furthermore, NASH is fully developed within 5 weeks of the MCD diet (209). In response to the MCD diet, mice show reduced hepatic TG secretion within VLDL particles, along with increased hepatic FA uptake (170). Furthermore, mice fed the MCD diet show reduced levels of *de novo* lipogenesis, while FA oxidation is elevated in response to the MCD diet compared to mice fed a diet supplemented with methionine and choline (210). The suppression of VLDL secretion in MCD fed animals is presumably due to impaired PC biosynthesis considering both methionine and choline are substrates for PC biosynthesis (203). All together, these studies have demonstrated that hepatic steatosis in mice fed the MCD diet is due to an imbalance in the relationship between FA storage (decreased *de novo* lipogenesis, increased FA uptake), and FA disposal (reduced TG secretion, increased FA oxidation).

Along with hepatic lipid accumulation, mice fed the MCD diet develop NASH, as indicated by increased markers of inflammation, hepatocellular apoptosis, increased plasma ALT activity, and the presence of lipid peroxidation (211). Although the mechanism(s) in which animals fed the MCD diet develop NASH are not entirely known, a recent study demonstrated that while both a choline-deficient or methionine-deficient diet induces hepatic steatosis, only methionine-deficiency and the MCD diet induces oxidative damage, inflammation and fibrosis in mouse livers (189,206). These studies suggest that methionine-deficiency, and not choline, is detrimental to hepatocytes. As methionine is an important

precursor for methylation reactions, protein synthesis, and PC biosynthesis, it is not surprising that methionine would be detrimental to hepatocytes, and would induce liver injury (212,213). However, as indicated, the MCD diet inhibits additional cellular processes other than PC biosynthesis, and therefore, it remains unclear of the exact role in which impaired PC biosynthesis may play on the development of NASH.

1.7.3 Phosphatidylcholine as a possible determinant of non-alcoholic steatohepatitis

As indicated, a diet deficient in either choline or both methionine and choline impairs PC biosynthesis, suggesting that impaired PC biosynthesis is a potential determinant of the pathogenesis of NASH. Further studies have also indicated that impaired PC biosynthesis may play a role in the pathogenesis of NASH. A recent lipidomic analysis has shown that hepatic PC is reduced by 25% in patients with steatosis compared with control patients; there was also a trend of decreased hepatic PC in NASH livers (214). In addition, a functional polymorphism (V175M substitution) within the *Pemt* gene has been found to be associated with NAFLD human livers (215). This polymorphism decreased the specific activity of PEMT when expressed in hepatoma cells and increased the susceptibility to NAFLD in patients with this polymorphism (215). Furthermore, mRNA expression of CT is reduced in NASH patients compared to patients without hepatic steatosis (216). These findings suggest that impaired hepatic PC homeostasis is a potential determinant of NASH in humans. In addition, *Pemt*$^{-/-}$ mice fed a choline-deficient diet develop severe steatohepatitis due to a dramatic reduction in the PC:PE phospholipid ratio resulting in loss of membrane integrity and consequently the induction of NASH (217). Interestingly, manipulation of the PC:PE ratio restored hepatocyte membrane integrity and attenuated NASH in *Pemt*$^{-/-}$ mice fed the choline-deficient diet (217)

indicating that the PC:PE ratio, rather than PC, is a determinant factor for the pathogenesis of NASH.

1.8 Phosphatidylcholine and Cell Death

1.8.1 Programmed Cell Death

Programmed cell death may be divided into two pathways: apoptosis and necrosis. As reviewed by Fiers (218), the typical features of apoptotic cells include: membrane blebbing, exposure of phosphatidylserine on the outer leaflet of the plasma membrane, cytosolic condensation, cellular shrinkage, nuclear condensation, breakdown of nuclear DNA , and the formation of apoptotic bodies. Furthermore, apoptotic cells are absorbed by neighbouring cells. On the other hand, necrotic cells tend to swell, round up, and have a loss of intracellular proteins and metabolites due to rupture of the plasma membrane (reviewed in (219)). Apoptosis and necrosis are often inseparable and share common mediators, such as the mitochondrial permeability transition (reviewed in (219)). Programmed cell death is conserved from *Caenorhabditis elegans* to humans (220) and is an essential process occurring in development, tissue remodelling, immune regulation, morphogenesis, and normal embryogenesis (reviewed in (218)). However, cell death has also been observed in pathologies, such as in bacterial meningitis (221).

An imbalance of PC homeostasis in mammalian cells leads to cell death. The fundamental role of PC in cellular survival has been underscored by several studies which demonstrate that genetic (222), pharmacological (223), and metabolic (224) disruption of PC biosynthesis leads to reduced cellular proliferation and the induction of apoptosis. Therefore, defining the mechanism of how impaired PC homeostasis induces cell death will allow insight into potential therapeutic mechanisms for treating various diseases.

1.8.2 Impairment of phosphatidylcholine biosynthesis induces cellular death

The first studies showing a correlation between impaired PC biosynthesis and cell death were performed in MT58 cells, which are ChoK1 cells with a thermo-sensitive mutation in CTα (225,226). When incubated at the permissive temperature of 33ºC, MT58 cells are phenotypically similar to the ChoK1 wild type cells. However, when shifted to the restrictive temperature of 40ºC, PC biosynthesis is impaired and the cellular PC content is dramatically decreased compared to control cells (225,226). Apoptosis is induced in MT58 cells after 30 hours of incubation at the restrictive temperature as indicated by the presence of membrane blebbing, DNA fragmentation, nuclear condensation, and cellular shrinkage (222,227). Interestingly, expression of PEMT in MT58 cells (which normally do not express PEMT) does not rescue cells from apoptosis even though the cells synthesize and maintain normal amounts of cellular PC (228). MT58 cells have increased PC degradation, even when incubated at the restrictive temperature (116). Thus, expression of PEMT did not prevent apoptosis of MT58 cells because PEMT was unable to maintain the high demand for cellular PC (229).

Other studies have also outlined the importance of PC biosynthesis in cell survival (111,221,223,230). A variety of cytotoxic drugs, many of which are used for cancer therapy, target the CDP-choline pathway to inhibit PC biosynthesis in order to impede cellular growth of the growing tumor cell (223,230,231). Bacterial infection in brain cells (neurons and microglia) by pneumoccal infections (221), and pulmonary infection with *Pseudomonas aeruginosa* (232) reduces PC biosynthesis resulting in apoptosis of both brain cells and lung cells. Injections of CDP-choline in mice could prevent hippocampal damage induced by infection with pneumoccal bacteria (221). Furthermore, acute lung injury in mice triggered by an infection with *P. aeruginosa* could be prevented with gene delivery of CTα (221,232,233). These studies demonstrated that unimpeded PC biosynthesis is essential for survival and function of lung and brain cells. Clearly, inhibition of PC biosynthesis is sufficient to induce apoptosis, and continual unimpeded PC metabolism is essential for cellular homeostasis.

1.8.3 Loss of membrane integrity induces cell death

PC is an essential component of mammalian membranes, and the integrity of cellular membranes may be compromised if mammalian membranes are deficient in PC content. Furthermore, loss of membrane integrity ultimately induces cellular death. Several lines of evidence have clearly demonstrated that choline-deficiency induces apoptosis, as indicated by the presence of DNA fragmentation, apoptotic morphology, and cell cycle arrest (224,234-236). Cellular PC content was 50% lower in cells cultured in choline-deficient medium, while choline-deficiency had no effect on cellular PE content (224,234,235). The loss of cellular PC induced by choline-deficiency may lead to loss of membrane integrity which would increase a cell's susceptibility to apoptosis.

A recent study utilizing *Pemt*$^{-/-}$ mice has highlighted the importance of membrane integrity in maintaining hepatic homeostasis. However, this study demonstrated that membrane integrity was influenced by a dramatic decrease in the PC:PE ratio, and did not result from the 50% loss of hepatic PC content (217). PC is a bilayer forming, cylindrical-shaped phospholipid which localizes primarily in the outer monolayer of the plasma membrane (Figure 1.8) (2). PE is a non-bilayer forming, cone-shaped phospholipid which primarily localizes within the inner monolayer of the plasma membrane (Figure 1.8) (2). Through manipulation of the PC:PE ratio, Vance and coworkers (217) demonstrated that a reduced hepatic PC:PE ratio alters the structure of hepatocyte plasma membranes (increased PE content in the outer leaflet of the plasma membrane) resulting in loss of membrane integrity and the induction of NASH (Figure 1.8) (217). A reduced hepatic PC:PE phospholipid ratio has been reported in other models of NASH and alcoholic steatohepatitis (188,237,238), as well as within brain microsomal membranes of apolipoprotein E-deficient mice (239). Furthermore, a recent study has demonstrated that the PC:PE ratio may be important for maintaining mitochondrial membrane fluidity as a reduced mitochondrial PC:PE ratio in a mouse model of steatohepatitis resulted in depletion of mitochondrial glutathione (189). These studies suggest that the PC:PE ratio influences membrane integrity. Therefore, a reduced PC:PE ratio, rather than the reduction of cellular PC, may play a pivotal role in the induction of apoptosis due to compromised cellular membranes.

1.9 Thesis Objectives

Thesis Objective 1:

Several lines of evidence have suggested that impaired PC biosynthesis may contribute to the pathogenesis of NASH in both humans and animals (210,214); however, the direct role of impaired PC biosynthesis (without dietary reduction of PC precursors) in the pathogenesis of NASH has not been investigated. In chapters 2 and 3, we have utilized LCTα$^{-/-}$ mice to investigate whether impaired PC biosynthesis is a determinant factor in the pathogenesis of NASH. As LCTα$^{-/-}$ mice develop mild steatosis when fed a chow diet (155,156), the mice were challenged with a high fat diet in an attempt to induce NASH. Surprisingly, CTα-deficient livers develop NASH within one week of high fat feeding. From this, all subsequent experiments were performed in LCTα$^{-/-}$ mice fed the high fat diet for one week to investigate the mechanisms involved in the pathogenesis of NASH during the initial stages of development. To identify the mechanism(s) involved in the development of steatosis (the "first hit") and NASH (the "second hit"), we employed various techniques, such as *in vivo* radiolabelling experiments, hepatic lipid analysis, and quantitative PCR.

In addition, to characterize the role of impaired PC biosynthesis in the pathogenesis of NASH, we treated mice with LPC, betaine, choline, and CDP-choline, all of which may be incorporated into PC. Furthermore, we also utilized adenoviral delivery of CTα into CTα-deficient livers to stimulate PC biosynthesis. All together, we found that hepatic steatosis was largely attributed to reduced TG secretion. Furthermore, we found that impaired PC biosynthesis contributes to hepatic steatosis, which increases the susceptibility of CTα-deficient livers to develop NASH. However, PC is not the only determinant factor contributing to the pathogenesis of NASH in LCTα$^{-/-}$ mice.

Thesis Objective 2:

It is well established that impaired PC biosynthesis and reduced cellular PC content is sufficient to induce cellular death. However, a reduction in cellular PC ultimately results in a reduced PC:PE ratio. The PC:PE ratio has been shown to be a predictor of membrane integrity and a reduced PC:PE ratio leads to loss of membrane integrity, leading to the development of NASH (217). Therefore, a reduced PC:PE ratio, rather than the reduction of cellular PC, may play a pivotal role in the induction of apoptosis due to compromised cellular membranes. In chapter 4, we utilized the MT58 cell line to understand whether a reduced PC:PE ratio contributes to cellular death. We hypothesized that if the reduced PC:PE ratio is sufficient to induce cellular death, then normalization of the ratio should rescue MT58 cells from cellular death. In an attempt to normalize the PC:PE, we utilized silencing RNA to knockdown the two key enzymes involved in PE biosynthesis which should decreased PE mass, and normalize the PC:PE ratio. MT58 cells were also treated with LPC which should increased PC and normalize the PC:PE ratio. We found that the total amount of cellular PC and PE, and not the reduced PC:PE ratio, influences cellular integrity of MT58 cells. The reduced PC:PE ratio reflects an imbalance of the phospholipid homeostasis.

Lesion	Scoring Criteria (score out of 3)
Steatosis (Percentage of hepatocytes)	**1** - <33% **2** - 33-67% **3** - >68
Lobular Inflammation (Neutrophil cluster)	**1** - 1 focus **2** - 2-10 foci **3** - >10 foci
Ballooning Degeneration	**1** – mild **2** - moderate **3** – severe
Portal Inflammation	**1** – nonexpansile **2** – expansile, minority of triads **3** – expansile, majority of triads
Grade of NASH **(Total score of lesions)**	Grade 0 = Score 0 Grade 1 = Score 1-4 Grade 2 = Score 5-8 Grade 3 = Score 9-12
Fibrosis Staging Criteria	Stage 0 = no fibrosis Stage 1 = perivenular Stage 2 = perivenular and periportal Stage 3 = perivenular, periportal and bridging fibrosis Stage 4 = cirrhosis

Table 1.1 Grading and staging of non-alcoholic steatohepatitis. Liver histology is scored for the severity of each lesion (steatosis, ballooning degeneration, lobular inflammation and portal inflammation). The grade of non-alcoholic steatohepatitis (NASH) is defined by the total score of all lesions. The stage of fibrosis is defined by the extent of collagen deposition, and the location of fibrosis.

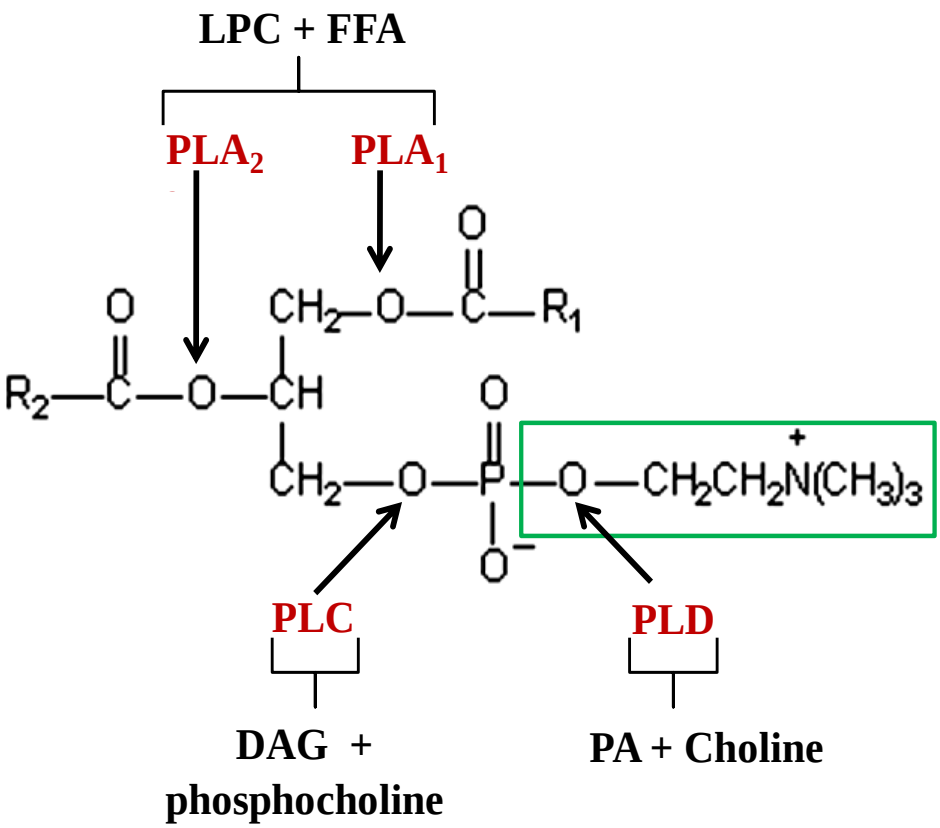

Figure 1.1 Structure and catabolism of phosphatidylcholine. The picture represents the basic structure of a phosphatidylcholine (PC) molecule. The two fatty acid hydrocarbon chains which are esterified to the glycerol back bone are depicted by R_1 and R_2. The variation of the side chains allows for the large diversity among PC molecules. The choline head group is outlined by the green box. More than one phospholipase (PL) degrades PC generating important signalling molecules. PLA_1 and PLA_2 hydrolyze PC at the *sn*-1 (PLA_1) or *sn*-2 (PLA_2) position generating lysophosphatidylcholine (LPC) and a free fatty acid (FFA). PLC and PLD are phosphodiesterases as they cleave a phosphodiester bond. Degradation of PC by PLC generates diacylglycerol (DAG) and phosphocholine, while cleavage by PLD generates phosphatidic acid (PA) and choline.

Figure 1.2 Phosphatidylcholine biosynthesis. Phosphatidylcholine (PC) is generated via the CDP-choline pathway (pathway depicted on the left of the figure). This pathway begins with the phosphorylation of choline catalyzed by choline kinase (CK). Through the action of CTP:phosphocholine cytidylyltransferase (CT), phosphocholine is converted into CDP-choline. Finally, CDP-choline reacts with diacylglycerol (DAG) to generate PC via CDP-choline:1,2-diacylglycerol cholinephosphotransferase (CPT). Regulation of PC biosynthesis via the CDP-choline pathway is modulated by the association of CT with cellular membranes. Membrane-bound CT is active, while the soluble form of CT is inactive. Activation and deactivation of CT is modulated by changes in cellular levels of PC and DAG, and by changes within the phosphorylation status of CT. The liver may also generate PC via the phosphatidylethanolamine *N*-methyltransferase (PEMT) pathway (pathway depicted on the bottom of the figure). This pathway begins with the methylation of phosphatidylethanolamine (PE) into phosphatidylmonomethylethanolamine (PMME). PMME is subsequently converted into phosphatidyldimethylethanolamine (PDME) via a second methylation reaction. The third methylation reaction converts PDME into PC. PEMT catalyzes each methylation reaction within the pathway. *S*-sdenosylmethionine (AdoMet) is the other substrate for each methylation reaction, and *S*-adenosylhomocysteine (AdoHcy) is produced during each reaction.

Figure 1.2

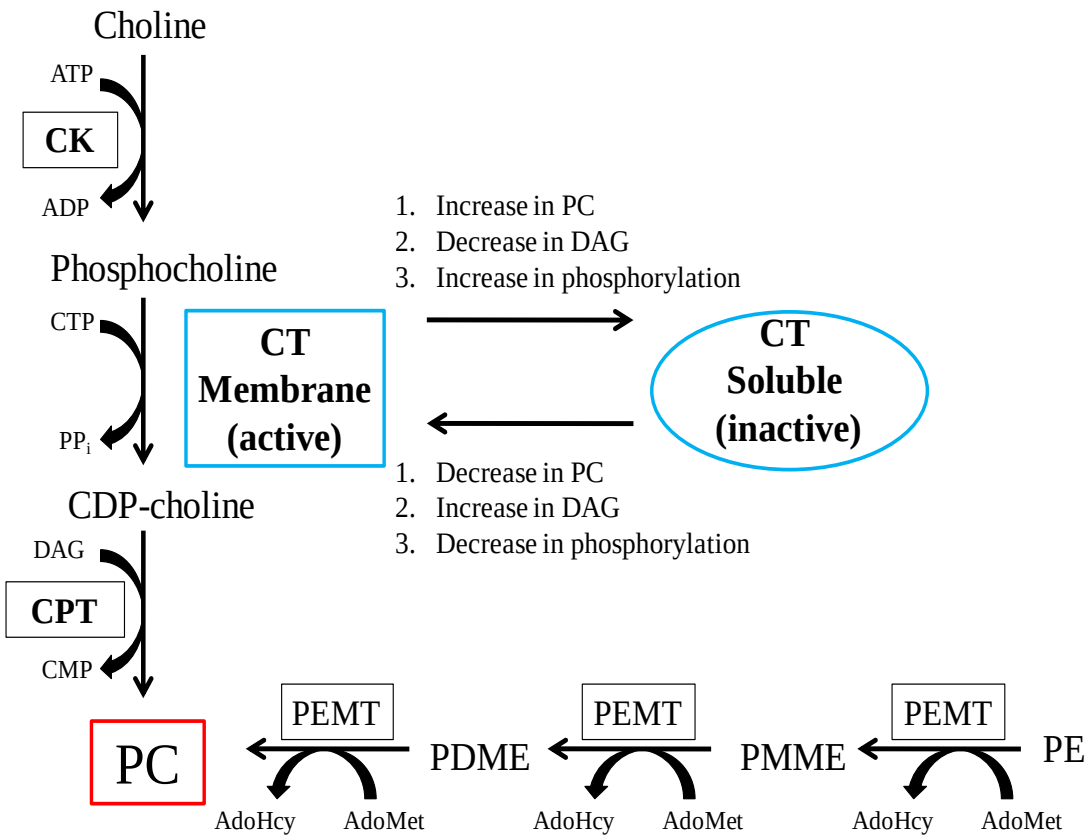
Choline
ATP
CK
ADP
Phosphocholine
CTP
PPi
CDP-choline
DAG
CPT
CMP
PC
CT Membrane (active)
CT Soluble (inactive)
1. Increase in PC
2. Decrease in DAG
3. Increase in phosphorylation
1. Decrease in PC
2. Increase in DAG
3. Decrease in phosphorylation
PEMT
PDME
PEMT
PMME
PEMT
PE
AdoHcy
AdoMet
AdoHcy
AdoMet
AdoHcy
AdoMet

Figure 1.3 Metabolic fates of choline. Choline may be converted into phosphatidylcholine (PC) via the CDP-choline pathway through the actions of three consecutive enzymes: choline kinase (CK), CTP:phosphocholine cytidylyltransferase (CT), and CDP-choline:1,2-diacylglycerol cholinephosphotransferase (CPT). In neuronal cells, choline is a precursor for acetylcholine and this reaction is catalyzed by the enzyme choline acetyltransferase (ChAT). In the liver and kidney, choline is oxidized to betaine through the coordinated action of choline dehydrogenase (CHDH) and betaine aldehyde dehydrogenase (BADH). Betaine serves as a methyl donor for the methionine cycle, and transfers its methyl group to homocysteine (Hcy) catalyzed via betaine:homocyteine methyltransferase (BHMT). Methionine synthase (MS) catalyzes the methylation of Hcy using 5-methyltetrahydrofolate (CH_3THF) as the methyl donor, producing tetrahydrofolate (THF) and methionine. The methionine cycle begins with the adenylation of methionine (Met) into *S*-adenosylmethionine (AdoMet) via the action of methionine adenosyltransferase (MAT). AdoMet is the methyl donor for most biological methylation reactions, including the phosphatidylethanolamine *N*-methyltransferase (PEMT) pathway. All methylation reactions produce *S*-adenosylhomocysteine (AdoHcy) which is cleaved by *S*-adenosylhomocysteine hydrolase (AHCY) to from adenosine and Hcy. Hcy may either be methylated for re-entry into the methionine cycle, or is further catabolised to cysteine via the transsulfuration enzymes cystathionine β-synthase (CBS) and cystathionine γ-lyase (CBL). Modified from Stead, L.M., *et. al.*(2006) *Am J Clin Nutr* 83, 5-10.

Figure 1.3

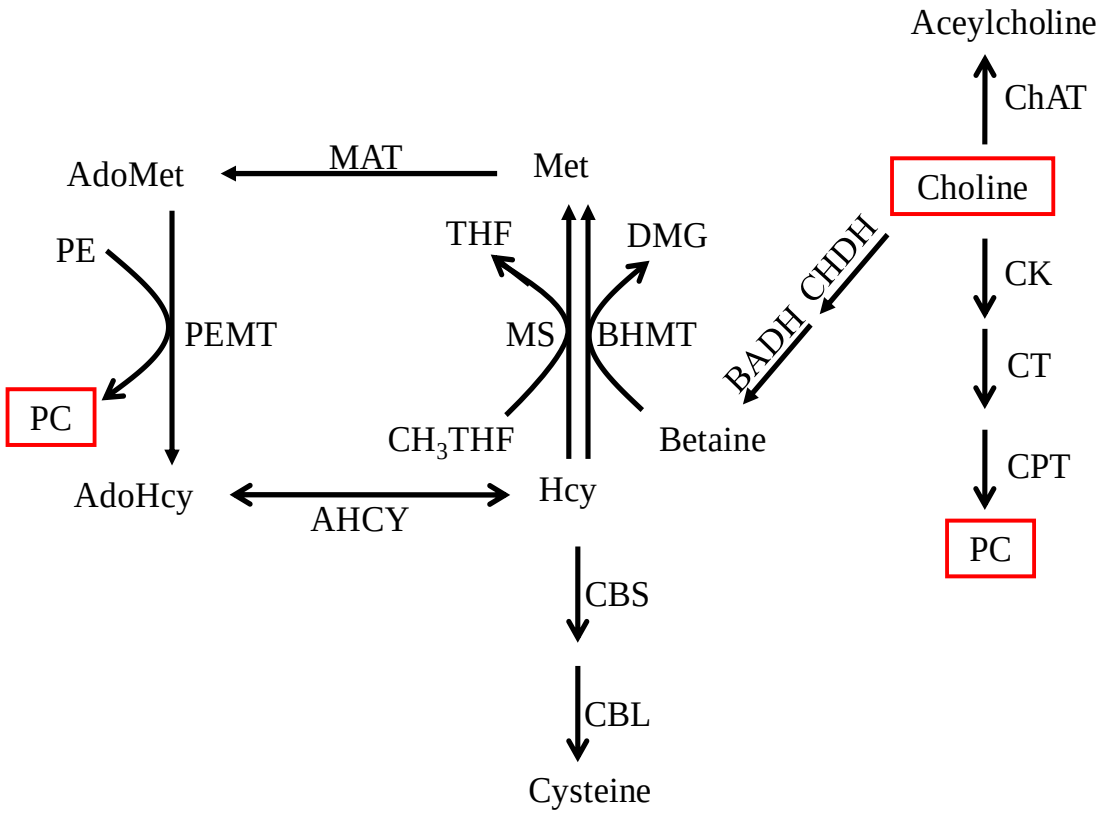
Aceylcholine
ChAT
Choline
CK
CT
CPT
PC
MAT
AdoMet
Met
PE
PEMT
PC
THF
DMG
MS
BHMT
BADH CHDH
CH3THF
Betaine
AdoHcy
AHCY
Hcy
CBS
CBL
Cysteine

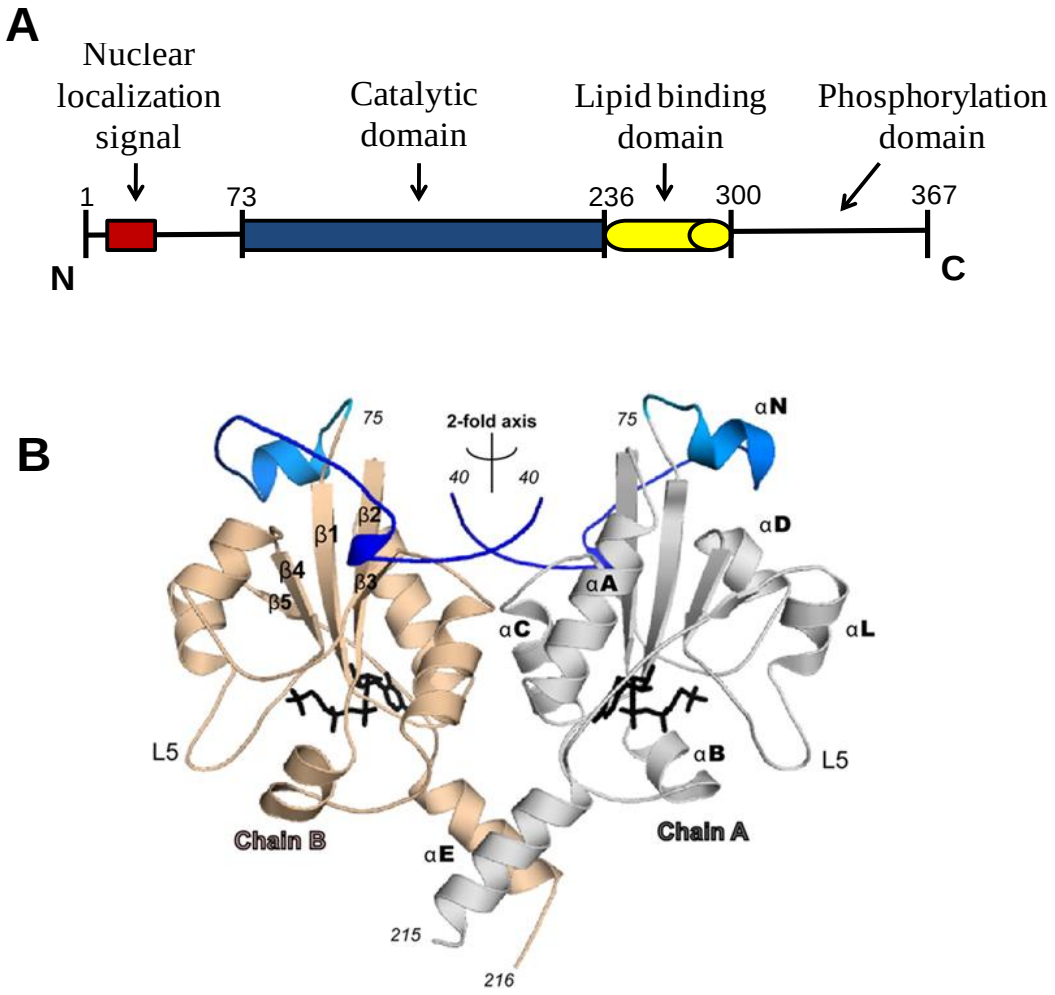

Figure 1.4 Structure of CTP:phosphocholine cytidylyltransferase-α. (A) Domain structures of CTP:phosphocholine cytidylyltransferase-α (CTα). CTα contains an N-terminal nuclear localization signal, a catalytic domain, an amphipathic helical (lipid binding) domain, and a C-terminal phosphorylation domain. Modified from Johnson, J.E., *et al.* (2003) *J. Biol. Chem.* 278, 514-522. (B) Crystal structure of the catalytic domain of CTα (residues 1-236) as a homodimer in complex with CDP-choline (black). Domains within the structure include the N-terminus (blue), and the catalytic domain (grey and brown). Reproduced from Lee, J., *et. al.* (2009) *J. Biol. Chem.* 284m 33535-33548.

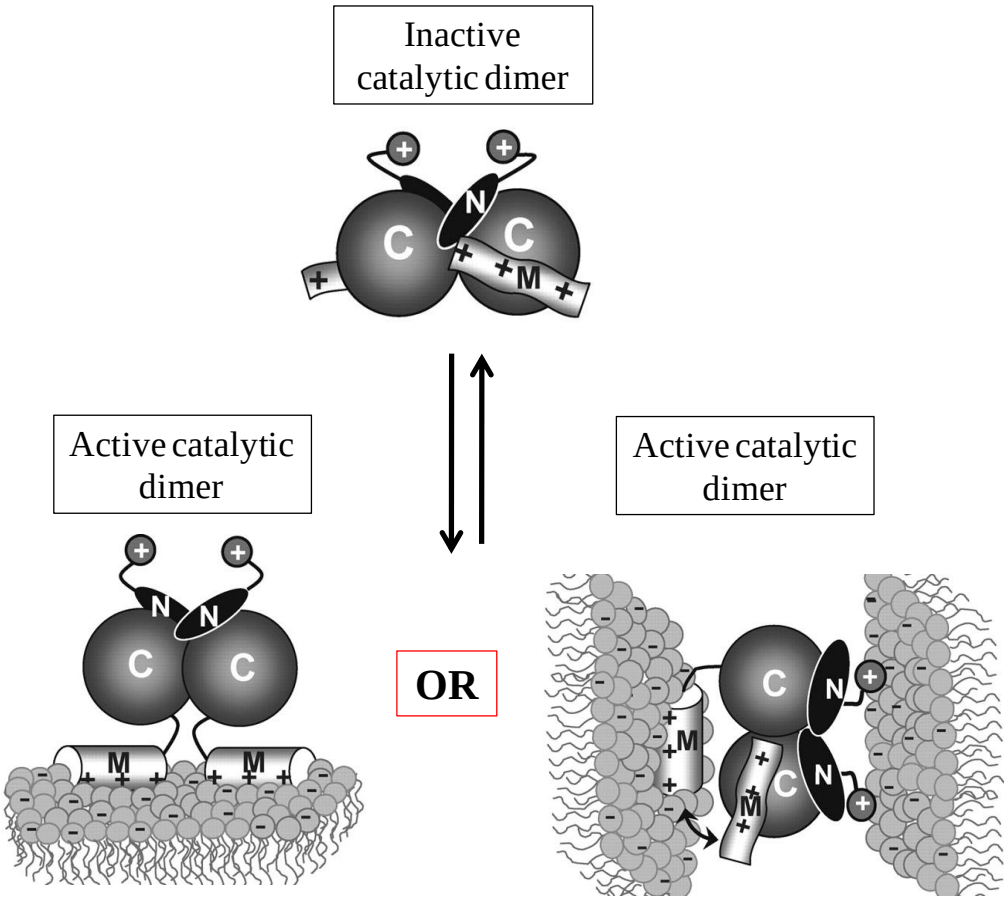

Figure 1.5 Association of CTP:phosphocholine cytidylyltransferase-α with biological membranes. CTP: phosphocholine cytidylyltransferase-α (CTα) is an inactive homodimer in its soluble form. However, upon activation by various stimulus (i.e. diacylglycerol), the CTα homodimer becomes active and partitions into biological membranes, thereby regulating PC biosynthesis via the CDP-choline pathway. The classical view of membrane-binding includes the partitioning of the CTα dimer into a single membrane using both lipid-binding domains (left panel). However, another model includes tethering of two membranes by the CTα homodimer (right panel). In this model, only a single lipid-binding domain binds to the cellular membrane, while both nuclear localization signals tether a second biological membrane (right panel). Modified from Taneva, S., *et. al.* (2008) *J. Biol. Chem.* 283, 28137-28148.

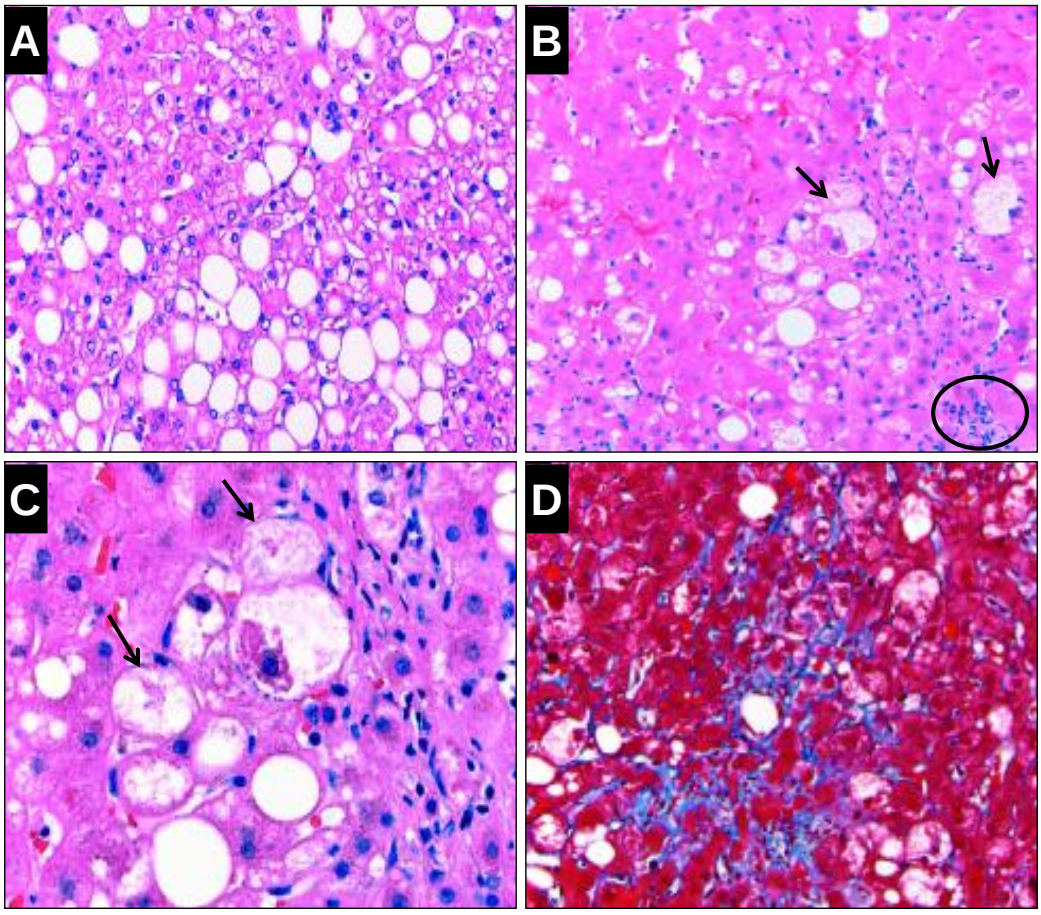

Figure 1.6 Pathogenesis of non-alcoholic fatty liver disease. (A) Liver histology stained with hematoxylin and eosin (H&E) showing benign steatosis, with occasional foci of inflammatory cells. (B) Liver histology stained with H&E stain showing non-alcoholic steatohepatitis. Hepatocyte ballooning degeneration (indicated by arrows), and inflammatory cells (indicated within the circle) are mixed with hepatocytes containing steatosis. (C) H&E stained liver histology showing Mallory hyaline with ropy inclusions (indicated by arrows) in the cytoplasm of hepatocytes. (D) Liver histology stained with masson trichrome showing perivenular fibrosis. The fibrosis is shown in blue. Reproduced from Yeh, M. M., and Brunt, E.M. (2007) *Am. J. Clin. Pathol.* 128, 837-847.

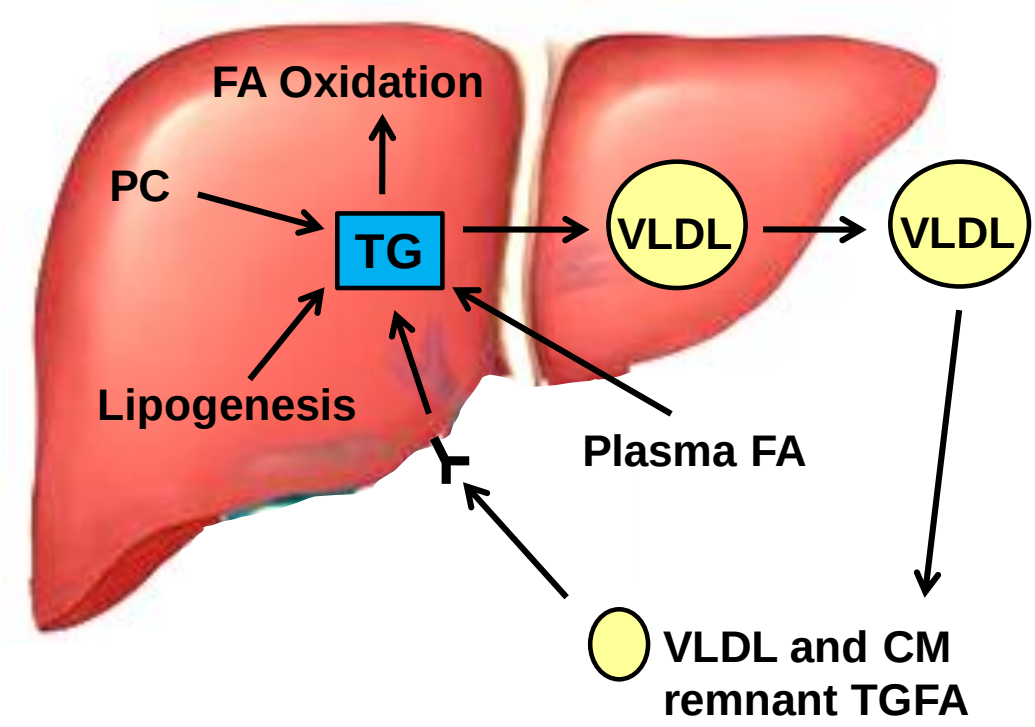

Figure 1.7 Homeostasis of hepatic triacylglycerol. Hepatic triacylglycerol (TG) homeostasis is maintained through a balance between: delivery of plasma free fatty acids (FA) and FA from TG within the remnant lipoprotein particles (very-low-density lipoproteins, VLDL, and chylomicrons, CM); *de novo* synthesis of FA via lipogenesis; oxidation of FA; the assembly and secretion of TG in the form of VLDL; and the conversion of phosphatidylcholine (PC) to TG. Modified from Ginsberg, H.N. (2006) *Cell Metabolism* 4, 179-181

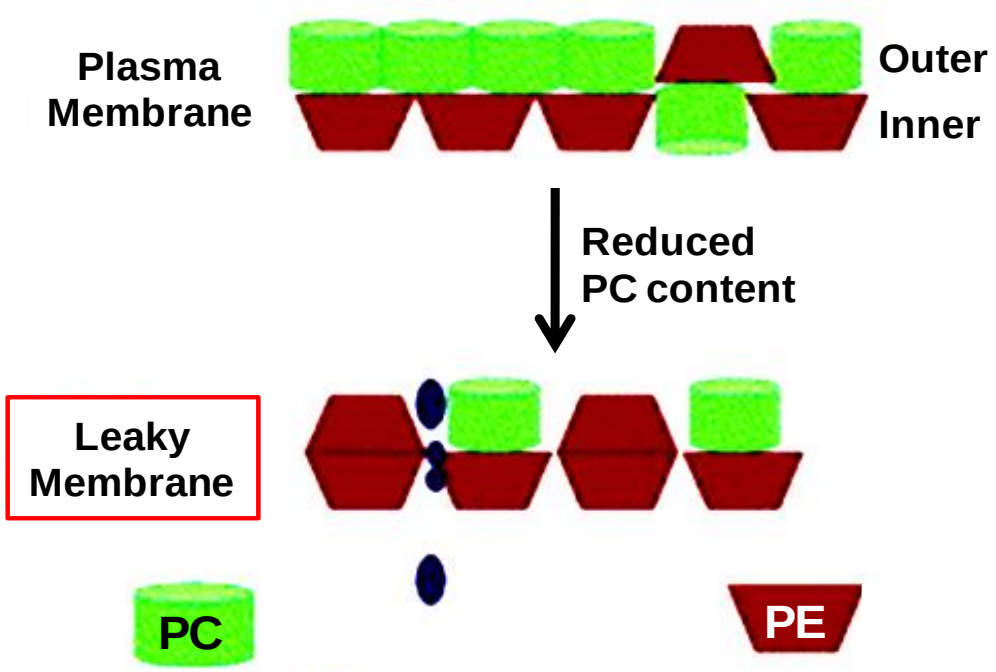

Figure 1.8 Membrane integrity is influenced by the phosphatidylcholine to phosphatidylethanolamine ratio. Phosphatidylcholine (PC) molecules form cylindrical structures (green), while phosphatidylethanolamine (PE) molecules form conical structures (red). Under normal conditions, where the phospholipid homeostasis is maintained, PCs primarily localize to the outer leaflet of the plasma membrane, while PEs primarily localize to the inner leaflet of the plasma membrane. However, a reduction in cellular PC content results in a reduction in the proportion of PC to PE within cellular membranes. As a result, more PE molecules may localize to the outer leaflet of the plasma membrane, compromising the membrane integrity of cells. Reproduced from Li, Z., *et. al.* (2006) *Cell Metabolism* 5, 321-331.

1.10 References

1. Kent, C. (1995) *Annu Rev Biochem* **64**, 315-343

2. W. Downhan, M. B., and E. Mileykovskaya. (2008) Functional roles of lipids in membranes. in *BIochemistiry of Lipids, Lipoproteins and Membranes, 5th edition* (Vance DE and Vance JE ed.), Elsevier, Amsterdam. pp 1-37

3. Vance DE and Vance JE (2008) Phospholipid biosynthesis in eukaryotes. in *Biochemistry of Lipids, Lipoproteins, and Membranes, 5th Edition* (Vance DE and Vance JE ed.), Elsevier, Amsterdam. pp 213-244

4. Exton, J. H. (1990) *J Biol Chem* **265**, 1-4

5. Billah, M. M., and Anthes, J. C. (1990) *Biochem J* **269**, 281-291

6. Phillips, A. J. a. M. C. (2008) Lipoprotein Structure. in *Biochemistry of Lipids, Lipoproteins and Membranes, 5th edition* (J.E., V. D. E. a. V. ed.), Elsevier, Amsterdam. pp 485-506

7. Chapman, M. J. (1986) *Methods Enzymol* **128**, 70-143

8. Hay, D. W., Cahalane, M. J., Timofeyeva, N., and Carey, M. C. (1993) *J Lipid Res* **34**, 759-768

9. Agellon, L. B., Walkey, C. J., Vance, D. E., Kuipers, F., and Verkade, H. J. (1999) *Hepatology* **30**, 725-729

10. Kuipers, F., Oude Elferink, R. P., Verkade, H. J., and Groen, A. K. (1997) *Subcell Biochem* **28**, 295-318

11. Patton, G. M., Fasulo, J. M., and Robins, S. J. (1994) *J Lipid Res* **35**, 1211-1221

12. Smit, J. J., Schinkel, A. H., Oude Elferink, R. P., Groen, A. K., Wagenaar, E., van Deemter, L., Mol, C. A., Ottenhoff, R., van der Lugt, N. M., van Roon, M. A., and et al. (1993) *Cell* **75**, 451-462

13. Goerke, J. (1998) *Biochim Biophys Acta* **1408**, 79-89

14. Wilton, D. C. (2008) Phospholipases. in *Biochemsitry of Lipids, Lipoproteins and Membranes, 5th edition* (Vance, D. E. V. a. J. E. ed.), Elsevier, Amsterdam. pp 305-329

15. Cuadrado, A., Carnero, A., Dolfi, F., Jimenez, B., and Lacal, J. C. (1993) *Oncogene* **8**, 2959-2968

16. Baburina, I., and Jackowski, S. (1999) *J Biol Chem* **274**, 9400-9408

17. Barbour, S. E., Kapur, A., and Deal, C. L. (1999) *Biochim Biophys Acta* **1439**, 77-88

18. Chiu, C. H., and Jackowski, S. (2001) *Biochem Biophys Res Commun* **287**, 600-606

19. Robichaud, J. C., van der Veen, J. N., Yao, Z., Trigatti, B., and Vance, D. E. (2009) *Biochim Biophys Acta* **1790**, 538-551

20. Minahk, C., Kim, K. W., Nelson, R., Trigatti, B., Lehner, R., and Vance, D. E. (2008) *J Biol Chem* **283**, 6449-6458

21. Kennedy, E. P. (1957) *Annu Rev Biochem* **26**, 119-148

22. Kennedy, E. P., and Weiss, S. B. (1956) *J Biol Chem* **222**, 193-214

23. Bremer, J., and Greenberg, D. M. (1959) *Biochim Biophys Acta* **35**, 287-288

24. Vance, D. E., and Ridgway, N. D. (1988) *Prog Lipid Res* **27**, 61-79

25. Reo, N. V., Adinehzadeh, M., and Foy, B. D. (2002) *Biochim Biophys Acta* **1580**, 171-188

26. Sundler, R., and Akesson, B. (1975) *J Biol Chem* **250**, 3359-3367

27. DeLong, C. J., Shen, Y. J., Thomas, M. J., and Cui, Z. (1999) *J Biol Chem* **274**, 29683-29688

28. Li, Z., and Vance, D. E. (2008) *J Lipid Res* **49**, 1187-1194

29. Deves, R., and Krupka, R. M. (1979) *Biochim Biophys Acta* **557**, 469-485

30. Simon, J. R., Atweh, S., and Kuhar, M. J. (1976) *J Neurochem* **26**, 909-922

31. van Rossum, G. D., and Boyd, C. A. (1998) *J Membr Biol* **162**, 147-156

32. Stead, L. M., Brosnan, J. T., Brosnan, M. E., Vance, D. E., and Jacobs, R. L. (2006) *Am J Clin Nutr* **83**, 5-10

33. Mudd, S. H., and Poole, J. R. (1975) *Metabolism* **24**, 721-735

34. Best, C. H., and Huntsman, M. E. (1932) *J Physiol* **75**, 405-412

35. Zeisel, S. H., Da Costa, K. A., Franklin, P. D., Alexander, E. A., Lamont, J. T., Sheard, N. F., and Beiser, A. (1991) *FASEB J* **5**, 2093-2098

36. Blusztajn, J. K. (1998) *Science* **281**, 794-795

37. Zeisel, S. H., Mar, M. H., Zhou, Z., and da Costa, K. A. (1995) *J Nutr* **125**, 3049-3054

38. Wittenberg, J., and Kornberg, A. (1953) *J Biol Chem* **202**, 431-444

39. Aoyama, C., Yamazaki, N., Terada, H., and Ishidate, K. (2000) *J Lipid Res* **41**, 452-464

40. Uchida, T. (1994) *J Biochem* **116**, 508-518

41. Uchida, T., and Yamashita, S. (1992) *J Biol Chem* **267**, 10156-10162

42. Aoyama, C., Nakashima, K., Matsui, M., and Ishidate, K. (1998) *Biochim Biophys Acta* **1390**, 1-7

43. Aoyama, C., Liao, H., and Ishidate, K. (2004) *Prog Lipid Res* **43**, 266-281

44. Aoyama, C., Ohtani, A., and Ishidate, K. (2002) *Biochem J* **363**, 777-784

45. Ishidate, K., Tsuruoka, M., and Nakazawa, Y. (1980) *Biochem Biophys Res Commun* **96**, 946-952

46. Ishidate, K., Kihara, M., Tadokoro, K., and Nakazawa, Y. (1982) *Biochim Biophys Acta* **713**, 94-102

47. Ishidate, K., Tsuruoka, M., and Nakazawa, Y. (1982) *Biochim Biophys Acta* **713**, 103-111

48. Ishidate, K., Enosawa, S., and Nakazawa, Y. (1983) *Biochem Biophys Res Commun* **111**, 683-689

49. Aoyama, C., Ishidate, K., Sugimoto, H., and Vance, D. E. (2007) *Biochim Biophys Acta* **1771**, 1148-1155

50. Iorio, E., Mezzanzanica, D., Alberti, P., Spadaro, F., Ramoni, C., D'Ascenzo, S., Millimaggi, D., Pavan, A., Dolo, V., Canevari, S., and Podo, F. (2005) *Cancer Res* **65**, 9369-9376

51. Eliyahu, G., Kreizman, T., and Degani, H. (2007) *Int J Cancer* **120**, 1721-1730

52. Hernando, E., Sarmentero-Estrada, J., Koppie, T., Belda-Iniesta, C., Ramirez de Molina, V., Cejas, P., Ozu, C., Le, C., Sanchez, J. J., Gonzalez-Baron, M., Koutcher, J., Cordon-Cardo, C., Bochner, B. H., Lacal, J. C., and Ramirez de Molina, A. (2009) *Oncogene* **28**, 2425-2435

53. Wu, G., Aoyama, C., Young, S. G., and Vance, D. E. (2008) *J Biol Chem* **283**, 1456-1462

54. Sher, R. B., Aoyama, C., Huebsch, K. A., Ji, S., Kerner, J., Yang, Y., Frankel, W. N., Hoppel, C. L., Wood, P. A., Vance, D. E., and Cox, G. A. (2006) *J Biol Chem* **281**, 4938-4948

55. Wu, G., Sher, R. B., Cox, G. A., and Vance, D. E. (2009) *Biochim Biophys Acta* **1791**, 347-356

56. Wu, G., Sher, R. B., Cox, G. A., and Vance, D. E. (2010) *Biochim Biophys Acta* **1801**, 446-454

57. Cornell, R. B., and Northwood, I. C. (2000) *Trends Biochem Sci* **25**, 441-447

58. Taneva, S., Johnson, J. E., and Cornell, R. B. (2003) *Biochemistry* **42**, 11768-11776

59. Johnson, J. E., Xie, M., Singh, L. M., Edge, R., and Cornell, R. B. (2003) *J Biol Chem* **278**, 514-522

60. Johnson, J. E., Rao, N. M., Hui, S. W., and Cornell, R. B. (1998) *Biochemistry* **37**, 9509-9519

61. Pelech, S. L., Pritchard, P. H., Brindley, D. N., and Vance, D. E. (1983) *J Biol Chem* **258**, 6782-6788

62. Sleight, R., and Kent, C. (1983) *J Biol Chem* **258**, 836-839

63. Sleight, R., and Kent, C. (1983) *J Biol Chem* **258**, 831-835

64. Karim, M., Jackson, P., and Jackowski, S. (2003) *Biochim Biophys Acta* **1633**, 1-12

65. Lykidis, A., Baburina, I., and Jackowski, S. (1999) *J Biol Chem* **274**, 26992-27001

66. Tang, W., Keesler, G. A., and Tabas, I. (1997) *J Biol Chem* **272**, 13146-13151

67. Wang, Y., MacDonald, J. I., and Kent, C. (1995) *J Biol Chem* **270**, 354-360

68. Lee, J., Johnson, J., Ding, Z., Paetzel, M., and Cornell, R. B. (2009) *J Biol Chem* **284**, 33535-33548

69. Henneberry, A. L., Wistow, G., and McMaster, C. R. (2000) *J Biol Chem* **275**, 29808-29815

70. Henneberry, A. L., and McMaster, C. R. (1999) *Biochem J* **339 (Pt 2)**, 291-298

71. Henneberry, A. L., Wright, M. M., and McMaster, C. R. (2002) *Mol Biol Cell* **13**, 3148-3161

72. Lim, P., Cornell, R., and Vance, D. E. (1986) *Biochem Cell Biol* **64**, 692-698

73. Cui, Z., Vance, J. E., Chen, M. H., Voelker, D. R., and Vance, D. E. (1993) *J Biol Chem* **268**, 16655-16663

74. Shields, D. J., Lehner, R., Agellon, L. B., and Vance, D. E. (2003) *J Biol Chem* **278**, 2956-2962

75. Vance, D. E., Walkey, C. J., and Cui, Z. (1997) *Biochim Biophys Acta* **1348**, 142-150

76. Shields, D. J., Altarejos, J. Y., Wang, X., Agellon, L. B., and Vance, D. E. (2003) *J Biol Chem* **278**, 35826-35836

77. Ridgway, N. D., and Vance, D. E. (1987) *J Biol Chem* **262**, 17231-17239

78. Walkey, C. J., Cui, Z., Agellon, L. B., and Vance, D. E. (1996) *J Lipid Res* **37**, 2341-2350

79. Sesca, E., Perletti, G. P., Binasco, V., Chiara, M., and Tessitore, L. (1996) *Biochem Biophys Res Commun* **229**, 158-162

80. Cui, Z., Shen, Y. J., and Vance, D. E. (1997) *Biochim Biophys Acta* **1346**, 10-16

81. Tessitore, L., Cui, Z., and Vance, D. E. (1997) *Biochem J* **322 (Pt 1)**, 151-154

82. Houweling, M., Cui, Z., Tessitore, L., and Vance, D. E. (1997) *Biochim Biophys Acta* **1346**, 1-9

83. Cole, L. K., and Vance, D. E. (2010) *J Biol Chem* **285**, 11880-11891

84. Banchio, C., Schang, L. M., and Vance, D. E. (2003) *J Biol Chem* **278**, 32457-32464

85. Walkey, C. J., Donohue, L. R., Bronson, R., Agellon, L. B., and Vance, D. E. (1997) *Proc Natl Acad Sci U S A* **94**, 12880-12885

86. Walkey, C. J., Yu, L., Agellon, L. B., and Vance, D. E. (1998) *J Biol Chem* **273**, 27043-27046

87. Waite, K. A., Cabilio, N. R., and Vance, D. E. (2002) *J Nutr* **132**, 68-71

88. Li, Z., and Vance, D. E. (2007) *Biochim Biophys Acta* **1771**, 486-490

89. Waite, K. A., and Vance, D. E. (2004) *Biochim Biophys Acta* **1636**, 175-182

90. Noga, A. A., and Vance, D. E. (2003) *J Biol Chem* **278**, 21851-21859

91. Noga, A. A., Zhao, Y., and Vance, D. E. (2002) *J Biol Chem* **277**, 42358-42365

92. Robichaud, J. C., Francis, G. A., and Vance, D. E. (2008) *J Biol Chem* **283**, 35496-35506

93. Glass, C. K., and Witztum, J. L. (2001) *Cell* **104**, 503-516

94. Zhao, Y., Su, B., Jacobs, R. L., Kennedy, B., Francis, G. A., Waddington, E., Brosnan, J. T., Vance, J. E., and Vance, D. E. (2009) *Arterioscler Thromb Vasc Biol* **29**, 1349-1355

95. Kowala, M. C., Recce, R., Beyer, S., Gu, C., and Valentine, M. (2000) *Atherosclerosis* **149**, 323-330

96. Cole, L. K., Dolinsky, V. W., Dyck, J. R., and Vance, D. E. (2011) *Circ Res* **108**, 686-694

97. Plump, A. S., and Breslow, J. L. (1995) *Annu Rev Nutr* **15**, 495-518

98. Jacobs, R. L., Zhao, Y., Koonen, D. P., Sletten, T., Su, B., Lingrell, S., Cao, G., Peake, D. A., Kuo, M. S., Proctor, S. D., Kennedy, B. P., Dyck, J. R., and Vance, D. E. (2010) *J Biol Chem* **285**, 22403-22413

99. Wang, Y., Sweitzer, T. D., Weinhold, P. A., and Kent, C. (1993) *J Biol Chem* **268**, 5899-5904

100. DeLong, C. J., Qin, L., and Cui, Z. (2000) *J Biol Chem* **275**, 32325-32330

101. Northwood, I. C., Tong, A. H., Crawford, B., Drobnies, A. E., and Cornell, R. B. (1999) *J Biol Chem* **274**, 26240-26248

102. Lagace, T. A., and Ridgway, N. D. (2005) *Mol Biol Cell* **16**, 1120-1130

103. Gehrig, K., Cornell, R. B., and Ridgway, N. D. (2008) *Mol Biol Cell* **19**, 237-247

104. Gehrig, K., and Ridgway, N. D. (2011) *Biochim Biophys Acta* **1811**, 377-385

105. Ridsdale, R., Tseu, I., Wang, J., and Post, M. (2001) *J Biol Chem* **276**, 49148-49155

106. Fagone, P., Sriburi, R., Ward-Chapman, C., Frank, M., Wang, J., Gunter, C., Brewer, J. W., and Jackowski, S. (2007) *J Biol Chem* **282**, 7591-7605

107. Houweling, M., Cui, Z., Anfuso, C. D., Bussiere, M., Chen, M. H., and Vance, D. E. (1996) *Eur J Cell Biol* **69**, 55-63

108. Agassandian, M., Chen, B. B., Schuster, C. C., Houtman, J. C., and Mallampalli, R. K. (2010) *FASEB J* **24**, 1271-1283

109. Zhou, J., Ryan, A. J., Medh, J., and Mallampalli, R. K. (2003) *J Biol Chem* **278**, 37032-37040

110. Lagace, T. A., and Ridgway, N. D. (2005) *Biochem J* **392**, 449-456

111. Lagace, T. A., Miller, J. R., and Ridgway, N. D. (2002) *Mol Cell Biol* **22**, 4851-4862

112. Gehrig, K., Morton, C. C., and Ridgway, N. D. (2009) *J Lipid Res* **50**, 966-976

113. Guo, Y., Walther, T. C., Rao, M., Stuurman, N., Goshima, G., Terayama, K., Wong, J. S., Vale, R. D., Walter, P., and Farese, R. V. (2008) *Nature* **453**, 657-661

114. Tian, Y., Pate, C., Andreolotti, A., Wang, L., Tuomanen, E., Boyd, K., Claro, E., and Jackowski, S. (2008) *J Cell Biol* **181**, 945-957

115. Skinner, H. B., McGee, T. P., McMaster, C. R., Fry, M. R., Bell, R. M., and Bankaitis, V. A. (1995) *Proc Natl Acad Sci U S A* **92**, 112-116

116. Testerink, N., van der Sanden, M. H., Houweling, M., Helms, J. B., and Vaandrager, A. B. (2009) *J Lipid Res* **50**, 2182-2192

117. Lykidis, A., Jackson, P., and Jackowski, S. (2001) *Biochemistry* **40**, 494-503

118. Friesen, J. A., Campbell, H. A., and Kent, C. (1999) *J Biol Chem* **274**, 13384-13389

119. Taneva, S., Dennis, M. K., Ding, Z., Smith, J. L., and Cornell, R. B. (2008) *J Biol Chem* **283**, 28137-28148

120. Sleight, R., and Kent, C. (1983) *J Biol Chem* **258**, 824-830

121. Utal, A. K., Jamil, H., and Vance, D. E. (1991) *J Biol Chem* **266**, 24084-24091

122. Jamil, H., Utal, A. K., and Vance, D. E. (1992) *J Biol Chem* **267**, 1752-1760

123. Hatch, G. M., Jamil, H., Utal, A. K., and Vance, D. E. (1992) *J Biol Chem* **267**, 15751-15758

124. Jamil, H., and Vance, D. E. (1990) *Biochem J* **270**, 749-754

125. Jamil, H., Yao, Z. M., and Vance, D. E. (1990) *J Biol Chem* **265**, 4332-4339

126. Yao, Z. M., Jamil, H., and Vance, D. E. (1990) *J Biol Chem* **265**, 4326-4331

127. Kent, C. (1997) *Biochim Biophys Acta* **1348**, 79-90

128. Wang, Y., and Kent, C. (1995) *J Biol Chem* **270**, 17843-17849

129. Cornell, R. B., Kalmar, G. B., Kay, R. J., Johnson, M. A., Sanghera, J. S., and Pelech, S. L. (1995) *Biochem J* **310 (Pt 2)**, 699-708

130. Yang, W., and Jackowski, S. (1995) *J Biol Chem* **270**, 16503-16506

131. Jackowski, S. (1994) *J Biol Chem* **269**, 3858-3867

132. Houweling, M., Jamil, H., Hatch, G. M., and Vance, D. E. (1994) *J Biol Chem* **269**, 7544-7551

133. Agassandian, M., Zhou, J., Tephly, L. A., Ryan, A. J., Carter, A. B., and Mallampalli, R. K. (2005) *J Biol Chem* **280**, 21577-21587

134. Shiratori, Y., Houweling, M., Zha, X., and Tabas, I. (1995) *J Biol Chem* **270**, 29894-29903

135. Tessner, T. G., Rock, C. O., Kalmar, G. B., Cornell, R. B., and Jackowski, S. (1991) *J Biol Chem* **266**, 16261-16264

136. Houweling, M., Tijburg, L. B., Jamil, H., Vance, D. E., Nyathi, C. B., Vaartjes, W. J., and van Golde, L. M. (1991) *Biochem J* **278 (Pt 2)**, 347-351

137. Houweling, M., Tijburg, L. B., Vaartjes, W. J., Batenburg, J. J., Kalmar, G. B., Cornell, R. B., and Van Golde, L. M. (1993) *Eur J Biochem* **214**, 927-933

138. Ryan, A. J., McCoy, D. M., Mathur, S. N., Field, F. J., and Mallampalli, R. K. (2000) *J Lipid Res* **41**, 1268-1277

139. Bakovic, M., Waite, K., Tang, W., Tabas, I., and Vance, D. E. (1999) *Biochim Biophys Acta* **1438**, 147-165

140. Bakovic, M., Waite, K. A., and Vance, D. E. (2000) *J Lipid Res* **41**, 583-594

141. Sugimoto, H., Bakovic, M., Yamashita, S., and Vance, D. E. (2001) *J Biol Chem* **276**, 12338-12344

142. Sugimoto, H., Okamura, K., Sugimoto, S., Satou, M., Hattori, T., Vance, D. E., and Izumi, T. (2005) *J Biol Chem* **280**, 40857-40866

143. Marcucci, H., Elena, C., Gilardoni, P., and Banchio, C. (2008) *Biochim Biophys Acta* **1781**, 254-262

144. Terce, F., Brun, H., and Vance, D. E. (1994) *J Lipid Res* **35**, 2130-2142

145. Golfman, L. S., Bakovic, M., and Vance, D. E. (2001) *J Biol Chem* **276**, 43688-43692

146. Elena, C., and Banchio, C. (2010) *Biochim Biophys Acta* **1801**, 537-546

147. Banchio, C., Schang, L. M., and Vance, D. E. (2004) *J Biol Chem* **279**, 40220-40226

148. Wang, L., Magdaleno, S., Tabas, I., and Jackowski, S. (2005) *Mol Cell Biol* **25**, 3357-3363

149. Jackowski, S., Rehg, J. E., Zhang, Y. M., Wang, J., Miller, K., Jackson, P., and Karim, M. A. (2004) *Mol Cell Biol* **24**, 4720-4733

150. Carter, J. M., Demizieux, L., Campenot, R. B., Vance, D. E., and Vance, J. E. (2008) *J Biol Chem* **283**, 202-212

151. Carter, J. M., Waite, K. A., Campenot, R. B., Vance, J. E., and Vance, D. E. (2003) *J Biol Chem* **278**, 44988-44994

152. Tian, Y., Zhou, R., Rehg, J. E., and Jackowski, S. (2007) *Mol Cell Biol* **27**, 975-982

153. Fagone, P., Gunter, C., Sage, C. R., Gunn, K. E., Brewer, J. W., and Jackowski, S. (2009) *J Biol Chem* **284**, 6847-6854

154. Zhang, D., Tang, W., Yao, P. M., Yang, C., Xie, B., Jackowski, S., and Tabas, I. (2000) *J Biol Chem* **275**, 35368-35376

155. Jacobs, R. L., Devlin, C., Tabas, I., and Vance, D. E. (2004) *J Biol Chem* **279**, 47402-47410

156. Jacobs, R. L., Lingrell, S., Zhao, Y., Francis, G. A., and Vance, D. E. (2008) *J Biol Chem* **283**, 2147-2155

157. Ludwig, J., Viggiano, T. R., McGill, D. B., and Oh, B. J. (1980) *Mayo Clin Proc* **55**, 434-438

158. Browning, J. D., and Horton, J. D. (2004) *J Clin Invest* **114**, 147-152

159. Yeh, M. M., and Brunt, E. M. (2007) *Am J Clin Pathol* **128**, 837-847

160. Angulo, P. (2002) *N Engl J Med* **346**, 1221-1231

161. Farrell, G. C., and Larter, C. Z. (2006) *Hepatology* **43**, S99-S112

162. Postic, C., and Girard, J. (2008) *J Clin Invest* **118**, 829-838

163. Brunt, E. M. (2001) *Semin Liver Dis* **21**, 3-16

164. Parekh, S., and Anania, F. A. (2007) *Gastroenterology* **132**, 2191-2207

165. Brunt, E. M., Janney, C. G., Di Bisceglie, A. M., Neuschwander-Tetri, B. A., and Bacon, B. R. (1999) *Am J Gastroenterol* **94**, 2467-2474

166. Day, C. P., and James, O. F. (1998) *Gastroenterology* **114**, 842-845

167. Musso, G., Gambino, R., and Cassader, M. (2009) *Prog Lipid Res* **48**, 1-26

168. Donnelly, K. L., Smith, C. I., Schwarzenberg, S. J., Jessurun, J., Boldt, M. D., and Parks, E. J. (2005) *J Clin Invest* **115**, 1343-1351

169. Horton, J. D., Shimomura, I., Ikemoto, S., Bashmakov, Y., and Hammer, R. E. (2003) *J Biol Chem* **278**, 36652-36660

170. Rinella, M. E., Elias, M. S., Smolak, R. R., Fu, T., Borensztajn, J., and Green, R. M. (2008) *J Lipid Res* **49**, 1068-1076

171. Koonen, D. P., Jacobs, R. L., Febbraio, M., Young, M. E., Soltys, C. L., Ong, H., Vance, D. E., and Dyck, J. R. (2007) *Diabetes* **56**, 2863-2871

172. Doege, H., Grimm, D., Falcon, A., Tsang, B., Storm, T. A., Xu, H., Ortegon, A. M., Kazantzis, M., Kay, M. A., and Stahl, A. (2008) *J Biol Chem* **283**, 22186-22192

173. Newberry, E. P., Xie, Y., Kennedy, S., Han, X., Buhman, K. K., Luo, J., Gross, R. W., and Davidson, N. O. (2003) *J Biol Chem* **278**, 51664-51672

174. Moon, Y. A., Hammer, R. E., and Horton, J. D. (2009) *J Lipid Res* **50**, 412-423

175. Shimomura, I., Bashmakov, Y., and Horton, J. D. (1999) *J Biol Chem* **274**, 30028-30032

176. Shimomura, I., Matsuda, M., Hammer, R. E., Bashmakov, Y., Brown, M. S., and Goldstein, J. L. (2000) *Mol Cell* **6**, 77-86

177. Fujita, K., Nozaki, Y., Wada, K., Yoneda, M., Fujimoto, Y., Fujitake, M., Endo, H., Takahashi, H., Inamori, M., Kobayashi, N., Kirikoshi, H., Kubota, K., Saito, S., and Nakajima, A. (2009) *Hepatology* **50**, 772-780

178. Ip, E., Farrell, G. C., Robertson, G., Hall, P., Kirsch, R., and Leclercq, I. (2003) *Hepatology* **38**, 123-132

179. Yang, S. Q., Lin, H. Z., Lane, M. D., Clemens, M., and Diehl, A. M. (1997) *Proc Natl Acad Sci U S A* **94**, 2557-2562

180. Kirsch, R., Clarkson, V., Verdonk, R. C., Marais, A. D., Shephard, E. G., Ryffel, B., and de la, M. H. P. (2006) *J Gastroenterol Hepatol* **21**, 174-182

181. Feldstein, A. E., Canbay, A., Angulo, P., Taniai, M., Burgart, L. J., Lindor, K. D., and Gores, G. J. (2003) *Gastroenterology* **125**, 437-443

182. Crespo, J., Cayon, A., Fernandez-Gil, P., Hernandez-Guerra, M., Mayorga, M., Dominguez-Diez, A., Fernandez-Escalante, J. C., and Pons-Romero, F. (2001) *Hepatology* **34**, 1158-1163

183. Yin, M., Wheeler, M. D., Kono, H., Bradford, B. U., Gallucci, R. M., Luster, M. I., and Thurman, R. G. (1999) *Gastroenterology* **117**, 942-952

184. Ribeiro, P. S., Cortez-Pinto, H., Sola, S., Castro, R. E., Ramalho, R. M., Baptista, A., Moura, M. C., Camilo, M. E., and Rodrigues, C. M. (2004) *Am J Gastroenterol* **99**, 1708-1717

185. Haukeland, J. W., Damas, J. K., Konopski, Z., Loberg, E. M., Haaland, T., Goverud, I., Torjesen, P. A., Birkeland, K., Bjoro, K., and Aukrust, P. (2006) *J Hepatol* **44**, 1167-1174

186. Feldstein, A. E., Werneburg, N. W., Canbay, A., Guicciardi, M. E., Bronk, S. F., Rydzewski, R., Burgart, L. J., and Gores, G. J. (2004) *Hepatology* **40**, 185-194

187. Tomita, K., Tamiya, G., Ando, S., Ohsumi, K., Chiyo, T., Mizutani, A., Kitamura, N., Toda, K., Kaneko, T., Horie, Y., Han, J. Y., Kato, S., Shimoda, M., Oike, Y., Tomizawa, M., Makino, S., Ohkura, T., Saito, H., Kumagai, N., Nagata, H., Ishii, H., and Hibi, T. (2006) *Gut* **55**, 415-424

188. Mas, E., Danjoux, M., Garcia, V., Carpentier, S., Segui, B., and Levade, T. (2009) *PLoS One* **4**, e7929

189. Caballero, F., Fernandez, A., Matias, N., Martinez, L., Fucho, R., Elena, M., Caballeria, J., Morales, A., Fernandez-Checa, J. C., and Garcia-Ruiz, C. (2010) *J Biol Chem* **285**, 18528-18536

190. Leclercq, I. A., Farrell, G. C., Field, J., Bell, D. R., Gonzalez, F. J., and Robertson, G. R. (2000) *J Clin Invest* **105**, 1067-1075

191. Mari, M., Caballero, F., Colell, A., Morales, A., Caballeria, J., Fernandez, A., Enrich, C., Fernandez-Checa, J. C., and Garcia-Ruiz, C. (2006) *Cell Metab* **4**, 185-198

192. Vendemiale, G., Grattagliano, I., Caraceni, P., Caraccio, G., Domenicali, M., Dall'Agata, M., Trevisani, F., Guerrieri, F., Bernardi, M., and Altomare, E. (2001) *Hepatology* **33**, 808-815

193. Ozcan, U., Cao, Q., Yilmaz, E., Lee, A. H., Iwakoshi, N. N., Ozdelen, E., Tuncman, G., Gorgun, C., Glimcher, L. H., and Hotamisligil, G. S. (2004) *Science* **306**, 457-461

194. Ozcan, U., Yilmaz, E., Ozcan, L., Furuhashi, M., Vaillancourt, E., Smith, R. O., Gorgun, C. Z., and Hotamisligil, G. S. (2006) *Science* **313**, 1137-1140

195. Kammoun, H. L., Chabanon, H., Hainault, I., Luquet, S., Magnan, C., Koike, T., Ferre, P., and Foufelle, F. (2009) *J Clin Invest* **119**, 1201-1215

196. Oyadomari, S., Harding, H. P., Zhang, Y., Oyadomari, M., and Ron, D. (2008) *Cell Metab* **7**, 520-532

197. Wang, D., Wei, Y., and Pagliassotti, M. J. (2006) *Endocrinology* **147**, 943-951

198. Ota, T., Gayet, C., and Ginsberg, H. N. (2008) *J Clin Invest* **118**, 316-332

199. Macfarlane, D. P., Zou, X., Andrew, R., Morton, N. M., Livingstone, D. E., Aucott, R. L., Nyirenda, M. J., Iredale, J. P., and Walker, B. R. (2011) *Am J Physiol Endocrinol Metab* **300**, E402-409

200. Lombardi, B., Pani, P., and Schlunk, F. F. (1968) *J Lipid Res* **9**, 437-446

201. Yao, Z. M., and Vance, D. E. (1990) *Biochem Cell Biol* **68**, 552-558

202. Vermeulen, P. S., Lingrell, S., Yao, Z., and Vance, D. E. (1997) *J Lipid Res* **38**, 447-458

203. Yao, Z. M., and Vance, D. E. (1988) *J Biol Chem* **263**, 2998-3004

204. Yao, Z. M., and Vance, D. E. (1989) *J Biol Chem* **264**, 11373-11380

205. Merrill, A. H., Jr., Lingrell, S., Wang, E., Nikolova-Karakashian, M., Vales, T. R., and Vance, D. E. (1995) *J Biol Chem* **270**, 13834-13841

206. Vetelainen, R., van Vliet, A., and van Gulik, T. M. (2007) *J Gastroenterol Hepatol* **22**, 1526-1533

207. Cui, Z., and Vance, D. E. (1996) *J Biol Chem* **271**, 2839-2843

208. Larter, C. Z., and Yeh, M. M. (2008) *J Gastroenterol Hepatol* **23**, 1635-1648

209. Dela Pena, A., Leclercq, I., Field, J., George, J., Jones, B., and Farrell, G. (2005) *Gastroenterology* **129**, 1663-1674

210. Rizki, G., Arnaboldi, L., Gabrielli, B., Yan, J., Lee, G. S., Ng, R. K., Turner, S. M., Badger, T. M., Pitas, R. E., and Maher, J. J. (2006) *J Lipid Res* **47**, 2280-2290

211. Lee, G. S., Yan, J. S., Ng, R. K., Kakar, S., and Maher, J. J. (2007) *J Lipid Res* **48**, 1885-1896

212. Zeisel, S. H., and Blusztajn, J. K. (1994) *Annu Rev Nutr* **14**, 269-296

213. Niculescu, M. D., and Zeisel, S. H. (2002) *J Nutr* **132**, 2333S-2335S

214. Puri, P., Baillie, R. A., Wiest, M. M., Mirshahi, F., Choudhury, J., Cheung, O., Sargeant, C., Contos, M. J., and Sanyal, A. J. (2007) *Hepatology* **46**, 1081-1090

215. Song, J., da Costa, K. A., Fischer, L. M., Kohlmeier, M., Kwock, L., Wang, S., and Zeisel, S. H. (2005) *FASEB J* **19**, 1266-1271

216. Saibara, T., and Ono, M. (2007) *J Hepatol* **47**, 869-870

217. Li, Z., Agellon, L. B., Allen, T. M., Umeda, M., Jewell, L., Mason, A., and Vance, D. E. (2006) *Cell Metab* **3**, 321-331

218. Fiers, W., Beyaert, R., Declercq, W., and Vandenabeele, P. (1999) *Oncogene* **18**, 7719-7730

219. Lemasters, J. J. (1999) *Am J Physiol* **276**, G1-6

220. Yuan, J. (1996) *J Cell Biochem* **60**, 4-11

221. Zweigner, J., Jackowski, S., Smith, S. H., Van Der Merwe, M., Weber, J. R., and Tuomanen, E. I. (2004) *J Exp Med* **200**, 99-106

222. Cui, Z., Houweling, M., Chen, M. H., Record, M., Chap, H., Vance, D. E., and Terce, F. (1996) *J Biol Chem* **271**, 14668-14671

223. Baburina, I., and Jackowski, S. (1998) *J Biol Chem* **273**, 2169-2173

224. Yen, C. L., Mar, M. H., Meeker, R. B., Fernandes, A., and Zeisel, S. H. (2001) *FASEB J* **15**, 1704-1710

225. Esko, J. D., and Raetz, C. R. (1980) *Proc Natl Acad Sci U S A* **77**, 5192-5196

226. Esko, J. D., Wermuth, M. M., and Raetz, C. R. (1981) *J Biol Chem* **256**, 7388-7393

227. van der Sanden, M. H., Houweling, M., van Golde, L. M., and Vaandrager, A. B. (2003) *Biochem J* **369**, 643-650

228. Houweling, M., Cui, Z., and Vance, D. E. (1995) *J Biol Chem* **270**, 16277-16282

229. Waite, K. A., and Vance, D. E. (2000) *J Biol Chem* **275**, 21197-21202

230. van der Luit, A. H., Budde, M., Ruurs, P., Verheij, M., and van Blitterswijk, W. J. (2002) *J Biol Chem* **277**, 39541-39547

231. Anthony, M. L., Zhao, M., and Brindle, K. M. (1999) *J Biol Chem* **274**, 19686-19692

232. Henderson, F. C., Miakotina, O. L., and Mallampalli, R. K. (2006) *J Lipid Res* **47**, 2314-2324

233. Zhou, J., Wu, Y., Henderson, F., McCoy, D. M., Salome, R. G., McGowan, S. E., and Mallampalli, R. K. (2006) *Gene Ther* **13**, 974-985

234. Yen, C. L., Mar, M. H., and Zeisel, S. H. (1999) *FASEB J* **13**, 135-142

235. Zeisel, S. H., Albright, C. D., Shin, O. H., Mar, M. H., Salganik, R. I., and da Costa, K. A. (1997) *Carcinogenesis* **18**, 731-738

236. Holmes-McNary, M. Q., Baldwin, A. S., Jr., and Zeisel, S. H. (2001) *J Biol Chem* **276**, 41197-41204

237. Ji, C., Shinohara, M., Vance, D., Than, T. A., Ookhtens, M., Chan, C., and Kaplowitz, N. (2008) *Alcohol Clin Exp Res* **32**, 1049-1058

238. Fast, D. G., and Vance, D. E. (1995) *Biochim Biophys Acta* **1258**, 159-168

239. Lomnitski, L., Oron, L., Sklan, D., and Michaelson, D. M. (1999) *J Neurosci Res* **58**, 586-592

CHAPTER 2

Hepatic CTP: phosphocholine cytidylyltransferase-α deficient mice are susceptible to diet induced non-alcoholic steatohepatitis

2.1 Introduction

In all nucleated cells, PC is made via the CDP-choline pathway and flux through this pathway is regulated by CTP:phosphocholine cytidylyltransferase (CT) (1,2). Although two isoforms of CT exist (CTα and CTβ), CTα is believed to be the predominant isoform in the liver (3). In the liver, PC can also be made via the phosphatidylethanolamine *N*-methyltransferase (PEMT) pathway in which PC is synthesized from sequential methylation reactions of phosphatidylethanolamine (PE) (4).

Previously, we have generated mice deficient in either PEMT or hepatic CTα. Studies on *Pemt*$^{-/-}$ mice demonstrated that normal very-low-density lipoprotein (VLDL) secretion requires PEMT, and that disruption of this pathway causes hepatic steatosis (5,6). CTα is also important for hepatic VLDL metabolism since liver-specific CTα knockout (LCTα$^{-/-}$) mice have impaired apoB-100 secretion (7). Furthermore, on a chow diet hepatic PC in LCTα$^{-/-}$ mice was 5-20% lower, and triacylglycerol (TG) was 25-40% higher, than in LCTα$^{+/+}$ mice (7). These data demonstrate the importance of CTα in controlling hepatic VLDL secretion. That LCTα$^{-/-}$ mice develop hepatic steatosis when fed a chow diet suggests that CTα-deficient livers may be susceptible to the development of non-alcoholic fatty liver disease (NAFLD) if challenged to additional cellular stress.

NAFLD encompasses a wide spectrum of liver damage including steatosis, non-alcoholic steatohepatitis (NASH), fibrosis and cirrhosis. The prevalence of NAFLD in the general population in North America is 10-24%, and is 25-75% in the obese and diabetic population (8-10). The progression from steatosis to NASH has been described as a “two-hit” model in which the “first hit” constitutes hepatic TG accumulation and the “second hit” involves cellular stresses causing inflammation and apoptosis (11).

Hepatic TG accumulation results from an imbalance between the availability of fatty acids (FA) for storage, and the disposal of FAs from the liver (12). Sources of free FA include: hepatic uptake from plasma non-esterified FA (NEFA) pool; hepatic uptake of FA from dietary TG within remnant lipoprotein particles (chylomicrons and VLDL); or from increased *de novo* lipogenesis (13). Disposal of hepatic FAs include oxidation of FAs, or secretion of hepatic TG in VLDL particles. Defects in FA storage or disposal are associated with the development of hepatic steatosis (14-17). The transition of hepatic steatosis to NASH includes a "second hit" which leads to hepatocellular injury. Excessive accumulation of hepatic TG increases the sensitivity of the liver to several types of cellular injury, including inflammation, oxidative damage, and endoplasmic reticulum (ER) stress (18-23).

Since impaired VLDL secretion is induced by LCTα-deficiency, we challenged LCTα$^{-/-}$ mice with a high fat (HF) diet to determine whether CTα-deficient livers have increased sensitivity to cellular injury. Surprisingly, within 7 days of HF feeding, LCTα$^{-/-}$ mice developed moderate NASH. Therefore, subsequent experiments were performed after 7 days of HF feeding to identify the mechanisms involved in the development of hepatic steatosis and the cellular stresses leading to the pathogenesis of NASH in LCTα$^{-/-}$ mice.

2.2 Experimental Procedures

2.2.1 Animal handling and diets

All procedures were approved by the University of Alberta's Institutional Animal Care Committee in accordance with guidelines of the Canadian Council on Animal Care. Female C57BL/6:129P2 floxed (control) and LCTα$^{-/-}$ mice (2-4 months old) (7) were fed the HF diet (Bioserve, #F3282) for 7 days. Mice were fasted for 12 h before collection of blood by cardiac puncture. Plasma was stored at -80ºC. Liver samples were freeze clamped and stored at -80ºC.

2.2.2 Histology and assessment of non-alcoholic fatty liver disease

Liver samples were preserved in 10% phosphate-buffered formalin, pH 7.0. Formalin-preserved liver samples were subjected to hematoxylin and eosin staining. Hematoxylin and eosin stained liver histology were clinically assessed by a pathologist for the presence of the histological features associated with NASH (lobular inflammation, portal inflammation and hepatocyte ballooning degeneration) using the method developed by Brunt *et. al.* (24).

2.2.3 Plasma parameters

Female C57BL/6:129P2 floxed and LCTα$^{-/-}$ mice were fed the HF diet for 7 days and blood was collected after an overnight fast. Total ketone bodies, NEFA, TG and alanine aminotransferase were quantified in 10 µl plasma using commercially available kits (Waco Inc., Roche Diagnostics, and Biotron Diagnostics Inc.).

2.2.4 Glucose, insulin and pyruvate tolerance tests

Floxed and LCTα$^{-/-}$ mice were fed the high fat diet for 7 days. Glucose tolerance test: after an overnight fast, the mice were administered 2g of glucose/kg body weight via intraperitoneal injection. Blood glucose levels were monitored after 15, 30 45, 60, 90 and 120 min. Insulin tolerance test: after 6 h fast, the mice were administered 1U of insulin/kg body weight via intraperitoneal injection. Blood glucose levels were monitored after 15, 30, 45, 60, 90 and 120 min. Pyruvate tolerance test: after an overnight fast, the mice were administered 2g of pyruvate/kg body weight via intraperitoneal injection. Blood glucose levels were monitored after 15, 30, 45, 60, 90 and 120 min. Area under the curve was measured for each test as a measure to compare floxed and LCTα$^{-/-}$ mice.

2.2.5 Quantification of hepatic lipids

Hepatic lipids were extracted from liver samples by the method of Folch *et al.* (25). Briefly, total lipids were extracted from liver homogenates (1 mg of protein) with chloroform:methanol (2:1). Phospholipids were separated by thin-layer chromatography in chloroform:methanol:acetic acid:water (25:15:4:2, v/v). Bands corresponding to PC and PE were scraped and the mass of PC and PE was quantified by a phosphorus assay (26). For quantification of hepatic TG, lipids were extracted from liver homogenate (1 mg of protein) as described above. The organic phase was dried under N_2, re-suspended in chloroform containing 1% tritonX-100 and further dried under N_2. Lipid extracts were re-suspended in water, and 10 µl (10 µg of protein) of sample was used to quantify hepatic TG using a commercially available kit (Roche Diagnostics).

Hepatic diacylglycerol (DAG) and ceramide levels were measured by the DAG kinase assay (27). Briefly, lipids were extracted from liver homogenates (1 mg of protein) as described above. The organic phase was dried under N_2, and resuspended in octyl-β-glucoside/cardiolipin and assay buffer (100 mM imidazole, 100 mM NaCl, 25 mM $MgCl_2$, 2 mM EGTA). DAG kinase (5 µg) and [γ-^{32}P]ATP (2µCi/mmol cold ATP) were added to the samples and incubated at 25ºC for 30 min. The reaction was stopped using chloroform: methanol (2:1). The [γ-^{32}P]phosphatidic acid and [γ-^{32}P]ceramide 1-phosphate produced in the reaction were separated by thin-layer chromatography in chloroform:hexane:methanol:acetic acid (10:6:2:1, v/v). Bands corresponding to phosphatidic acid and ceramide 1-phosphate were scraped and radioactivity was determined. Hepatic DAG and ceramide mass, which are proportional to phosphatidic acid and ceramide 1-phosphate, were quantified from a standard curve.

2.2.6 Real-time quantitative PCR

Total liver RNA was isolated using TRIzol reagent (Invitrogen) according to the manufacturer's instructions. Hepatic RNA was treated with DNaseI (Invitrogen) and reverse-transcribed using an oligo(dT)12-18 primer and Superscript II reverse transcriptase (Invitrogen) according to the manufacturer's instructions. Real-time quantitative PCR (qPCR) was performed using a Rotor-Gene 3000 instrument (Montreal Biotech). Hepatic gene expression was normalized to cyclophilin mRNA. Primer sets utilized for quantification of gene expression are shown in table 2.1.

2.2.7 In Vivo lipid radiolabelling

Floxed and LCTα$^{-/-}$ mice were fed the HF diet for 7 days followed by a 12 h fast. To assess *de novo* lipogenesis, the mice received an intraperitoneal injection of 100 µL of sterile saline containing 10 µCi of [^{3}H]glycerol (0.0125 µmole) and 10 µCi of [^{14}C]acetic acid (1.67 nmole) with 250 µM sodium acetate and 250 µM glycerol. Livers were collected 2 h post-injection. Lipids were extracted from liver homogenates (5 mg of protein) as described above. Neutral lipids were separated by thin-layer chromatography in hexane:diisopropyl ether:acetic acid (65:35:2, v/v) and phospholipids were separated by thin-layer chromatography in chloroform:methanol:acetic acid: water (25:15:4:2, v/v). Bands corresponding to TG, DAG, PC and PE were scraped and radioactivity was determined.

To assess FA uptake, the mice received a tail vein injection of 100 µl of sterile saline containing 10 µCi of [^{3}H]oleic acid (0.22 nmole) with 250 µM oleic acid. Livers were collected 30 min post-injection. Livers were homogenized in homogenization buffer (10 mM tris-HCl, pH 7.4, 150 mM NaCl, 1 mM EDTA) and radioactivity in liver homogenate (50 µg of protein) was determined as a measure of FA uptake.

2.2.8 Immunoblot analysis

Equal amounts of total protein (25 µg) from liver homogenates were boiled in buffer containing 1% SDS, and proteins were separated on a SDS-PAGE gel. Proteins were transferred to an immobilon-P transfer membrane and probed with antibodies immunoreactive towards fatty acid synthase, FAS (dilution 1:2500), phosphorylated acetyl-CoA carboxylase, p-ACC (dilution 1:2500), total ACC (dilution 1:2500), CCAAT/-enhancer-binding protein homologous protein, CHOP (dilution 1:2500), and glyceraldehyde 3-phosphate dehydrogenase, GAPDH (dilution1:5000).

Immunoreactive bands were visualized by enhanced chemiluminescence (Amersham Biosciences).

2.2.9 Oxidative stress analysis

To assess hepatic lipid peroxidation, hepatic thiobarbituric acid reactive substances (TBARS) was quantified in fasted livers from floxed and LCTα$^{-/-}$ mice fed the HF diet for 7 days. TBARS was quantified in liver homogenates (250 µg of protein) using a commercially available kit (Cayman Chemical).

Reduced glutathione (GSH) was quantified in fasted livers from floxed and LCTα$^{-/-}$ mice fed the HF for 7 days. Proteins were extracted from liver homogenates (1 mg) using 5% (w/v) trichloroacetic acid and 200 µl of the supernatant incubated with 200 µl of 5,5'-dithiobis-(2-nitrobenzoic acid) (5 mM) at 37ºC for 5 min. The absorbance was read at 412 nm.

2.2.10 Statistical analysis

Data are presented as means ± S.E. Comparisons between two groups were performed using a two-way *t* test, where $p < 0.05$ was considered significant. Four to eight mice were used per experimental group.

2.3 Results

2.3.1 High fat feeding induces moderate steatohepatitis in livers of LCTα-deficient mice

After one week of HF feeding, the body weights of LCTα$^{-/-}$ mice were comparable to floxed control mice (Table 2.2). However, CTα-deficient livers were 1.3-fold larger than livers from floxed mice (Table 2.2) suggesting CTα-deficient livers accumulate lipids. Liver histology revealed markedly altered morphology of livers from CTα-deficient mice fed the HF diet for 7 days (Figure 2.1A). To investigate the presence of NASH, liver histology was assessed for the appearance of steatosis, intra-acinar and portal inflammation, and ballooning degeneration of hepatocytes. Clinical assessment of liver histology revealed an increased presence of all lesions associated with NAFLD in CTα-deficient livers (Figure 2.1B), resulting in a steatohepatitis grade 2 (Figure 2.1C). Plasma alanine aminotransferase content was 7-fold higher in the LCTα$^{-/-}$ mice compared to floxed controls, further verifying the presence of liver injury (Table 2.2). These data show that CTα-deficient livers develop moderate NASH within one week of HF feeding.

2.3.2 Hepatic and plasma lipid profiles are altered in LCTα-deficient mice

Consistent with the changes in liver histology, hepatic CTα-deficiency resulted in a 3-fold higher level of hepatic TG compared to that in floxed livers (Figure 2.2A). The amount of TG was 60% lower in plasma of LCTα$^{-/-}$ mice than floxed mice (Table 2.2). Hepatic PC levels were 25% lower in LCTα$^{-/-}$ mice than in floxed controls, while PE levels were the same (Figure 2.2B). These results support earlier studies (7), and suggest that decreased hepatic PC biosynthesis impairs VLDL secretion, resulting in hepatic steatosis. A recent study has demonstrated that a reduced

hepatic PC:PE ratio may be a contributing factor to the pathogenesis of NASH (28). However, the PC:PE ratio in CTα-deficient livers is comparable to floxed livers (Figure 2.2B) indicating that a reduced PC:PE ratio does not contribute to the pathogenesis of NASH in LCTα$^{-/-}$ mice. Interestingly, the mass of hepatic DAG and ceramide was approximately 2-fold higher in LCTα$^{-/-}$ mice than in floxed controls (Figure 2.2C).

2.3.3 LCTα-deficient mice are not insulin resistant after one week of high fat feeding

Elevated hepatic DAG, ceramide and TG are associated with the development of hepatic insulin resistance (reviewed in (29,30)). Therefore, we performed glucose and insulin tolerance tests as a measure of whole-body insulin sensitivity. However, despite elevated hepatic lipids, LCTα$^{-/-}$ mice are not insulin resistant after 7 days of HF feeding as indicated by the insulin tolerance test (Table 2.2). The glucose tolerance test further indicates that whole-body glucose metabolism is not altered by LCTα deficiency after one week of HF feeding (Table 2.2). Since insulin down-regulates gluconeogenesis, we performed a pyruvate tolerance test as a measure of hepatic insulin sensitivity. However, LCTα$^{-/-}$ mice showed no difference in the pyruvate challenge compared to floxed mice (Table 2.2) suggesting that CTα-deficient livers have normal hepatic insulin sensitivity after 7 days of the HF diet.

2.3.4 Triacylglycerol production is unaltered by LCTα deficiency

To determine if *de novo* lipogenesis contributed to the hepatic steatosis in LCTα$^{-/-}$ mice, mRNAs encoding lipogenic genes were quantified (Figure 2.3A). The amount of mRNAs encoding liver X receptor α (LXRα) and diacylglycerol acyltransferase 2 (DGAT2) were lower in LCTα$^{-/-}$ mice than in floxed mice, whereas the expression of peroxisome proliferator receptor γ (PPARγ) mRNA was almost 3-fold higher in the LCTα$^{-/-}$ mice. Other hepatic mRNAs involved in lipogenesis were not altered by LCTα deficiency (Figure 2.3). In addition, protein expression of FAS, p-ACC and total ACC were not altered by LCTα deficiency (Figure 2.4). As a measure of TG synthesis, floxed and LCTα$^{-/-}$ mice were injected with [^{3}H]glycerol or [^{14}C]acetic acid. Incorporation of [^{3}H]glycerol into hepatic TG and DAG was not altered by LCTα deficiency (Figure 2.5A, B). Incorporation of [^{14}C]acetic acid also showed that *de novo* lipogenesis was not altered in livers of LCTα$^{-/-}$ mice (Figure 2.5C). In agreement with the decrease in hepatic PC mass in LCTα$^{-/-}$ livers (Figure 2.2B), the incorporation of [^{3}H]glycerol into PC, but not PE, was reduced by 45% by LCTα deficiency (Figure 2.5D).

2.3.5 Hepatic fatty acid uptake and oxidation are altered by LCTα deficiency

LCTα$^{-/-}$ mice showed a 60% reduction in plasma NEFA compared to floxed mice (Table 2.2) suggesting that FA uptake may be elevated by LCTα deficiency. However, the amounts of hepatic mRNAs encoding genes of FA uptake (fatty acid transport proteins 2 and 5: FATP2, FATP5) and the mRNA encoding liver fatty acid binding protein (LABP) were decreased by LCTα deficiency (Figure 2.6). *In vivo* labelling with [^{3}H]oleic acid indicated that FA uptake by LCTα$^{-/-}$ livers was 33% lower than by floxed livers (Figure 2.7). Therefore, the reduction of plasma NEFA is

unlikely to result from altered hepatic FA uptake. Although the reduction in plasma NEFA is unknown, adipose tissue in LCTα$^{-/-}$ mice may have reduced lipolysis resulting in decreased plasma NEFA. In addition, despite no change in hepatic mRNAs encoding FA oxidation genes (Figure 2.6), plasma ketone bodies were higher in LCTα$^{-/-}$ mice than in floxed control mice (Table 2.2) indicating that FA oxidation is enhanced by LCTα-deficiency.

2.3.6 Hepatic inflammation induces non-alcoholic steatohepatitis in CTα-deficient livers

Hepatic mRNAs encoding F4/80 and CD68, two prominent inflammation markers, were both increased in livers of CTα-deficient mice compared to floxed control mice (Figure 2.8A), indicating that CTα-deficient livers develop inflammation after one week of the HF diet. Furthermore, hepatic mRNA encoding NADPH oxidase, an oxidative stress marker, was also increased in livers of CTα-deficient mice, further indicating liver injury (Figure 2.8A). The NADPH oxidase complex is an abundant source of cellular reactive oxygen species generated by inflammatory cells (31,32). Therefore, the up-regulation of hepatic mRNA encoding NADPH oxidase may further indicate the presence of inflammation in CTα-deficient livers.

Hepatic mRNA encoding glucose regulated/immunoglobulin protein 78 (GRP78) (Figure 2.8A), and protein expression of CHOP (figure 2.8B) were unaltered in CTα-deficient livers indicating that ER stress is not the cellular insult contributing to the pathogenesis of NASH in LCTα$^{-/-}$ mice. Furthermore, hepatic mRNA encoding uncoupling protein 2 (UCP2) was unaltered by LCTα-deficiency (Figure 2.8A), while there was a 2-fold decrease in hepatic mRNA encoding cytochrome P450 2E1 (Cyp2E1) (Figure 2.8A). These data suggest that oxidative stress is not involved in

the pathogenesis of NASH in LCTα$^{-/-}$ mice. Additionally, hepatic TBARS, a marker of hepatic lipid peroxidation, was unaltered by LCTα deficiency (Figure 2.9A), while CTα-deficient livers showed a 2-fold increase in hepatic levels of GSH (Figure 2.9B). These data provide further evidence that oxidative stress is not a contributing factor to the pathogenesis of NASH in LCTα$^{-/-}$ mice.

2.4 Discussion

LCTα$^{-/-}$ mice have impaired VLDL secretion and develop mild steatosis when fed a chow diet (7,33). We hypothesized that the reduced VLDL secretion, as a result of impaired PC biosynthesis, would increase the susceptibility of CTα-deficient livers to develop NASH. Therefore, we challenged LCTα$^{-/-}$ mice with the HF diet to determine whether CTα-deficient livers were more sensitive to liver injury. LCTα$^{-/-}$ mice proved to be an attractive model for studies on NASH as liver disease developed within one week of feeding the HF diet as indicated by elevated levels of plasma alanine aminotransferase, increased hepatic gene expression of inflammation markers, and clinical assessment of liver histology which revealed the presence of histological markers associated with NASH. The data presented show that in addition to an impairment of PC biosynthesis, hepatic TG was increased by 75% by LCTα deficiency and plasma TG was reduced by 60% indicating that TG secretion is impaired by LCTα deficiency. These data support previous findings that CTα plays a role in controlling VLDL secretion (7,33). Hence, the hepatic steatosis in LCTα$^{-/-}$ mice could be largely attributed to decreased TG secretion. Many other studies have established a role for impaired TG secretion in the development of hepatic steatosis (14,34-36). For example, liver-specific knockout of microsomal transfer protein results in reduction of TG in VLDL and a reduction in plasma apoB-100 which were accompanied by hepatic

steatosis (35,36). We found that hepatic *de novo* TG synthesis was unchanged by LCTα deficiency indicating that impaired VLDL secretion, rather than increased lipogenesis, underlies the hepatic steatosis in LCTα$^{-/-}$ mice. Furthermore, CTα-deficient livers have altered FA uptake and oxidation in an attempt to eliminate excess hepatic TG, which further underscores the role of impaired VLDL secretion in the development of hepatic steatosis in LCTα$^{-/-}$ mice.

2.4.1 Inflammation contributes to the pathogenesis of non-alcoholic steatohepatitis

As predicted, CTα-deficient livers are more susceptible to the pathogenesis of NASH as a result of imbalanced TG homeostasis. Previous studies have linked systemic inflammation with the development of NASH (37,38). For instance, inflammatory cytokines (interleukin-6, CC-chemokine ligand 2, tumor necrosis factor α) are increased in plasma from patients with NASH compared to control patients (37). In the current study, hepatic gene expression of inflammation markers was significantly increased by LCTα deficiency after one week of HF feeding. These data indicate that systemic inflammation is associated with the pathogenesis of NASH in livers of LCTα$^{-/-}$ mice.

Oxidative stress and ER stress are cellular insults which are also associated with the pathogenesis of NASH (21,22,39,40). However, the ER stress markers, GRP78 and Chop, were not induced in response to LCTα deficiency after one week of HF feeding. Furthermore, hepatic gene expression of UCP2, a protein associated with mitochondrial bioenergetics and oxidative stress (41), was not altered in CTα-deficient livers compared to floxed livers. However, hepatic gene expression of Cyp2E1, a cytochrome P450 protein involved in lipid peroxidation (42), was significantly reduced, while hepatic TBARS was unchanged by LCTα

deficiency. Furthermore, hepatic levels of GSH, an anti-oxidant, were increased in response to LCTα-deficiency. These results indicate that oxidative stress is not induced in the livers of LCTα$^{-/-}$ mice. Together, these data indicate that systemic inflammation is the cellular insult leading to the pathogenesis of NASH in LCTα$^{-/-}$ mice after one week of the HF diet, while ER and oxidative stress are not involved the initial stages of NASH development.

2.4.2 Why does diacylglycerol accumulate?

Both liver-specific knockout and whole-body single allele knockdown of CTP: phosphoethanolamine cytidylyltransferase, a key enzyme involved in PE biosynthesis, decreased hepatic PE levels (43,44). Consequently, hepatic DAG mass was increased rendering it available for increased TG synthesis which might be expected to lead to hepatic steatosis (43,44). Similarly, we show that hepatic DAG accumulates in LCTα$^{-/-}$ mice. I*n vivo* [^{3}H]glycerol labelling of hepatic DAG, TG and phospholipids was unchanged by LCTα deficiency. Since DAG is a substrate for PC, PE and TG biosynthesis, we calculated the sum of [^{3}H]glycerol label incorporated into total hepatic PC, PE, TG and DAG; the incorporation of radiolabel into these glycerolipids was not different between floxed and LCTα$^{-/-}$ mice (floxed: 3428 ± 625.1 dpm/mg protein; LCTα$^{-/-}$: 3393±248.7 dpm/mg protein). This indicates that DAG accumulation does not result from increased DAG synthesis. However, the hepatic accumulation of DAG may result from impaired PC biosynthesis since the CDP-choline pathway utilizes DAG to produce PC.

DAG may accumulate in CTα-deficient livers as a result of increased TG hydrolysis. Both hormone sensitive lipase (HSL) and adipose triglyceride lipase (ATGL) have shown to be involved in hepatic TG hydrolysis in mice (45-47). HSL and ATGL are known target genes of

the transcription factor PPARγ (48,49). Although normally present in low levels in the liver, HSL has been reported to be up-regulated in livers with increased expression of PPARγ (45). Furthermore, ablation of ATGL in mice results in hepatic steatosis (46). Interestingly, hepatic over-expression of HSL or ATGL in *ob/ob* mice, an obese mouse model, ameliorated hepatic steatosis via promotion of FA oxidation (47). In the current study, hepatic gene expression of PPARγ was up-regulated by LCTα-deficiency. In addition, LCTα$^{-/-}$ mice showed enhance FA oxidation. Together, these results suggest that HSL and/or ATGL may be up-regulated in CTα-deficient livers resulting in increased FA oxidation, and elevated levels of hepatic DAG.

2.4.3 Why does ceramide accumulate?

It is currently unknown why ceramide accumulates in response to LCTα-deficiency after HF feeding. Sphingomyelin synthase transfers the phosphocholine head group from PC to ceramide, generating sphingomyelin and DAG (reviewed in (50)). Therefore, reduced levels of hepatic PC in CTα-deficient livers may limit the availability of substrates required for sphingomyelin synthesis, resulting in an accumulation of hepatic ceramide. Another possible mechanism for ceramide accumulation is an increase in *de novo* synthesis of ceramide. Increased synthesis of ceramide via the *de novo* pathway has been implicated in the development of insulin resistance (51). However, hepatic mRNAs encoding subunits of the serine palmitoyltransferase heterodimer (Spt1 and Spt2), the key enzyme responsible for the first step of *de novo* ceramide synthesis (reviewed in (52)), was not altered by LCTα deficiency (Spt1, floxed: 1.00 ± 0.155, LCTα$^{-/-}$: 1.13 ± 0.19; Spt2, Floxed: 1.00 ± 0.16, LCTα$^{-/-}$: 1.314 ± 0.23). Therefore, the accumulation of hepatic ceramide in livers of LCTα$^{-/-}$ mice may not result from increased *de novo* ceramide synthesis. Hepatic ceramide accumulation in CTα-deficient livers may

also result from increased sphingomyelinase activity. Although the significance of hepatic ceramide accumulation in response to LCTα-deficiency is unknown, sphingomyelinase-generated ceramide has been shown to induce apoptosis (53). In addition, analyses of hepatic gene expression in patients with NAFLD have shown a positive correlation between genes involved in ceramide signalling and metabolism and hepatic TG content (54). Therefore, ceramide accumulation in CTα-deficient livers may induce hepatocellular injury leading to the pathogenesis of NASH in CTα-deficient livers.

2.4.4 Conclusion

As depicted in Figure 2.10, hepatic TG accumulation in LCTα$^{-/-}$ mice results from a reduction of TG secretion without a compensatory decrease in *de novo* lipogenesis after 7 days of HF feeding. Additionally, FA uptake and oxidation are altered in response to LCTα-deficiency, possibly in an attempt to prevent excess hepatic TG accumulation. Hepatic TG accumulation increases the sensitivity of CTα-deficient livers towards inflammation resulting in the development of NASH.

Table 2.1 Primer sequences utilized for real-time qPCR. Abbreviations are: FAS (fatty acid synthase); SCD1 (stearoyl-CoA desaturase 1); SREBP1c (sterol regulatory element binding protein 1c); LXRα (liver X receptor alpha); PPARγ (peroxisome proliferator activated receptor γ); DGAT1 and DGAT2 (diacylglycerol acyltransferase 1 and 2); PPARα (peroxisome proliferator activated receptor α); CPT1 (carnitine palmitoyl-CoA acyltransferase); MCAD (medium chain acyl-CoA dehydrogenase); ACOX (acyl-CoA oxidase); FATP 2, 4 and 5 (fatty acid transport protein 2, 4 and 5); LFABP (liver fatty acid binding protein); Cyp2E1(cytochrome P450 2E1); NADPHox (NADPH oxidase); UCP2 (uncoupling protein 2); GRP78 (glucose regulated/immunoglobulin protein 78); Cyc (cyclophilin).

Table 2.1

Gene	Forward Sequence	Reverse sequence
FAS	TTCCGTCACTTCCAGTTAGAG	TTCAGTGAGGCGTAGTAGACA
SCD1	GTTGCCAGTTTCTTTCGTG	GGGAAGCCAAGTTTCTACACA
SREBP1C	ATGGATTGCACATTTGAAGAC	CTCTCAGGAGAGTTGGCACC
LXRα	CAGAAGAACAGATCCGCTTGAAG	TGCAATGGGCCAAGGCGTGAC
PPARγ	TTGACATCAAGCCCTTTACCA	GGTTCTACTTTGATCGCACTTT
DGAT1	GGATCTGAGGTGCCATCGT	CCACCAGGATGCCATACTTG
DGAT2	GGCTACGTTGGCTGGTAACTT	TTCAGGGTGACTGCGTTCTT
PPARα	GACCTGAAAGATTCGGAAACT	CGTCTTCTCGGCCATACAC
CPT1	TGAGTGGCGTCCTCTTTGG	CAGCGAGTAGCGCATAGTCATG
MCAD	TTACCGAAGAGTTGGCGTATG	ATCTTCTGGCCGTTGATAACA
ACOX	GAGCAGGAGAAATGGATGCA	GGGCGTAGGTGCCAATTATCT
FATP2	CGGTCCGTGACGCAAAT	CCTCCAGCATAGCCAATAA
FATP4	CAGCACAGTGCCCGTCA	GTGGTGCCCGATGTGTAGATG
FATP5	GTTCTCTGCCTCCCGATTCTG	TGGCCAAGCGCACTGTATGTA
LFABP	CAGAAAGGGAAGGACATCAAG	TGGTCTCCAGTTCGCACTC
CD68	GCGGCTCCCTGTGTGTCTGAT	GGGCCTGTGGCTGGTCGTAG
F4/80	CCCTGCGGCTGTGAGATTGTG	TGGCCAAGGCAAGACATACCAG
Cyp2E1	GGTAATGAGGCCCGCATCCA	AGAGAATATCCGCAATGACA
NADPHox	GACTGGACGGAGGGGCTAT	ACTTGAGAATGGAGGCAAAGG
UCP2	GATTGGCCTCTACGACTCTG	GCCTGGAAGCGGACCTTTAC
Grp78	GAGGATGTGGGCACGGTGGT	CCCTGATCGTTGGCTATGAT
CYC	TTCAAAGACAGCAGAAAACTTTCG	TCTTCTTGCTGGTCTTGCCATTCC

Body Parameters	**Floxed**	**LCTα$^{-/-}$**
Body weight (g)	19.0± 0.96	18.4 ± 0.81
Liver weight (g)	0.79 ± 0.03	1.01 ± 0.07*
Liver/body (% b.w.)	4.2 ± 0.17	5.5 ± 0.22*
Blood/Plasma	**Floxed**	**LCTα$^{-/-}$**
ALT (U/L)	12.2 ± 5.2	84.7 ± 16.5*
Triacylglycerol (µg/ml)	280.9 ± 55.8	87.1 ± 26.9*
NEFA (µM)	270.7 ± 19.3	103.5 ± 28.9*
Ketone Bodies (µM)	123.2 ± 37.5	306.6 ± 31.7*
GTT (AUC)	1543 ± 251	1204 ± 164
ITT (AUC)	408 ± 42.6	317 ± 17
PTT (AUC)	871 ± 79.7	826 ± 62.4

Table 2.2 Plasma parameters following one week of a high fat diet. Floxed and liver-specific CTα (LCTα$^{-/-}$) knockout mice were fed a high fat diet for 7 days. ALT, alanine aminotransferase; NEFA, non-esterified fatty acids; GTT, glucose tolerance test; ITT, insulin tolerance test; PTT, pyruvate tolerance test; AUC, area under curve; b.w., body weight. Values are means ± S.E. *, $p < 0.05$

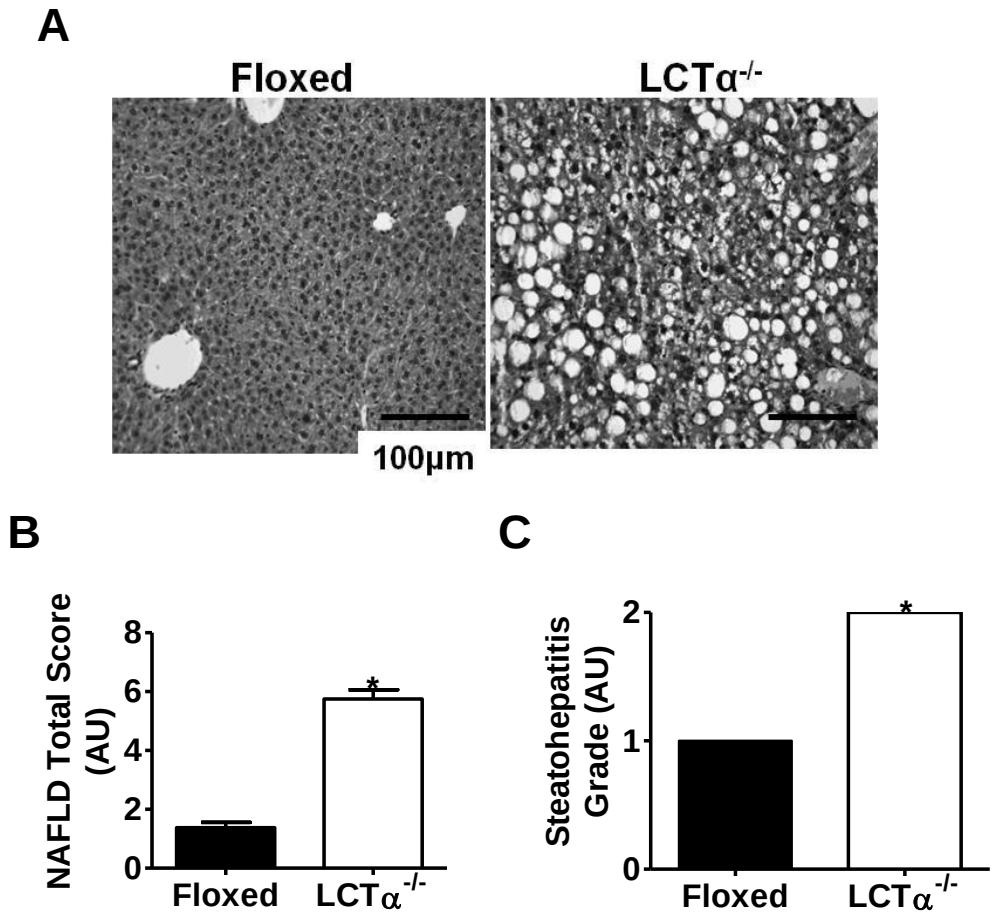

Figure 2.1 Livers from hepatic CTα deficient mice develop steatohepatitis when fed the high fat diet. (A) Liver samples from floxed and liver-specific CTα knockout ($LCT\alpha^{-/-}$) mice were fixed in 10% buffered formalin and stained with hematoxylin and eosin (n=8). A typical picture of each genotype is displayed. (B) Hematoxylin and eosin stained liver histology samples were analyzed by a clinical pathologist for the presence of NAFLD according to the level of steatosis, inflammation and hepatocyte ballooning. The total score for NAFLD was determined from the scores given for each histological legions associated with NAFLD (n=8). (C) The grade of steatohepatitis was pathologically determined from the total score of NAFLD (n=8). All data points were the same for histological data which contain no error bars. All data are means ± S.E. *, $p < 0.05$

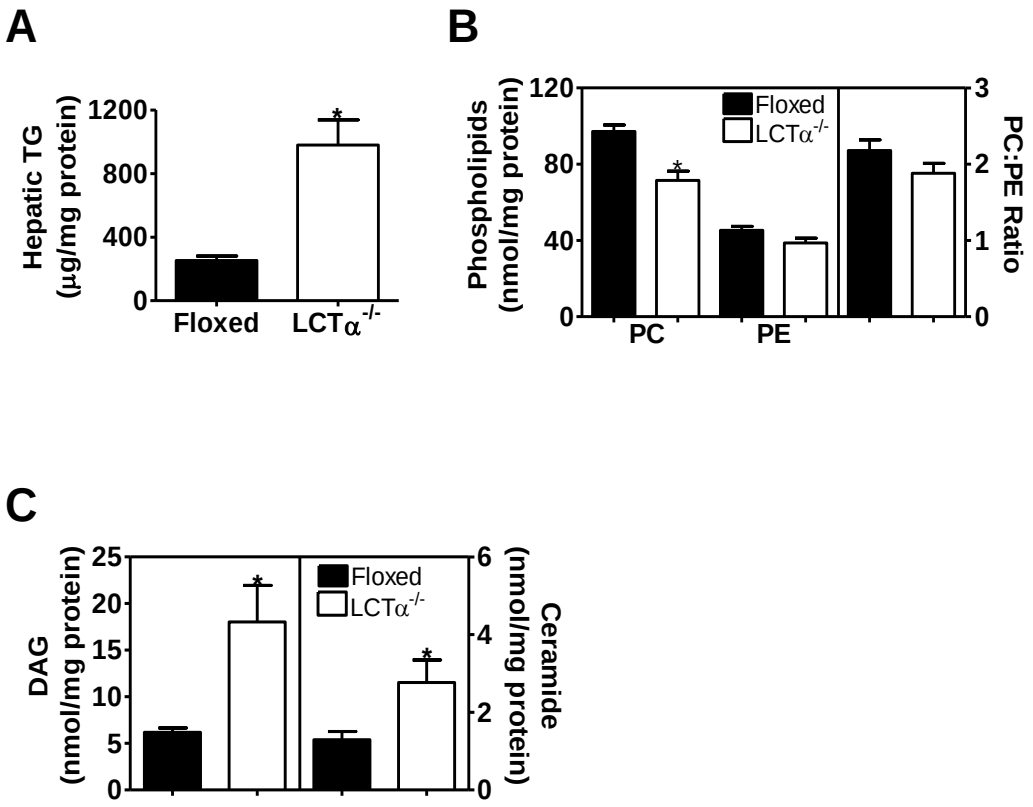

Figure 2.2 Hepatic lipids are altered by LCTα deficiency. Livers were collected from high fat-fed floxed and LCTα$^{-/-}$ mice after an overnight fast. (A) Quantitation of hepatic triacylglycerol (TG) (n=8). (B) The amounts of hepatic phosphatidylcholine (PC) and phosphatidylethanolamine (PE) were quantified by phosphorus assay. The PC:PE ratio was determined from the hepatic mass of PC and PE (n=7). (C) Hepatic diacylglycerol (DAG) and ceramide levels were quantified via a DAG kinase assay (n=5). All data are means ± S.E. *, $p < 0.05$

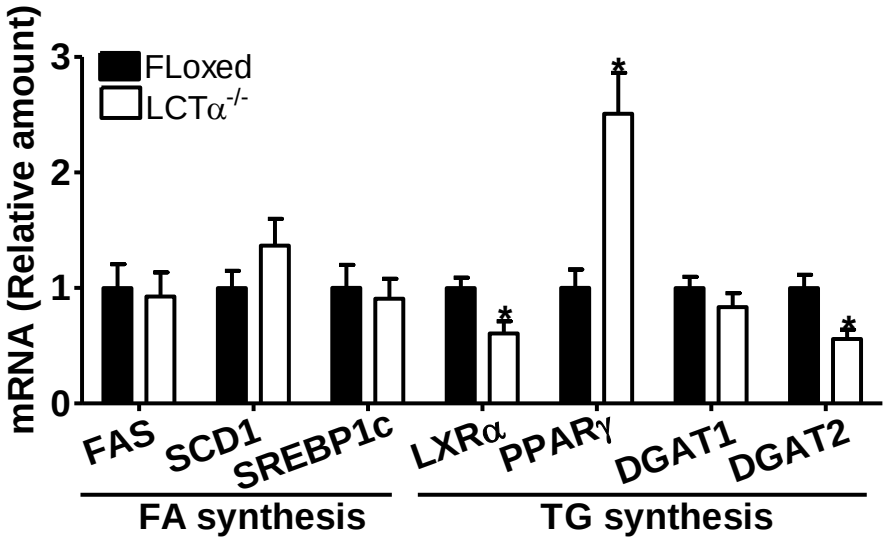

Figure 2.3 Hepatic genes involved in lipogenesis are unaltered by LCTα deficiency. Hepatic mRNA was isolated from fasted high fat-fed floxed and LCTα$^{-/-}$ mice. Relative mRNA levels were determined by real-time qPCR relative to cyclophilin mRNA. Hepatic genes encoding fatty acid synthesis and TG synthesis: FAS (fatty acid synthase); SCD1 (stearoyl-CoA desaturase 1); SREBP1c (sterol regulatory element binding protein 1c); LXRα (liver X receptor α); PPARγ (peroxisome proliferator activated receptor γ); DGAT1 and DGAT2 (diacylglycerol acyltransferase 1 and 2) (n=7 to 8). All data are means ± S.E. *, $p < 0.05$

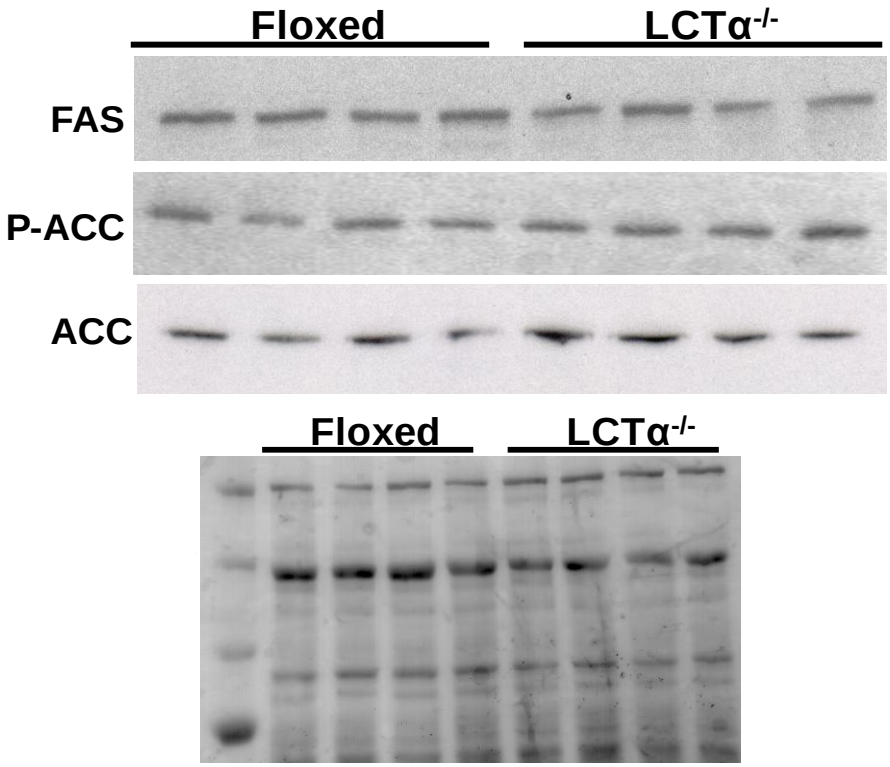

Figure 2.4 Hepatic proteins involved in lipogenesis are unaltered by LCTα deficiency. Amounts of hepatic FAS (Fatty acid synthase), p-ACC (phosphorylated acetyl-CoA carboxylase) and total ACC proteins were assessed by immunoblotting (left panel). To assess equal loading of protein, transfer membrane was stained with Ponceau S (right panel). A typical immunoblot is displayed (n=8).

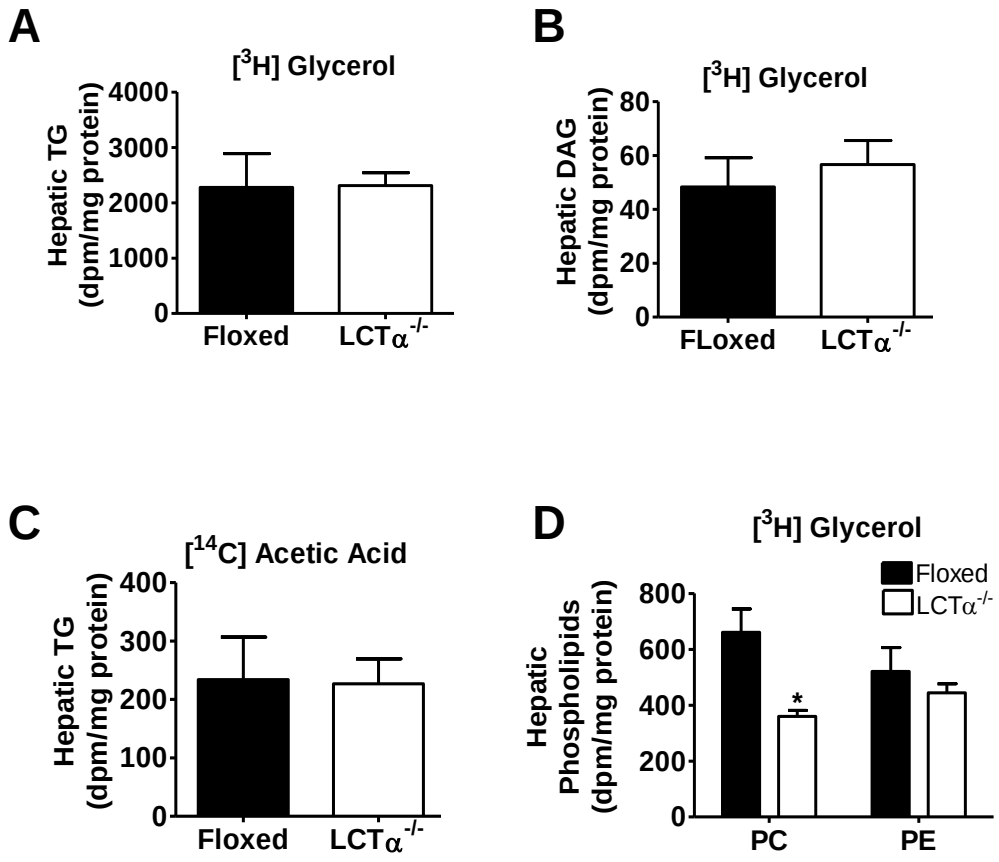

Figure 2.5 Hepatic lipogenesis is unaltered by LCTα deficiency. Floxed and LCTα$^{-/-}$ mice were fed the high fat diet for 7 days. After an overnight fast, lipogenesis was measured. Floxed and LCTα$^{-/-}$ mice were injected intraperitoneally with 10 µCi [^{3}H]glycerol and 10 µCi of [^{14}C]acetic acid. After 2 h, livers were collected and [^{3}H]glycerol or [^{14}C]acetic acid incorporation into hepatic lipids were quantified. (A,B) Incorporation of [^{3}H]glycerol into hepatic triacylglycerol (TG), and diacylglycerol (DAG) (n=5 to 7). (C) Incorporation of [^{14}C]acetic acid into hepatic TG (n=5 to 7). (D) Incorporation of [^{3}H]glycerol into phosphatidylcholine (PC) and phosphatidylethanolamine (PE) was measured (n=5 to 7). All data are means ± S.E. *, $p < 0.05$.

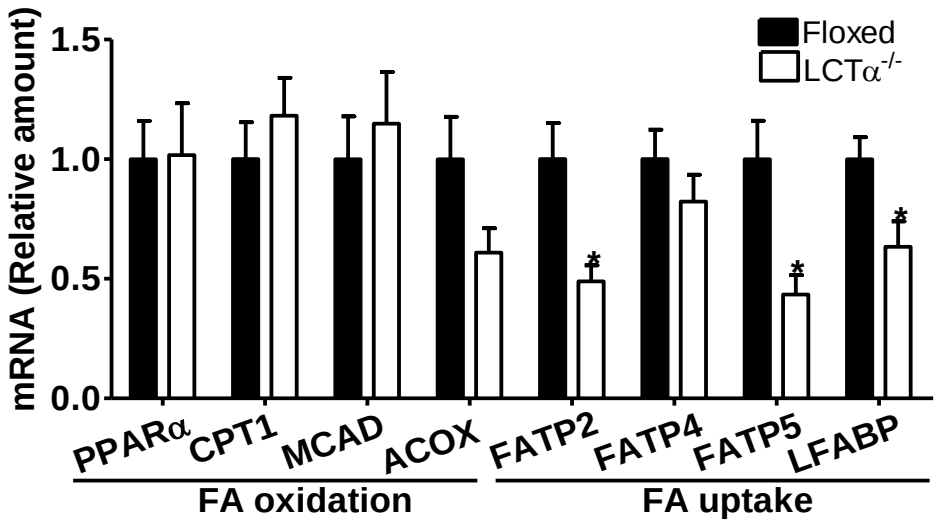

Figure 2.6 Hepatic genes involved in fatty acid uptake and oxidation. Hepatic mRNA was isolated from fasted high fat-fed floxed and LCTα$^{-/-}$ mice. Relative mRNA levels were determined by real-time qPCR relative to cyclophilin mRNA. Hepatic mRNAs involved in fatty acid oxidation and uptake: PPARα (peroxisome proliferator activated receptor alpha); CPT1 (carnitine palmitoyl-CoA acyltransferase); MCAD (medium chain acyl-CoA dehydrogenase); ACOX (acyl-CoA oxidase); FATP 2, 4 and 5 (fatty acid transport protein 2, 4 and 5); LFABP (liver fatty acid binding protein) (n=7 to 8). All data are means ± S.E. *, $p < 0.05$.

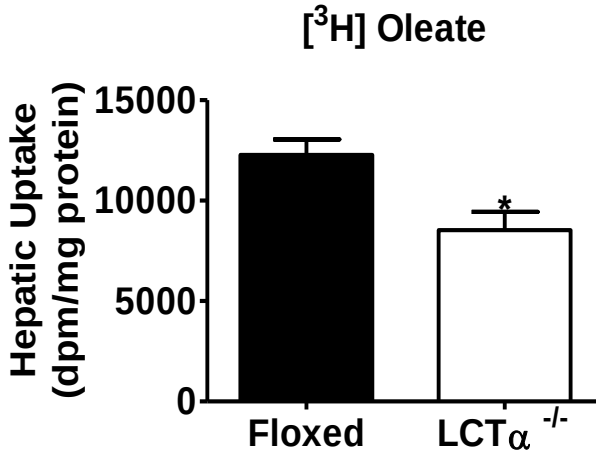

Figure 2.7 Hepatic fatty acid uptake is altered by LCTα deficiency. Floxed and LCTα$^{-/-}$ mice were fed the high fat diet for 7 days. After an overnight fast, fatty acid uptake was measured. Floxed and LCTα$^{-/-}$ mice were injected intravenously with 10 µCi [^{3}H]oleic acid. After 30 min, livers were collected and radiolabel was quantified in liver homogenates (measure of fatty acid uptake by the liver) (n=4 to 5). All data are means ± S.E. *, $p < 0.05$.

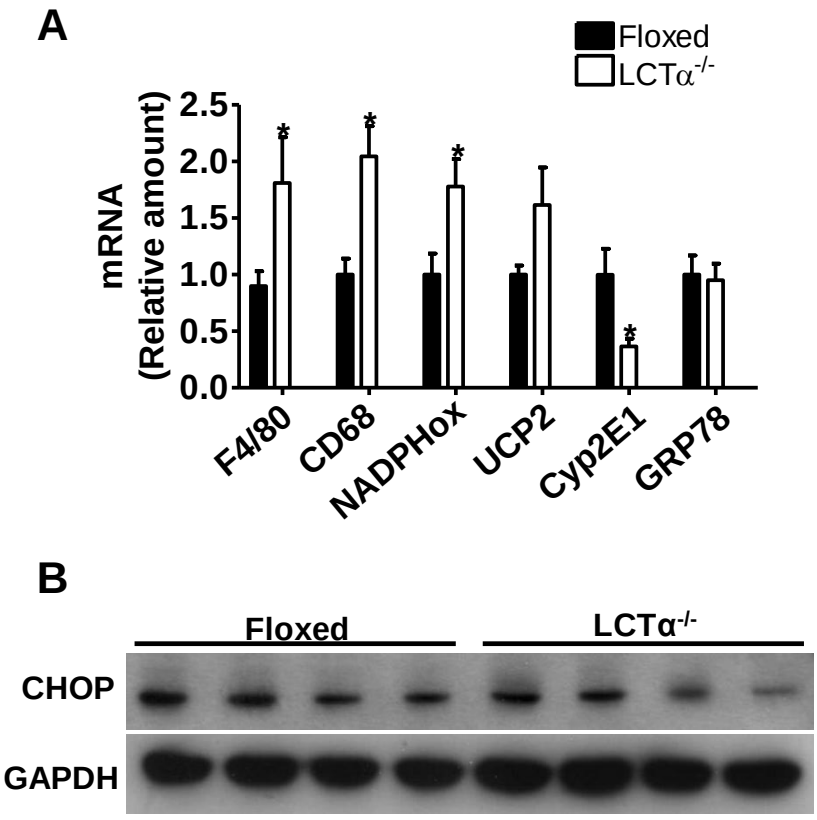

Figure 2.8 Inflammation contributes to non-alcoholic steatohepatitis in CTα-deficient livers. (A) Relative levels of mRNAs encoding genes involved in inflammation (CD68 and F4/80), oxidative stress (NADPHox, NADPH oxidase, UCP2, uncoupling protein 2, and Cyp2E1, cytochrome P450 2E1), and ER stress (GRP78, glucose regulated/immunoglobulin protein 78) were quantified by real-time PCR relative to cyclophilin mRNA (n=7 to 8). (B) Amounts of hepatic CHOP (CCAAT/ -enhancer-binding protein homologous protein) and GAPDH (glyceraldehyde 3-phosphate dehydrogenase) were assessed by immunoblotting. A typical immunoblot is displayed (n=8). All data are means ± S.E. *, $p < 0.05$.

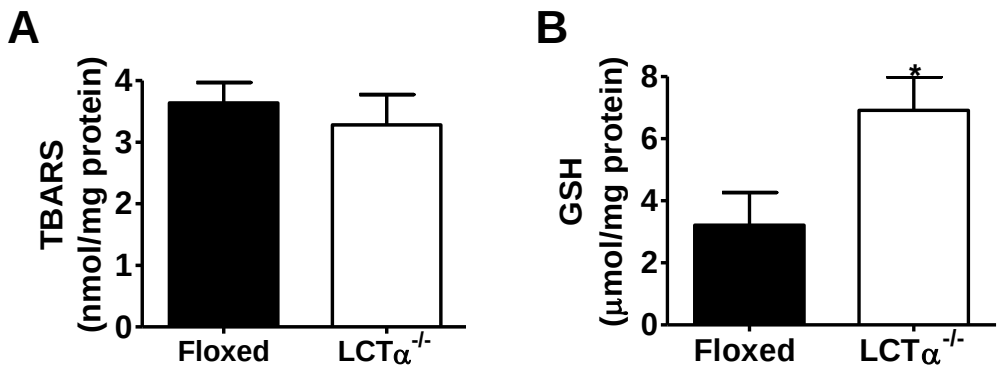

Figure 2.9 Oxidative stress does not contribute to non-alcoholic steatohepatitis in CTα-deficient livers. (A) Hepatic thiobarbituric acid reactive substances (TBARS) were quantified in floxed and LCTα-deficient livers after 7 days of the high fat diet (n=5). (B) Hepatic reduced glutathione (GSH) levels were quantified in floxed and LCTα-deficient livers after 7 days of the high fat diet (n=4). All data are means ± S.E. *, $p < 0.05$.

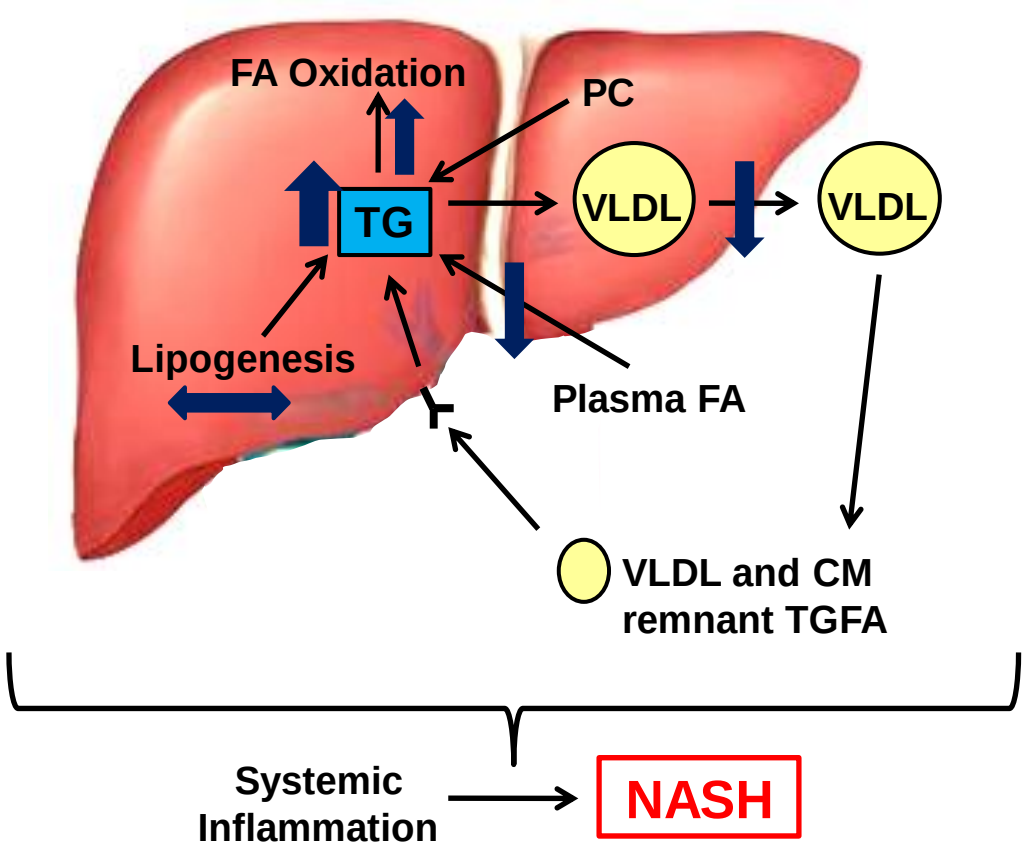

Figure 2.10 Schematic representation of altered hepatic triacylglycerol homeostasis in CTα-deficient livers. Hepatic triacylglycerol (TG) homeostasis is maintained through a balance between: delivery of plasma free fatty acids (FA) and FA from TG within the remnant lipoprotein particles; *de novo* synthesis of FA via lipogenesis; oxidation of FA; the assembly and secretion of TG in the form of very-low-density lipoproteins (VLDL); and the conversion of phosphatidylcholine (PC) to TG. However, hepatic TG accumulation in LCTα$^{-/-}$ mice results from impaired VLDL secretion without a compensatory reduction in *de novo* lipogenesis. FA uptake is reduced, while FA oxidation is increased in response to LCTα-deficiency. The imbalance of hepatic TG homeostasis in livers of LCTα$^{-/-}$ mice increases the livers sensitivity towards systemic inflammation which contributes to the pathogenesis of NASH (non-alcoholic steatohepatitis).

2.5 References

1. Kennedy, E. P., and Weiss, S. B. (1956) *J Biol Chem* **222**, 193-214

2. Vance DE and Vance JE (2008) Phospholipid biosynthesis in eukaryotes. in *Biochemistry of Lipids, Lipoproteins, and Membranes, 5th Edition* (Vance DE and Vance JE ed.), Elsevier, Amsterdam. pp 213-244

3. Karim, M., Jackson, P., and Jackowski, S. (2003) *Biochim Biophys Acta* **1633**, 1-12

4. Vance, D. E., and Ridgway, N. D. (1988) *Prog Lipid Res* **27**, 61-79

5. Noga, A. A., Zhao, Y., and Vance, D. E. (2002) *J Biol Chem* **277**, 42358-42365

6. Noga, A. A., and Vance, D. E. (2003) *J Biol Chem* **278**, 21851-21859

7. Jacobs, R. L., Devlin, C., Tabas, I., and Vance, D. E. (2004) *J Biol Chem* **279**, 47402-47410

8. Angulo, P. (2002) *N Engl J Med* **346**, 1221-1231

9. Browning, J. D., and Horton, J. D. (2004) *J Clin Invest* **114**, 147-152

10. Yeh, M. M., and Brunt, E. M. (2007) *Am J Clin Pathol* **128**, 837-847

11. Day, C. P., and James, O. F. (1998) *Gastroenterology* **114**, 842-845

12. Musso, G., Gambino, R., and Cassader, M. (2009) *Prog Lipid Res* **48**, 1-26

13. Donnelly, K. L., Smith, C. I., Schwarzenberg, S. J., Jessurun, J., Boldt, M. D., and Parks, E. J. (2005) *J Clin Invest* **115**, 1343-1351

14. Fujita, K., Nozaki, Y., Wada, K., Yoneda, M., Fujimoto, Y., Fujitake, M., Endo, H., Takahashi, H., Inamori, M., Kobayashi, N., Kirikoshi, H., Kubota, K., Saito, S., and Nakajima, A. (2009) *Hepatology* **50**, 772-780

15. Moon, Y. A., Hammer, R. E., and Horton, J. D. (2009) *J Lipid Res* **50**, 412-423

16. Shimomura, I., Bashmakov, Y., and Horton, J. D. (1999) *J Biol Chem* **274**, 30028-30032

17. Shimomura, I., Matsuda, M., Hammer, R. E., Bashmakov, Y., Brown, M. S., and Goldstein, J. L. (2000) *Mol Cell* **6**, 77-86

18. Feldstein, A. E., Canbay, A., Angulo, P., Taniai, M., Burgart, L. J., Lindor, K. D., and Gores, G. J. (2003) *Gastroenterology* **125**, 437-443

19. Feldstein, A. E., Werneburg, N. W., Canbay, A., Guicciardi, M. E., Bronk, S. F., Rydzewski, R., Burgart, L. J., and Gores, G. J. (2004) *Hepatology* **40**, 185-194

20. Caballero, F., Fernandez, A., Matias, N., Martinez, L., Fucho, R., Elena, M., Caballeria, J., Morales, A., Fernandez-Checa, J. C., and Garcia-Ruiz, C. (2010) *J Biol Chem* **285**, 18528-18536

21. Mari, M., Caballero, F., Colell, A., Morales, A., Caballeria, J., Fernandez, A., Enrich, C., Fernandez-Checa, J. C., and Garcia-Ruiz, C. (2006) *Cell Metab* **4**, 185-198

22. Ota, T., Gayet, C., and Ginsberg, H. N. (2008) *J Clin Invest* **118**, 316-332

23. Wang, D., Wei, Y., and Pagliassotti, M. J. (2006) *Endocrinology* **147**, 943-951

24. Brunt, E. M., Janney, C. G., Di Bisceglie, A. M., Neuschwander-Tetri, B. A., and Bacon, B. R. (1999) *Am J Gastroenterol* **94**, 2467-2474

25. Folch, J., Lees, M., and Sloane Stanley, G. H. (1957) *J Biol Chem* **226**, 497-509

26. Zhou, X., and Arthur, G. (1992) *J Lipid Res* **33**, 1233-1236

27. Modrak, D. E. (2005) *Methods Mol Med* **111**, 183-194

28. Li, Z., Agellon, L. B., Allen, T. M., Umeda, M., Jewell, L., Mason, A., and Vance, D. E. (2006) *Cell Metab* **3**, 321-331

29. Erion, D. M., and Shulman, G. I. (2010) *Nat Med* **16**, 400-402

30. Summers, S. A. (2006) *Prog Lipid Res* **45**, 42-72

31. Pollock, J. D., Williams, D. A., Gifford, M. A., Li, L. L., Du, X., Fisherman, J., Orkin, S. H., Doerschuk, C. M., and Dinauer, M. C. (1995) *Nat Genet* **9**, 202-209

32. Segal, B. H., Leto, T. L., Gallin, J. I., Malech, H. L., and Holland, S. M. (2000) *Medicine (Baltimore)* **79**, 170-200

33. Jacobs, R. L., Lingrell, S., Zhao, Y., Francis, G. A., and Vance, D. E. (2008) *J Biol Chem* **283**, 2147-2155

34. Mensenkamp, A. R., Havekes, L. M., Romijn, J. A., and Kuipers, F. (2001) *J Hepatol* **35**, 816-822

35. Minehira, K., Young, S. G., Villanueva, C. J., Yetukuri, L., Oresic, M., Hellerstein, M. K., Farese, R. V., Jr., Horton, J. D., Preitner, F., Thorens, B., and Tappy, L. (2008) *J Lipid Res* **49**, 2038-2044

36. Raabe, M., Veniant, M. M., Sullivan, M. A., Zlot, C. H., Bjorkegren, J., Nielsen, L. B., Wong, J. S., Hamilton, R. L., and Young, S. G. (1999) *J Clin Invest* **103**, 1287-1298

37. Haukeland, J. W., Damas, J. K., Konopski, Z., Loberg, E. M., Haaland, T., Goverud, I., Torjesen, P. A., Birkeland, K., Bjoro, K., and Aukrust, P. (2006) *J Hepatol* **44**, 1167-1174

38. dela Pena, A., Leclercq, I. A., Williams, J., and Farrell, G. C. (2007) *J Hepatol* **46**, 304-313

39. Oyadomari, S., Harding, H. P., Zhang, Y., Oyadomari, M., and Ron, D. (2008) *Cell Metab* **7**, 520-532

40. Vendemiale, G., Grattagliano, I., Caraceni, P., Caraccio, G., Domenicali, M., Dall'Agata, M., Trevisani, F., Guerrieri, F., Bernardi, M., and Altomare, E. (2001) *Hepatology* **33**, 808-815

41. Baffy, G. (2005) *Front Biosci* **10**, 2082-2096

42. Leclercq, I. A., Farrell, G. C., Field, J., Bell, D. R., Gonzalez, F. J., and Robertson, G. R. (2000) *J Clin Invest* **105**, 1067-1075

43. Fullerton, M. D., Hakimuddin, F., Bonen, A., and Bakovic, M. (2009) *J Biol Chem* **284**, 25704-25713

44. Leonardi, R., Frank, M. W., Jackson, P. D., Rock, C. O., and Jackowski, S. (2009) *J Biol Chem* **284**, 27077-27089

45. Yu, S., Matsusue, K., Kashireddy, P., Cao, W. Q., Yeldandi, V., Yeldandi, A. V., Rao, M. S., Gonzalez, F. J., and Reddy, J. K. (2003) *J Biol Chem* **278**, 498-505

46. Haemmerle, G., Lass, A., Zimmermann, R., Gorkiewicz, G., Meyer, C., Rozman, J., Heldmaier, G., Maier, R., Theussl, C., Eder, S., Kratky, D., Wagner, E. F., Klingenspor, M., Hoefler, G., and Zechner, R. (2006) *Science* **312**, 734-737

47. Reid, B. N., Ables, G. P., Otlivanchik, O. A., Schoiswohl, G., Zechner, R., Blaner, W. S., Goldberg, I. J., Schwabe, R. F., Chua, S. C., Jr., and Huang, L. S. (2008) *J Biol Chem* **283**, 13087-13099

48. Deng, T., Shan, S., Li, P. P., Shen, Z. F., Lu, X. P., Cheng, J., and Ning, Z. Q. (2006) *Endocrinology* **147**, 875-884

49. Kershaw, E. E., Schupp, M., Guan, H. P., Gardner, N. P., Lazar, M. A., and Flier, J. S. (2007) *Am J Physiol Endocrinol Metab* **293**, E1736-1745

50. Futerman, A. H., and Riezman, H. (2005) *Trends Cell Biol* **15**, 312-318

51. Holland, W. L., Brozinick, J. T., Wang, L. P., Hawkins, E. D., Sargent, K. M., Liu, Y., Narra, K., Hoehn, K. L., Knotts, T. A., Siesky, A., Nelson, D. H., Karathanasis, S. K., Fontenot, G. K., Birnbaum, M. J., and Summers, S. A. (2007) *Cell Metab* **5**, 167-179

52. Hanada, K. (2003) *Biochim Biophys Acta* **1632**, 16-30

53. Jana, A., and Pahan, K. (2004) *J Biol Chem* **279**, 51451-51459

54. Greco, D., Kotronen, A., Westerbacka, J., Puig, O., Arkkila, P., Kiviluoto, T., Laitinen, S., Kolak, M., Fisher, R. M., Hamsten, A., Auvinen, P., and Yki-Jarvinen, H. (2008) *Am J Physiol Gastrointest Liver Physiol* **294**, G1281-1287

CHAPTER 3

Phosphatidylcholine protects against steatosis in mice but not non-alcoholic steatohepatitis

3.1 Introduction

Non-alcoholic fatty liver disease (NAFLD) encompasses a wide spectrum of liver damage including steatosis, non-alcoholic steatohepatitis (NASH), fibrosis and cirrhosis. The prevalence of NAFLD in the general population in North America is 10-24%, and is 25-75% in the obese and diabetic population (1-3). The progression from steatosis to NASH has been described as a "two-hit" model in which the "first hit" constitutes hepatic triacylglycerol (TG) accumulation and the "second hit" involves cellular stresses causing inflammation and apoptosis (4). However, cellular determinants responsible for the pathogenesis of NASH from steatosis are relatively unknown.

One of the most commonly used nutritional models for studying NASH is a diet deficient in both methionine and choline (MCD). A choline-deficient diet is sufficient to induce hepatic steatosis due to impaired secretion of very-low-density lipoproteins (VLDL) particles, a consequence of impaired phosphatidylcholine (PC) biosynthesis (5). Recent evidence demonstrated that mice fed a choline-deficient diet develop hepatic steatosis without the transition to NASH (6,7). A diet deficient in both methionine and choline is required for the development of NASH in mouse livers (6,7). The MCD diet induces histological characteristics of NASH including steatosis, inflammation, and fibrosis. In response to the MCD diet, steatosis is also associated with reduced VLDL secretion, as a result of reduced PC biosynthesis (8,9). Clearly, impaired PC biosynthesis results in hepatic steatosis due to reduced VLDL secretion. However, aside from its role in VLDL secretion, it is unknown whether impaired PC biosynthesis plays a direct role in the pathogenesis of NASH.

In all nucleated cells, PC is made via the CDP-choline pathway and flux through this pathway is regulated by CTP:phosphocholine cytidylyltransferase (CT) (10,11). Although two isoforms of CT exist (CTα and CTβ), CTα is believed to be the predominant isoform in the liver (12). In the liver, PC can also be made via the phosphatidylethanolamine *N*-methyltransferase (PEMT) pathway in which PC is synthesized from sequential methylation reactions of phosphatidylethanolamine (PE) (13).

To understand the role of PC biosynthesis in controlling VLDL secretion, mice deficient in either PEMT or hepatic CTα were generated. Studies on *Pemt*$^{-/-}$ mice demonstrated that normal VLDL secretion requires PEMT, and that disruption of this pathway causes hepatic steatosis (14,15). CTα is also important for hepatic VLDL metabolism since liver-specific CTα knockout (LCTα$^{-/-}$) mice have impaired apoB-100 secretion (16). Furthermore, on a chow diet hepatic PC in LCTα$^{-/-}$ mice was 5-20% lower, and TG was 25-40% higher, than in LCTα$^{+/+}$ mice (16). These data demonstrate the importance of CTα in controlling hepatic VLDL secretion.

As indicated, the MCD diet impairs PC biosynthesis suggesting that impaired PC biosynthesis is a potential determinant in the pathogenesis of NASH. A recent lipidomic analysis has shown that hepatic PC is reduced by 25% in patients with steatosis compared with control patients; there was also a trend of decreased hepatic PC in NASH livers (17). In addition, a functional polymorphism (V175M substitution) within the *Pemt* gene is associated with NAFLD in humans (18). This polymorphism decreased the specific activity of PEMT when expressed in hepatoma cells and increased the susceptibility of patients to NAFLD (18). Furthermore, mRNA expression of CTα is reduced in NASH patients compared to patients without hepatic steatosis (19). These studies suggest that impaired hepatic PC homeostasis is a potential determinant of NASH in humans. Therefore, we challenged LCTα$^{-/-}$ mice with a high fat (HF) diet to determine whether or not impaired PC biosynthesis

contributes to the pathogenesis of NASH. If impaired PC biosynthesis is a determining factor in the pathogenesis of NASH, then restoring hepatic PC mass should attenuate the development of NASH induced by LCTα deficiency. To restore hepatic PC content, LCTα$^{-/-}$ mice were treated with a daily injection of cytidine 5'-diphosphocholine (CDP-choline) or lysophosphatidylcholine (LPC) (to bypass the CTα deficiency), or fed betaine or choline in the HF diet (to supply methyl groups for the PEMT pathway), all of which should be incorporated into hepatic PC. Furthermore, we hypothesized that adenoviral delivery of CTα would increase hepatic PC mass and prevent the development of NASH in CTα-deficient livers. However, the results show that impaired PC biosynthesis is not the only determinant of NASH in LCTα$^{-/-}$ mice.

3.2 Experimental Procedures

The following methods were described in Chapter 2: histology and assessment of non-alcoholic fatty liver disease and quantification of hepatic and plasma lipids and determination of plasma alanine aminotransferase.

3.2.1 Animal handling and diets

All procedures were approved by the University of Alberta's Institutional Animal Care Committee in accordance with guidelines of the Canadian Council on Animal Care. Female C57BL/6:129P2 floxed (control) and LCTα$^{-/-}$ mice (2-4 months old) (16) were fed the HF diet (Bioserve, #F3282) for 7 days. In some experiments, the HF diet was supplemented with 1% betaine (w/w) or with choline (2.7g choline/kg HF diet), and the mice were fed the diet for 7 days. For the CDP-choline experiment, mice were given the HF diet for 7 days together with a daily

intraperitoneal injection of either 150 µL of sterilized saline or 1 mg of CDP-choline/kg body weight (delivered in 150 µL of sterilized saline). For the LPC experiment, mice were given the HF diet for 7 days together with a daily intraperitoneal injection of either 150 µL of sterilized saline or 50 µM of LPC/kg body weight (delivered in 150 µL of sterilized saline). For all experiments, the mice were fasted for 12 h before collection of blood by cardiac puncture. Plasma was stored at -80ºC. Liver samples were freeze clamped and stored at -80ºC.

3.2.2 In vivo radiolabelling

Floxed and LCTα$^{-/-}$ mice were fed the HF diet for 7 days followed by a 12 h fast. The mice received an intraperitoneal injection of 100 µL of sterile saline containing 2.5 µCi of [^{3}H]choline (0.042 nmole) and 1 µCi of CDP-[^{14}C]choline (0.02 µmole) with 250 µM of choline chloride and 250 µM of CDP-choline. Livers were collected 4 h post-injection. Lipids were extracted from liver homogenates (5 mg of protein) as described above. Phospholipids were separated by thin-layer chromatography in chloroform:methanol:acetic acid: water (25:15:4:2, v/v). The bands corresponding to PC were scraped and radioactivity was determined. The aqueous phase was first dried under constant air flow and aqueous metabolites were separated by thin-layer chromatography in methanol:0.6% NaCl:ammonium hydroxide (10:10:0.9, v/v). Bands corresponding to choline, phosphocholine, betaine and CDP-choline were scraped and radioactivity was determined.

3.2.3 Adenoviral expression of CTP:phosphocholine cytidylyltransferase-α

Recombinant adenovirus encoding an HA-tagged CTα was propagated as previously described (20). A singled dose of adenoviruses (3×10^9 plaque-forming units) expressing GFP (Ad. GFP) or GFP together with HA-CTα (Ad.CTα) were injected into floxed or LCTα$^{-/-}$ mice via the tail vein. The mice were fed the HF diet for 7 days and after a 12 h fast, liver and plasma samples were collected.

To determine ectopic expression of CTα, total CT activity was measured from liver homogenates (25µg of protein) which express either GFP or HA-CTα by monitoring conversion of [^{3}H]phosphocholine into CDP-choline as previously described (21). Expression of GFP, and HA-CTα protein was assessed via immunoblotting using antibodies immunoreactive towards HA (dilution 1:5000), GFP (dilution 1:5000) and PDI, protein disulfide isomerase (dilution 1:5000). Immunoreactive bands were visualized by enhanced chemiluminescence (Amersham Biosciences)

Hepatic lipids were extracted from liver homogenates (1 mg of protein), and mass of PC, PE, TG DAG and ceramide were quantified as described above. Plasma TG content was quantified from 10 µl of plasma using a commercially available kit (Roche Diagnostics).

3.2.6 Statistical analysis

Data are means ± standard error of the mean (S.E.). Comparisons between two groups were performed using a two-way *t* test. Comparisons among multiple groups were performed via one-way ANOVA. In all cases, $p < 0.05$ was considered significant. Four to eight mice were used per experimental group.

3.3 Results

3.3.1 Normalizing the amount of hepatic phosphatidylcholine does not prevent non-alcoholic steatohepatitis

After one week of HF feeding, LCTα$^{-/-}$ mice develop moderate NASH as indicated by the histological presence of steatosis, inflammation and hepatocyte ballooning degeneration, pathological markers of NASH (Figure 3.1). We hypothesized that reduced hepatic PC content, as a result of impaired PC biosynthesis, is the determining factor in the pathogenesis of NASH in LCTα$^{-/-}$ mice. Thus, increasing hepatic PC should prevent the development of NASH in CTα-deficient livers. In an attempt to prevent NASH, and increase hepatic PC, LCTα$^{-/-}$ mice were fed the HF diet and administered a daily injection of CDP-choline. Since the conversion of CDP-choline to PC is independent of CT activity, we hypothesized treatment with CDP-choline would prevent NASH. First, floxed and LCTα$^{-/-}$ mice were injected with CDP-[^{14}C]choline to analyze whether choline derived from CDP-choline could be incorporated into hepatic PC. For comparison, floxed and LCTα$^{-/-}$ mice were also injected with [^{3}H]choline. As shown in figure 3.2A, choline derived from CDP-choline is incorporated into hepatic PC in LCTα$^{-/-}$ and floxed mice. Incorporation of [^{3}H]choline into hepatic PC was significantly lower in LCTα$^{-/-}$ mice compared with floxed mice (Figure 3.2A), confirming that hepatic PC biosynthesis is impaired by LCTα-deficiency. Curiously, incorporation of CDP-[^{14}C]choline into PC was also reduced by LCTα deficiency (Figure 3.2A) even though CDP-choline may be incorporated into hepatic PC via the last step of the CDP-choline pathway, independently of CTα. Therefore, these results suggest that CDP-choline may be metabolized to its intermediates prior to incorporation into hepatic PC. However, significantly more CDP-[^{14}C]choline than [^{3}H]choline was recovered in CDP-choline in both floxed and LCTα$^{-/-}$ mice (Figure 3.2B), while recovery of CDP-[^{14}C]choline and [^{3}H]choline in phosphocholine

was similar (Figure 3.2B). These results indicate that CDP-choline is not entirely metabolized and may be incorporated into hepatic PC independently of CTα. That CDP-[^{14}C]choline incorporated into hepatic PC was reduced by LCTα deficiency may suggest that the amount of CDP-[^{14}C]choline injected into the mice was not sufficient to restore PC biosynthesis in LCTα$^{-/-}$ mice. Together, this data shows that choline derived from CDP-choline is incorporated into hepatic PC in LCTα$^{-/-}$ mice.

Daily injection of CDP-choline for 7 days normalized the mass of PC (Figure 3.3A) and DAG (Figure 3.3B) to that in the floxed controls, but only partially reduced hepatic TG mass in CTα-deficient livers (Figure 3.3C). Partial prevention of hepatic steatosis in CTα-deficient livers was unlikely the result of increased TG secretion as plasma TG levels were not normalized with CDP-choline (Figure 3.3D). Administration of CDP-choline did not normalize the amount of hepatic ceramide (Figure 3.3B). Furthermore, despite normalization of the amount of hepatic PC (Figure 3.3A), clinical assessment of liver histology revealed that CDP-choline did not attenuate NASH in LCTα$^{-/-}$ mice (Figure 3.4A). In addition, hepatic mRNA encoding CD68, an inflammation marker, and NADPH oxidase, an oxidative stress marker, were not normalized by CDP-choline further indicating that CDP-choline did not prevent liver injury in LCTα$^{-/-}$ mice (Figure 3.4B).

As an alternative method for preventing NASH in LCTα$^{-/-}$ mice, the mice were fed the HF diet and given a daily injection of LPC. We hypothesized that LPC would prevent NASH since conversion of LPC into PC is independent of CT activity. As was the case for the CDP-choline administration, LPC increased hepatic PC, but did not prevent NASH in the LCTα$^{-/-}$ mice as indicated by the clinical assessment of liver histology (Figure 3.5A, B). The administration of LPC reduced hepatic DAG mass by 30% compared to that in the saline-treated mice, without altering hepatic ceramide or TG content (Figure 3.5C, D).

Interestingly, administration of LPC caused a modest, but significant increase in hepatic PE mass compared to that in the saline-treated mice (Figure 3.5A). Although it is unknown why LPC increased hepatic PE, the reduction in DAG mass together with the increase in PE mass suggests that administration of LPC stimulated PE biosynthesis. That hepatic PC was normalized with both CDP-choline and LPC without improvement of NASH suggests improving hepatic PC is not sufficient for prevention of NASH.

3.3.2 Betaine, but not choline, partially prevents non-alcoholic steatohepatitis

To further understand whether impaired PC biosynthesis is involved in the development of NASH, LCTα$^{-/-}$ mice were fed the HF diet supplemented with betaine. We hypothesized that since betaine would increase the supply of *S*-adenosylmethionine required for the PEMT pathway for PC synthesis, betaine might increase methylation-dependent PC biosynthesis. Betaine supplementation of the diet given to the LCTα$^{-/-}$ mice prevented hepatic steatosis as assessed by the accumulation of TG (Figure 3.6A) and DAG (Figure 3.6D) and normalized levels of these lipids (Figure 3.6A, D). However, betaine did not increase the amount of hepatic PC or plasma TG to the levels in the floxed mice (Figure 3.6B, C). Betaine supplementation of the LCTα$^{-/-}$ mice did not decrease ceramide levels (Figure 3.6D). Moreover, betaine improved portal inflammation, but not lobular inflammation or hepatocyte ballooning degeneration in CTα-deficient livers as determined by clinical assessment of liver histology (Figure 3.7A). In agreement with improved portal inflammation, betaine partially reduced plasma levels of alanine aminotransferase in LCTα$^{-/-}$ mice, further indicating improvement of liver function (Figure 3.7B). Since betaine attenuated NASH without increasing hepatic levels of PC further

indicates that reduced levels of hepatic PC is not a determining factor in the pathogenesis of NASH.

Choline (via the oxidation of betaine) is also a labile methyl donor which may increase the supply of *S*-adenosylmethionine required for the PEMT pathway for PC synthesis (22). Furthermore, *Pemt*$^{-/-}$ mice fed the HF diet are choline deficient due to a reduction in *de novo* choline production. As a result, the mice are resistant to HF diet-induced obesity and insulin resistance, both of which are reversed with choline supplementation, independently of PC (23). Taken together, we hypothesized that choline supplementation may prevent NASH in LCTα$^{-/-}$ mice, either by increasing methylation-dependent PC biosynthesis, or through mechanisms which are independent of improving hepatic PC. Choline supplementation did not normalize either hepatic PC or plasma TG levels in LCTα$^{-/-}$ mice (Figure 3.8A, B). Despite partial reduction of hepatic TG (Figure 3.8C), choline supplementation was not hepatoprotective as analyzed by clinical assessment of liver histology (Figure 3.8D). Therefore, unlike betaine, choline supplementation was unable to improve liver function in LCTα$^{-/-}$ mice.

3.3.3 Ectopic expression of CTα prevents hepatic steatosis CTα-deficient livers

To determine if expression of CTα in LCTα$^{-/-}$ mice prevented the development of NASH, adenoviruses containing cDNA encoding HA-tagged CTα were administered to LCTα$^{-/-}$ mice after which the mice were fed the HF diet for 7 days. Hepatic expression of CTα in LCTα$^{-/-}$ mice increased CT activity by 36% compared to control mice in which GFP was expressed via adenoviruses (Figure 3.9A). Increased expression of CTα via adenoviruses in LCTα$^{-/-}$ livers was confirmed by immunoblotting (Figure 3.9B). Liver histology (Figure 3.10A), as well as measurement of

hepatic TG mass (Figure 3.10B) revealed that ectopic expression of CTα in LCTα$^{-/-}$ mice prevents hepatic steatosis. Furthermore, the increase in CT activity was sufficient to increase the amount of plasma TG (Figure 3.10C). These data indicate that hepatic steatosis can be prevented by ectopic expression of CTα.

Ectopic expression of CTα in LCTα$^{-/-}$ mice partially normalized hepatic PC mass without altering hepatic PE mass (Figure 3.11A). Despite prevention of hepatic steatosis (Figure 3.10B), NASH was not prevented as indicated by the presence of lobular and portal inflammation and hepatocyte ballooning (Figure 3.11B). In addition, the hepatic concentration of ceramide and DAG were increased by 50% in LCTα$^{-/-}$ mice expressing CTα via adenoviruses (Figure 3.11C). That ectopic expression of CTα in LCTα$^{-/-}$ mice partially normalized hepatic PC mass without prevention of NASH further indicates that impaired PC synthesis is not a determining factor in the pathogenesis of NASH. However, these data indicate that impaired PC biosynthesis is a contributing factor to the development of hepatic steatosis.

3.3.4 Hepatic ceramide, but not phosphatidylcholine, correlates with non-alcoholic steatohepatitis

To further clarify the relationship between hepatic PC and the development of NASH, correlation curves were prepared containing data from treatment groups where hepatic PC was normalized. There was no correlation found between hepatic PC mass and the total score of NAFLD (R^2=0.10) (Figure 3.12A) further indicating that impaired PC biosynthesis is not a determining factor in the pathogenesis of NASH. Interestingly, a positive correlation was found between hepatic ceramide mass and total score of NAFLD (R^2=0.75) (Figure 3.12B), while there was no correlation found between hepatic levels of DAG and the pathology scores of NAFLD

(R^2=0.39) (Figure 3.12C). These correlation studies indicate an association between hepatic ceramide accumulation and the development of NASH in CTα-deficient livers.

3.4 Discussion

The cellular determinants which play key roles in the pathogenesis of NASH are not entirely understood. Recent studies have suggested that a deficiency in hepatic PC, and/or the enzymes involved in PC biosynthesis could play an important role in the development of NASH (17-19). We utilized LCTα$^{-/-}$ mice, without dietary reduction of PC precursors (choline and methionine), to investigate the relationship between impaired hepatic PC biosynthesis and NASH. To elucidate the role of impaired PC biosynthesis in the development of NASH, LCTα$^{-/-}$ mice were fed the HF diet supplemented with either betaine or choline, or were administered daily injections of either CDP-choline or LPC. Betaine, choline (via oxidation to betaine), CDP-choline and LPC may all be incorporated into hepatic PC independent of CTα. In addition, LCTα$^{-/-}$ mice received a single dose of adenoviruses expressing CTα in an attempt to prevent the development of NASH. Surprisingly, although impaired PC biosynthesis induces hepatic steatosis due to reduced VLDL secretion, the data presented illustrates that reduced levels of hepatic PC, as a result of impaired PC biosynthesis, is not the only determinant of NASH in LCTα$^{-/-}$ mice.

3.4.1 Betaine may be a potential treatment for non-alcoholic steatohepatitis

Betaine, a metabolite formed from the oxidation of choline, is an important methyl donor in the methionine-homocysteine cycle (24). The PEMT pathway utilizes methyl groups derived from betaine. Previous work in our lab has shown that flux through the PEMT pathway is increased in chow fed LCTα$^{-/-}$ mice, presumably as a mechanism for meeting the hepatic demand for PC (25). We hypothesized that the supply of methyl groups for PC synthesis via the PEMT pathway might limit PC synthesis in HF-fed LCTα$^{-/-}$ mice. Thus, supplementation of the HF diet with betaine would stimulate PC synthesis. In addition, a previous study has demonstrated that betaine can stimulate VLDL secretion (26) further indicating that betaine may stimulate TG secretion and improve NASH in LCTα$^{-/-}$ mice. Furthermore, previous studies have indicated that betaine may be beneficial for prevention of NASH and alcoholic steatohepatitis (27-31). Our studies demonstrated that betaine in the diet normalized hepatic TG mass in the LCTα$^{-/-}$ mice and eliminated portal vein inflammation indicating that betaine had reduced the severity of NASH in LCTα$^{-/-}$ mice, confirming the hepatoprotective effects of betaine. However, betaine supplementation did not normalize plasma TG levels in LCTα$^{-/-}$ mice suggesting that betaine supplementation had decreased hepatic TG mass without normalizing TG secretion. Dietary betaine has been shown to decrease hepatic mRNA and protein levels of sterol regulatory element binding protein 1c in models of NASH and alcoholic steatohepatitis suggesting that dietary betaine decreases lipogenesis (27,29). These observations are supported by our results in which betaine supplementation reduced hepatic content of TG and DAG suggesting that betaine reduces hepatic lipogenesis in LCTα$^{-/-}$ mice.

3.4.2 Decreased hepatic phosphatidylcholine may not directly induce non-alcoholic steatohepatitis

CDP-choline has been successfully used as a therapy for disorders such as brain ischemia and muscular dystrophy (32-34) in which PC biosynthesis is impaired. We, therefore, attempted to prevent NASH in LCTα$^{-/-}$ mice fed the HF diet by daily injection with CDP-choline. CDP-choline restored levels of both hepatic PC and DAG to those in floxed control mice and reduced the amount of hepatic TG. Nevertheless, NASH was not prevented suggesting that improving only hepatic PC mass is not sufficient for prevention of NASH. Similar results were obtained in LCTα$^{-/-}$ mice when hepatic PC mass were increased with LPC or with adenoviral expression of CTα. However, hepatic steatosis was prevented with ectopic expression of CTα in LCTα$^{-/-}$ mice suggesting that impaired PC biosynthesis is a determinant for hepatic steatosis. These data suggest that reduced levels of hepatic PC does not play a key role in the pathogenesis of NASH in LCTα$^{-/-}$ mice.

The failure of CDP-choline to restore TG secretion may indicate that not enough CDP-choline was supplied for sufficient TG secretion. Previous studies have reported that 16.4 μmole of hepatic PC is synthesized daily, where 70% of hepatic PC is produced via the CDP-choline pathway and the remainder 30% is synthesized by the PEMT pathway (35,36). In the current study, CDP-[^{14}C]choline was injected into both floxed and LCTα$^{-/-}$ mice to determine if choline derived from CDP-choline was incorporated into hepatic PC. From this experiment, we calculated that ~11 μmole of hepatic PC could be synthesized from the daily injected dose of CDP-choline, which would account for the daily amount of hepatic PC synthesized via the CDP-choline pathway. Thus, sufficient CDP-choline was supplied to accommodate daily hepatic PC biosynthesis via the CDP-choline pathway and to stimulate TG secretion.

Alternatively, compartmentation of the CDP-choline derived from the CT reaction may differ from that of the injected CDP-choline which may account for the failure of CDP-choline to restore TG secretion.

3.4.3 Other possible mechanisms involved in the development of non-alcoholic steatohepatitis

The CTα isoform contains a nuclear localization signal. However, the role of CT in the nucleus is unknown (37,38). Therefore, CTα may function in other pathways independently of PC biosynthesis. Knockdown of hepatic CTα could have affected a different function of the enzyme, resulting in decreased protection from NASH. More recently, it has been shown that knockdown of CTα in *Drosophila* S2 cells resulted in fewer, but larger lipid droplets (39). In these cells, the authors also found that CT localized to the surface of lipid droplets with incubation with oleate (39). Interestingly, knockdown of hepatic CTα also resulted in larger lipid droplets within hepatocytes (20). Therefore, it is possible that knockdown of hepatic CTα may have an effect on the lipid droplets, resulting in increased susceptibility of CTα-deficient livers to steatohepatitis.

3.4.4 Does ceramide play a key role in the pathogenesis of non-alcoholic steatohepatitis?

The hepatic mass of ceramide in LCTα$^{-/-}$ mice was double that in floxed controls. None of the treatments we used in this study normalized hepatic ceramide levels or fully prevented the development of NASH. In addition, our results show a positive correlation between hepatic levels of ceramide and the pathology score of NAFLD. Other studies in murine

models of NASH have also reported an accumulation of hepatic ceramide (7,40-42), however, the importance of ceramide accumulation in NASH livers is unknown.

Ceramide has been shown to activate NADPH oxidase leading to oxidative stress and apoptosis in many biological systems including endothelial cells, rat hepatocytes, primary neruons, and rat mesangial cells (43-46). In the current study, we found a 1.5-fold increase in hepatic gene expression of NADPH oxidase in LCTα$^{-/-}$ mice injected with saline, which was not restored to floxed levels with CDP-choline. Therefore, it is possible that in LCTα$^{-/-}$ mice, the accumulation of hepatic ceramide activated NADPH oxidase leading to hepatocellular apoptosis resulting in the development of NASH.

3.4.5 Conclusion

In summary, we show that impaired PC biosynthesis induced by LCTα-deficiency is a determinant factor in the development of hepatic steatosis. However, the data presented clearly indicate that lower levels of hepatic PC is not a major contributor in the transition of hepatic steatosis to NASH in CTα-deficient livers. Furthermore, these data suggest that hepatic accumulation of ceramide may play a potential role in the development of NASH in LCTα$^{-/-}$ mice.

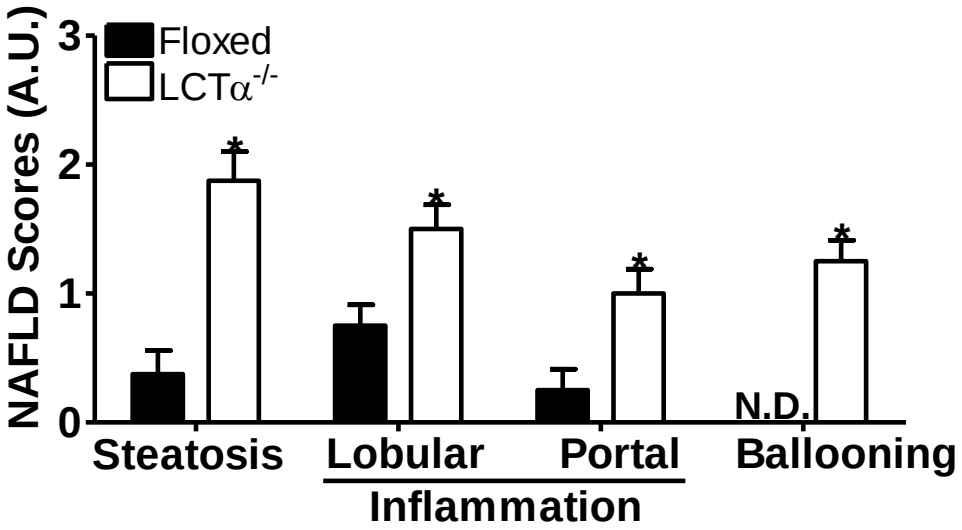

Figure 3.1 LCTα-deficient mice develop non-alcoholic steatohepatitis after one week of high fat feeding. LCTα$^{-/-}$ mice and floxed mice were fed the high fat (HF) diet for 7 days and livers were collected after an overnight fast. Hemotoxylin and eosin stained liver histology was clinically assessed for the presence of steatosis, lobular and portal inflammation and hepatocyte ballooning degeneration, which are histological markers of NAFLD (n=8). Score 0 = no histological presence**;** Score 3 = highest histological presence**.** All data are means ± S.E. *, $p < 0.05$

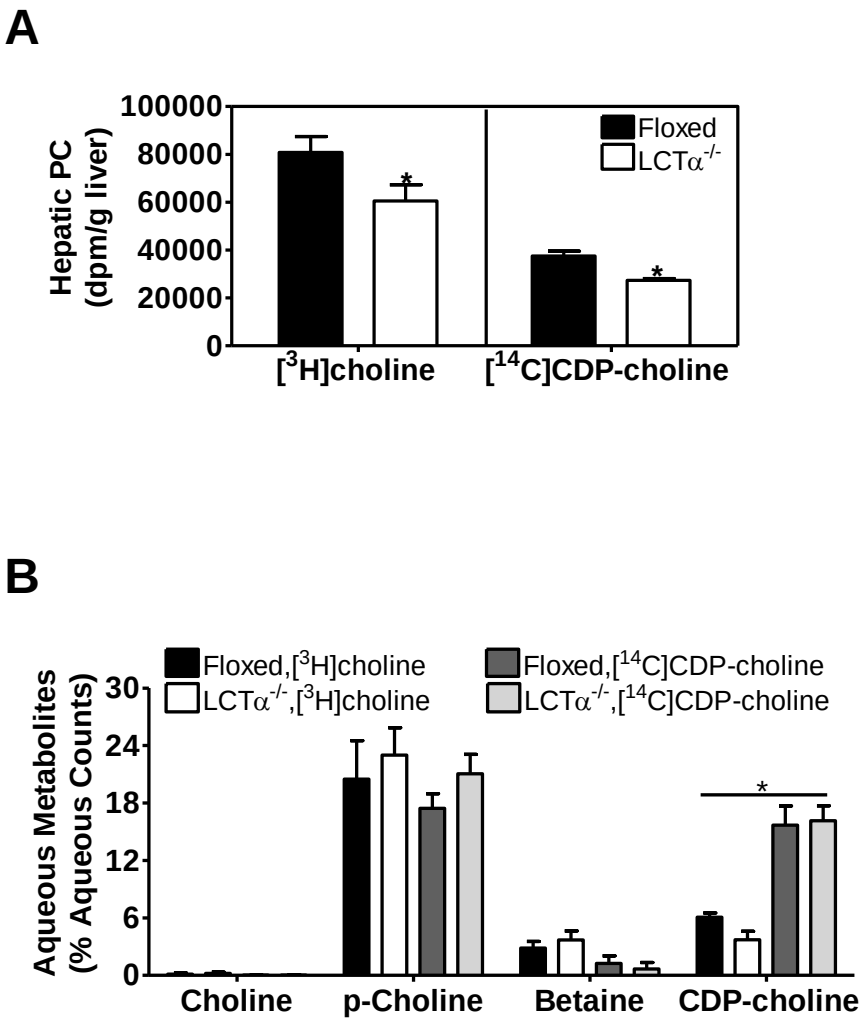

Figure 3.2 Choline derived from CDP-choline may be incorporated into hepatic phosphatidylcholine. LCTα$^{-/-}$ mice and floxed mice were fed the high fat (HF) diet for 7 days. After a 12 h fast, the mice were administered both 1 µCi CDP-[^{14}C]choline and 2.5 µCi [^{3}H]choline via intraperitoneal injection. Livers were collected 4 h post-injection. (A) Incorporation of [^{3}H]choline and CDP-[^{14}C]choline into hepatic PC (n=6). (B) Incorporation of [^{3}H]choline and CDP-[^{14}C]choline into hepatic choline, phosphocholine, betaine and CDP-choline (n=6). All data are means ± S.E. *, $p < 0.05$

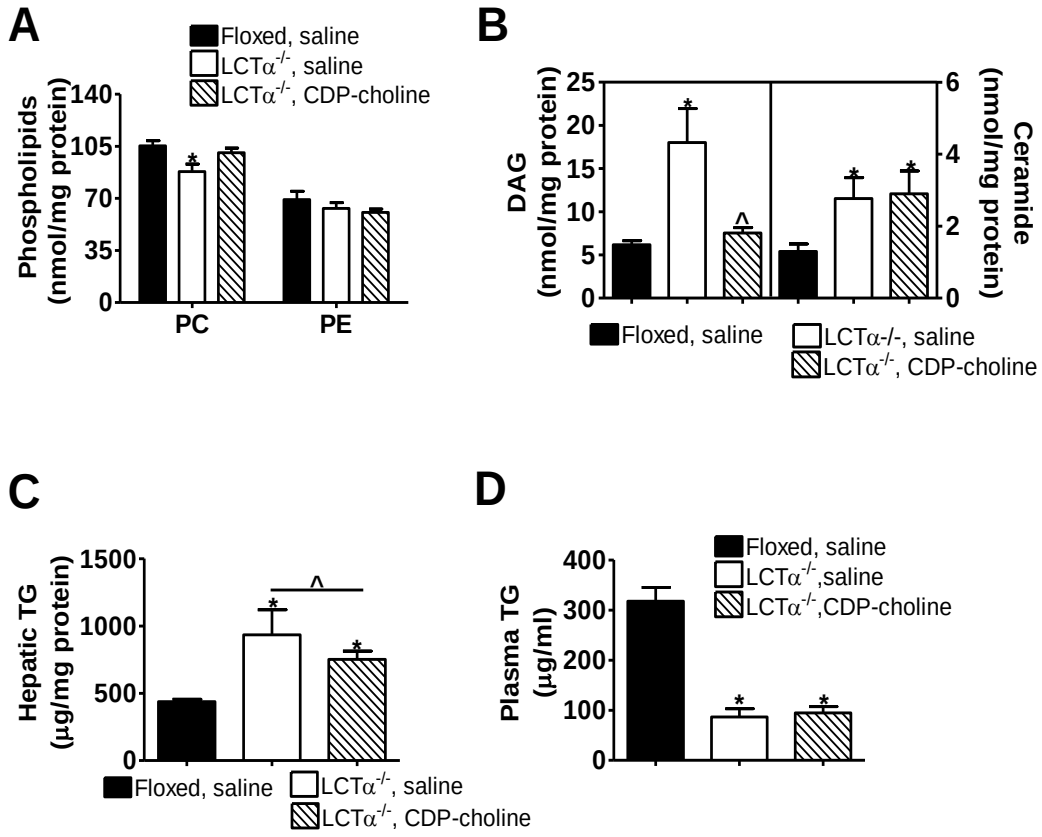

Figure 3.3 CDP-choline normalizes amounts of hepatic phosphatidylcholine and diacylglycerol, but not ceramide or triacylglycerol in LCTα deficient mice. LCTα$^{-/-}$ mice and floxed mice were fed the HF diet for 7 days during which the LCTα$^{-/-}$ mice were injected daily with either saline or 1 mg of CDP-choline/kg body weight; floxed mice were injected with saline. Livers and plasma were collected after an overnight fast. (A-C) Hepatic phosphatidylcholine (PC), phosphatidylethanolamine (PE), diacylglycerol (DAG), ceramide and triacylglycerol (TG) were quantified (n=5 to 8). (D) Plasma TG (n=5 to 8). All data are means ± S.E. *, $p < 0.05$ compared with floxed, saline. ^, $p < 0.05$ compared with LCTα$^{-/-}$, saline.

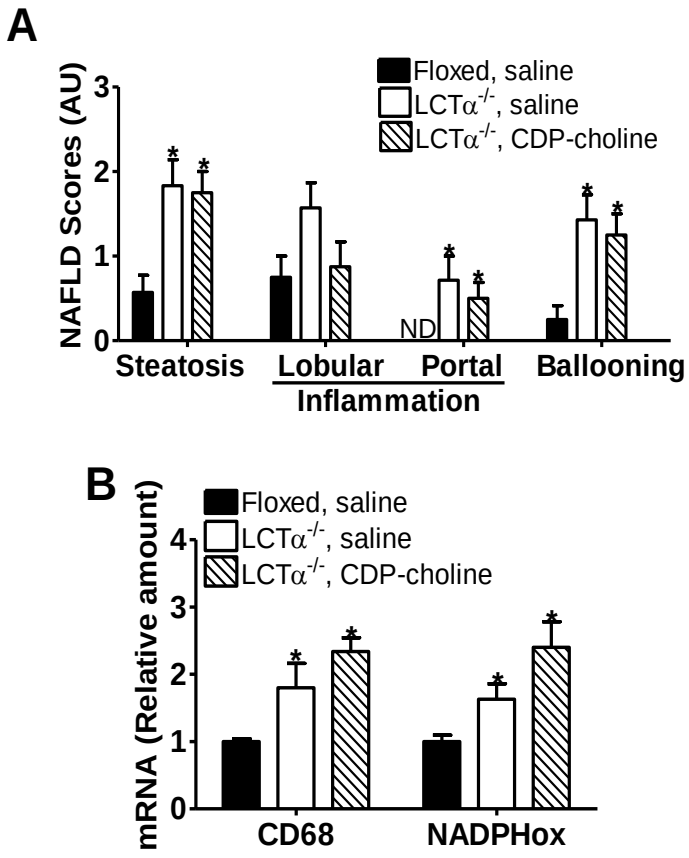

Figure 3.4 CDP-choline does not prevent the development of non-alcoholic steatohepatitis in LCTα deficient mice. LCTα$^{-/-}$ mice and floxed mice were fed the high fat (HF) diet for 7 days during which the LCTα$^{-/-}$ mice were injected daily with either saline or 1 mg of CDP-choline/kg body weight; floxed mice were injected with saline. Livers were collected after an overnight fast. (A) Hemotoxylin and eosin stained liver histology was clinically assessed for the presence of steatosis, lobular and portal inflammation and hepatocyte ballooning, which are histological markers of NAFLD (n=5). Score 0 = no histological presence; Score 3 = highest histological presence. (B) Relative levels of mRNAs encoding genes involved in inflammation (CD68 and NADPHox, NADPH oxidase) were quantified by real-time qPCR relative to cyclophilin mRNA (n=4). All data are means ± S.E. *, $p < 0.05$ compared with floxed, saline.

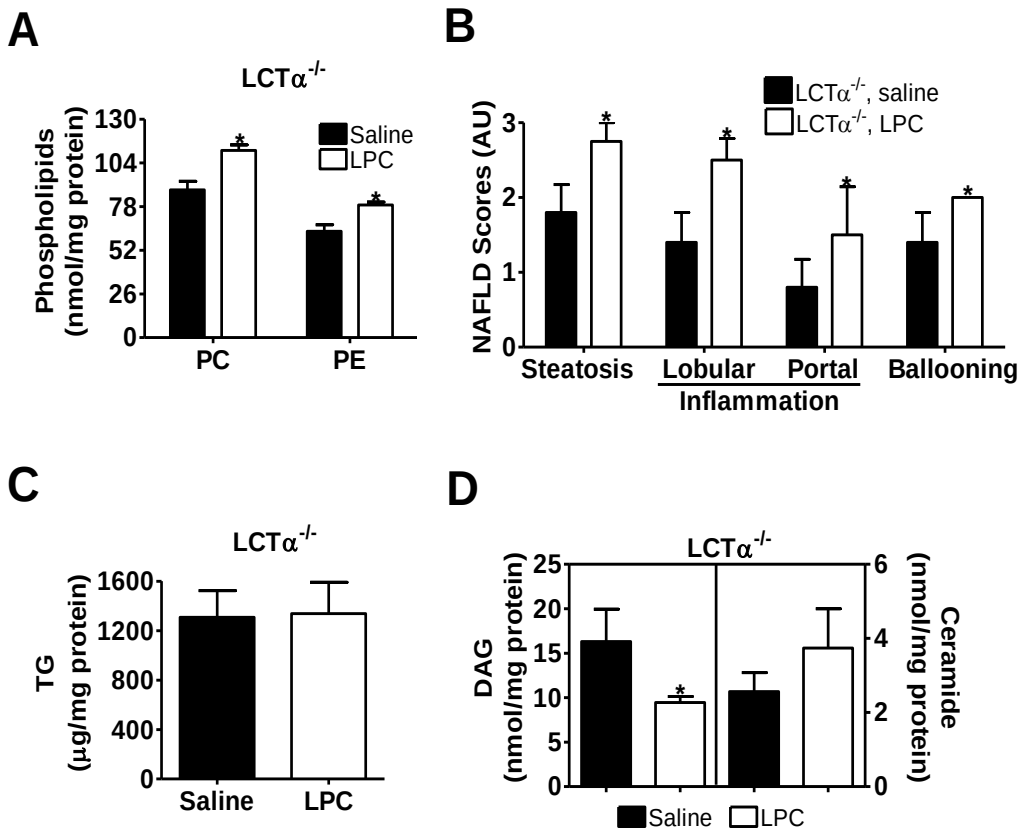

Figure 3.5 Lysophosphatidylcholine does not attenuate non-alcoholic steatohepatitis in LCTα deficient mice. LCTα$^{-/-}$ mice were fed the high fat diet for 7 days during which time they were injected daily with saline or 50 µM lysophosphatidylcholine (LPC)/kg body weight. After an overnight fast, livers were collected. (A) Hepatic phosphatidylcholine (PC), and phosphatidylethanolamine (PE) were quantified (n=4 to 6). (B) Liver histology was clinically assessed for the presence of steatosis, lobular and portal inflammation and hepatocyte ballooning, which are histological markers of NAFLD (n=4 to 6). Score 0 = no histological presence; Score 3 = highest histological presence. All data points were the same for histological data which contained no error bars. (C) Hepatic TG (n=4 to 6). (D) Hepatic levels of diacylglycerol (DAG) and ceramide were quantified by the DAG kinase assay (n=4 to 6). All data are means ± S.E. *, $p < 0.05$

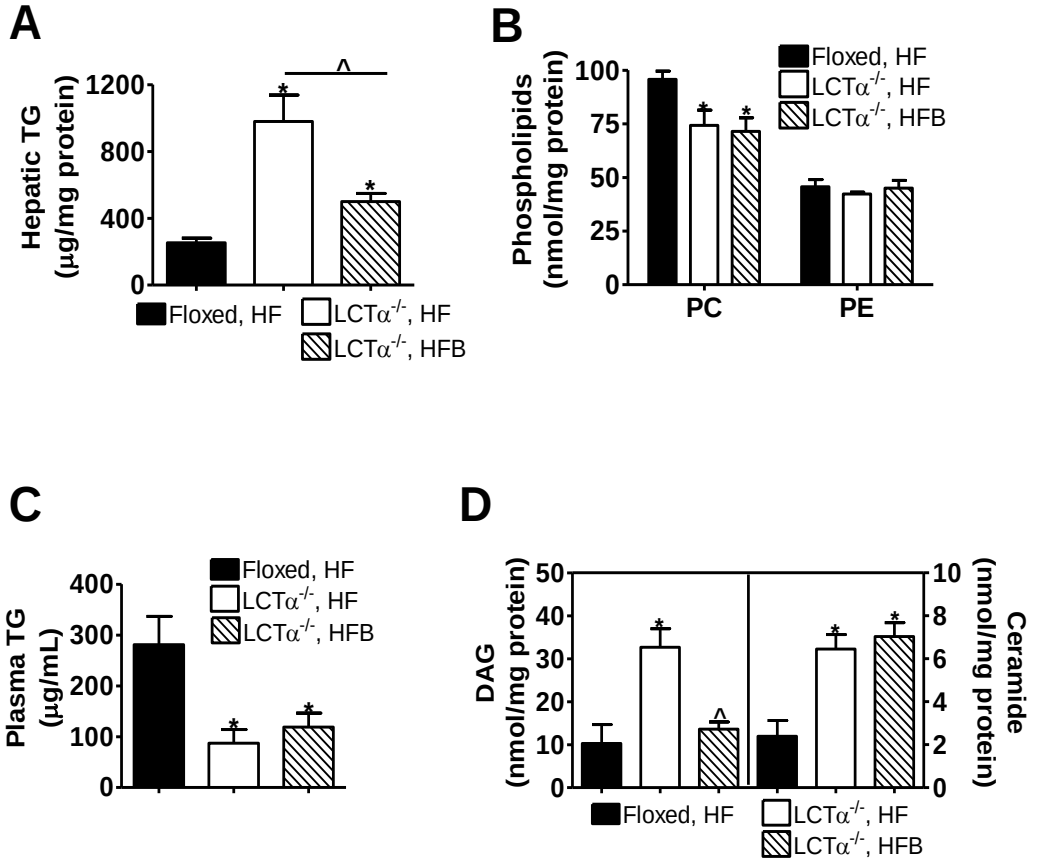

Figure 3.6 Dietary betaine prevents hepatic steatosis in LCTα deficient livers. LCTα$^{-/-}$ mice were fed either the high fat diet (HF), or the HF diet supplemented with 1% betaine (HFB) for 7 days; floxed mice were fed the HF diet. Livers and plasma were collected after an overnight fast. (A) Triacylglycerol (TG) (n=6 to 8). (B) Phosphatidylcholine (PC) and phosphatidylethanolamine (PE) (n=4). (C) Plasma TG (n=6 to 8). (D) Hepatic diacylglycerol (DAG) and ceramide (n=5 to 6). *, $p < 0.05$ compared with floxed, HF. ^, $p < 0.05$ compared with LCTα$^{-/-}$, HF.

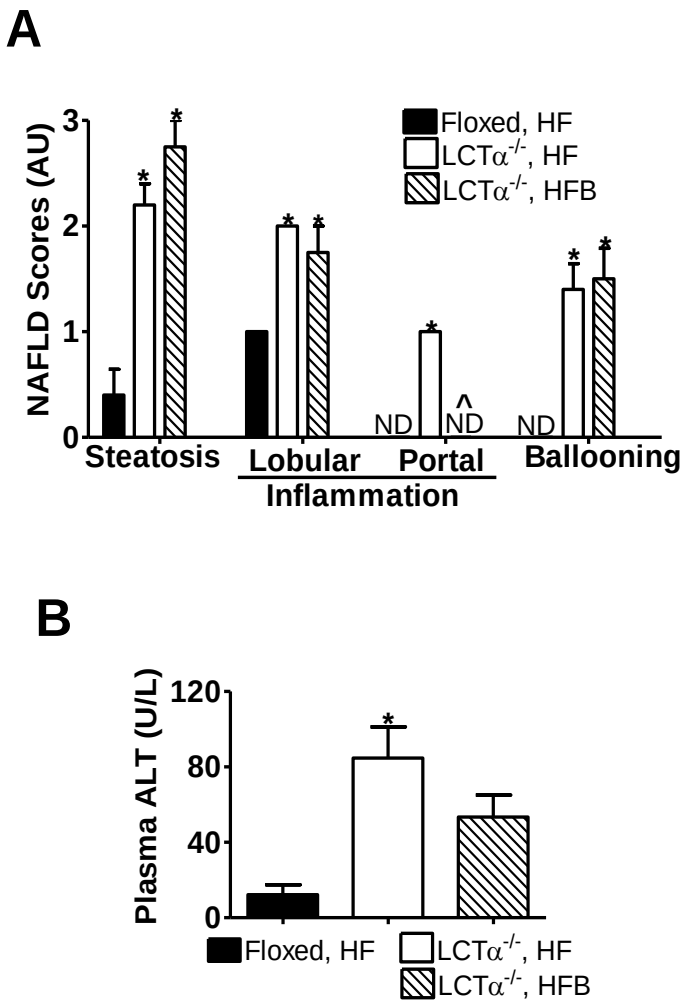

Figure 3.7 Dietary betaine reduced the severity of non-alcoholic steatohepatitis in LCTα deficient livers. LCTα$^{-/-}$ mice were fed either the high fat diet (HF), or the HF diet supplemented with 1% betaine (HFB) for 7 days; floxed mice were fed the HF diet. Livers and plasma were collected after an overnight fast. (A) Liver histology was clinically assessed for the presence lobular and portal inflammation and hepatocyte ballooning, which are histological markers of NAFLD (n = 4 to 6). Score 0 = no histological presence**;** Score 3 = highest histological presence. (B) Plasma levels of alanine aminotransferase (n = 5 to 6). All data are means ± S.E. *, $p < 0.05$ compared with floxed, HF diet. ^, $p < 0.05$ compared with LCTα$^{-/-}$, HF.

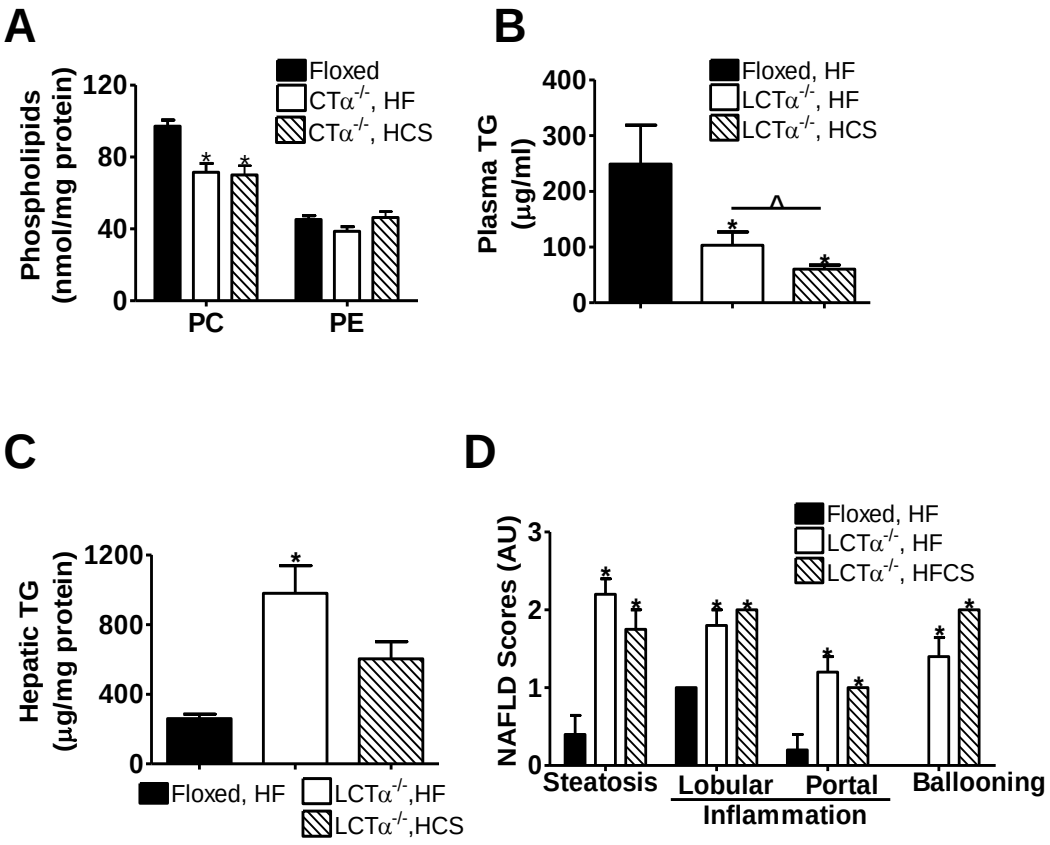

Figure 3.8 Dietary choline does not prevent non-alcoholic steatohepatitis induced by LCTα deficiency. LCTα$^{-/-}$ mice were fed either the high fat diet (HF), or the HF diet supplemented with 2.7 g of choline per kg diet (HFCS) for 7 days; floxed mice were fed the HF diet. Livers and plasma were collected after an overnight fast. (A) Hepatic phosphatidylcholine (PC) and phosphatidylethanolamine (PE) (n=5). (B) Plasma TG (n = 5). (C) Hepatic triacylglycerol (TG) (n=6 to 8). (D) Hematoxylin and eosin stained liver histology was clinically assessed for the presence of lobular and portal inflammation and hepatocyte ballooning, which are histological markers of NAFLD (n=5). Score 0 = no histological presence**;** Score 3 = highest histological presence. All data points were the same for histological data which contained no error bars. *, $p < 0.05$ compared with floxed, HF. ^, $p < 0.05$ compared with LCTα$^{-/-}$, HF.

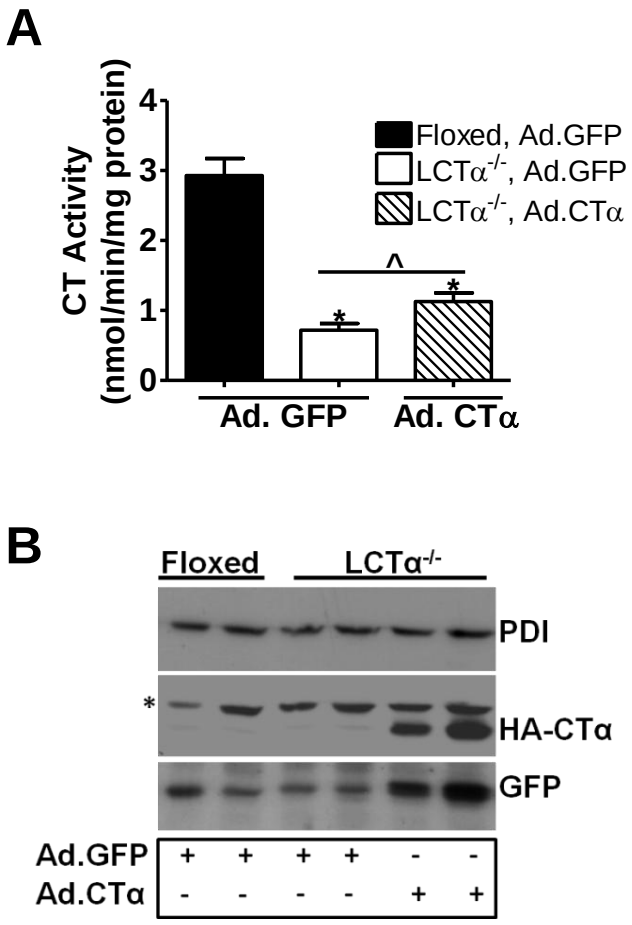

Figure 3.9 Adenoviral delivery of CTα in CTα-deficient livers. Floxed or LCTα$^{-/-}$ mice were injected via the tail vein with a single dose of adenoviruses encoding either green fluorescent protein (GFP) alone (Ad.GFP), or GFP with CTα (Ad.CTα) after which the mice were fed the high fat diet for 7 days. Livers were collected after an overnight fast. (A) CT activity was measured in liver homogenates from fasted mice (n=5). (B) Amounts of hepatic GFP, HA-tagged CTα, and PDI (protein disulfide isomerase) proteins were assessed by immunoblotting (* denotes non-specific band). A typical immunoblot is displayed (n=5). All data are means ± S.E. *, $p < 0.05$ compared to Floxed, Ad.GFP. ^, $p<0.05$ compared to LCTα$^{-/-}$, Ad.GFP.

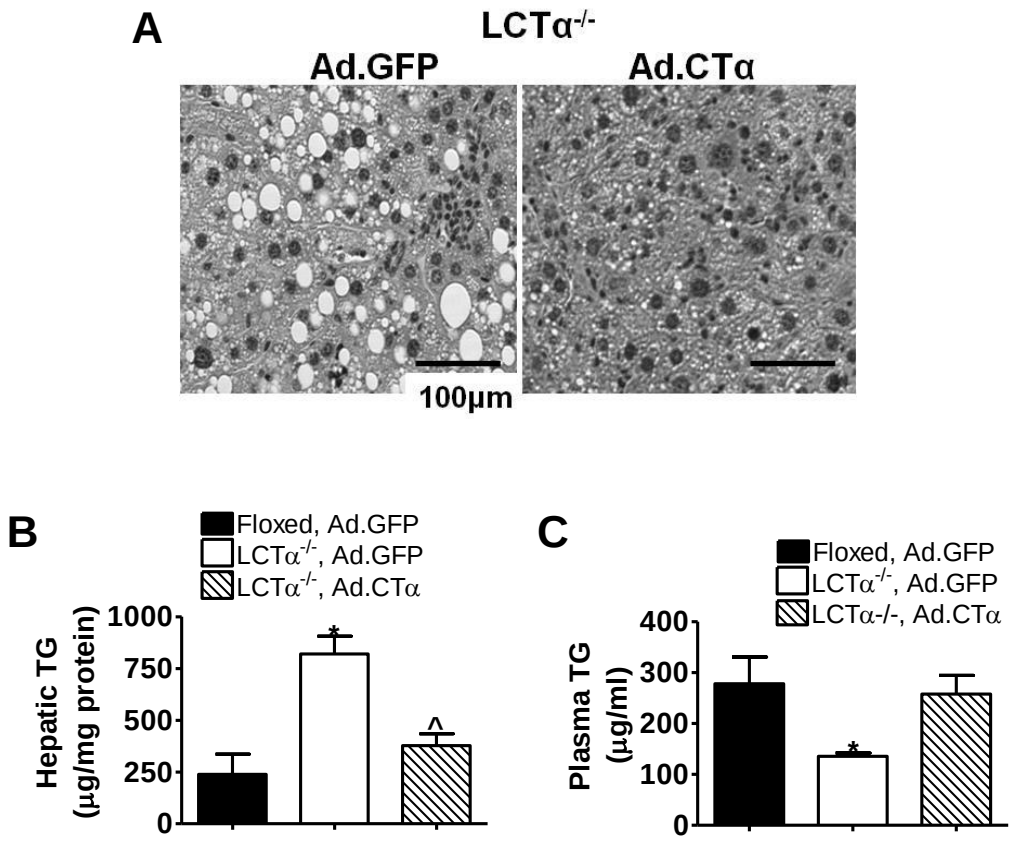

Figure 3.10 Adenoviral delivery of CTα prevents hepatic steatosis in LCTα deficient mice. Floxed or LCTα$^{-/-}$ mice were injected via the tail vein with a single dose of adenoviruses encoding either green fluorescent protein (GFP) alone (Ad.GFP), or GFP with CTα (Ad.CTα) after which the mice were fed the high fat diet for 7 days. Livers and plasma were collected after an overnight fast and lipids were quantified. A) Liver samples were fixed in 10% buffered formalin and stained with hematoxylin and eosin (n=4). (B) Hepatic triacylglycerol (TG) (n=5). (C) Plasma TG (n=5). All data are means ± S.E. *, $p < 0.05$ compared to Floxed, Ad.GFP. ^, $p < 0.05$ compared to LCTα$^{-/-}$, Ad.GFP.

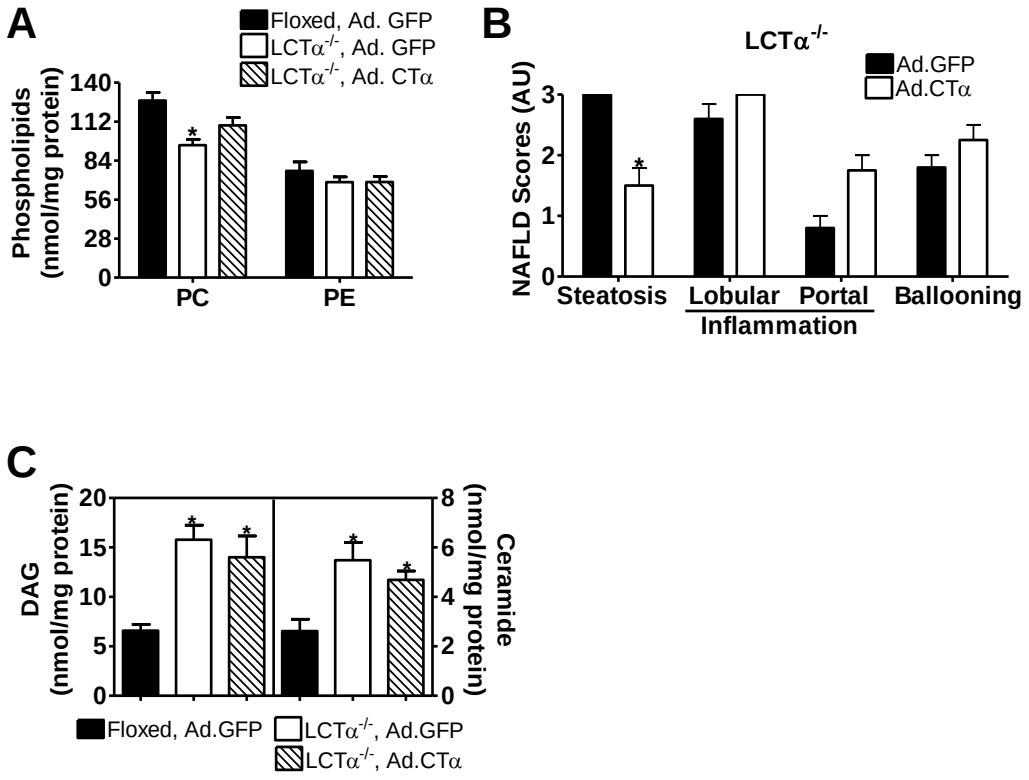

Figure 3.11 Adenoviral delivery of CTα normalizes hepatic phosphatidylcholine, but does not prevent non-alcoholic steatohepatitis in LCTα deficient mice. Floxed or LCTα$^{-/-}$ mice were injected with a single dose of adenoviruses encoding either green fluorescent protein (GFP) alone (Ad.GFP), or GFP with CTα (Ad.CTα) after which the mice were fed the high fat diet for 7 days. Livers were collected after an overnight fast and lipids were quantified. (A) Phosphatidylcholine (PC) and phosphatidylethanolamine (PE) (n=5). (B) Liver histology from LCTα$^{-/-}$ mice were clinically assessed for the presence of steatosis, lobular and portal inflammation and hepatocyte ballooning, which are histological markers of NAFLD (n=4). Score 0 = no histological presence; Score 3 = highest histological presence. All data points were the same for histological data which contained no error bars. (C) Hepatic diacylglycerol (DAG) and ceramide (n=5). All data are means ± S.E. *, $p < 0.05$ compared with floxed, Ad.GFP

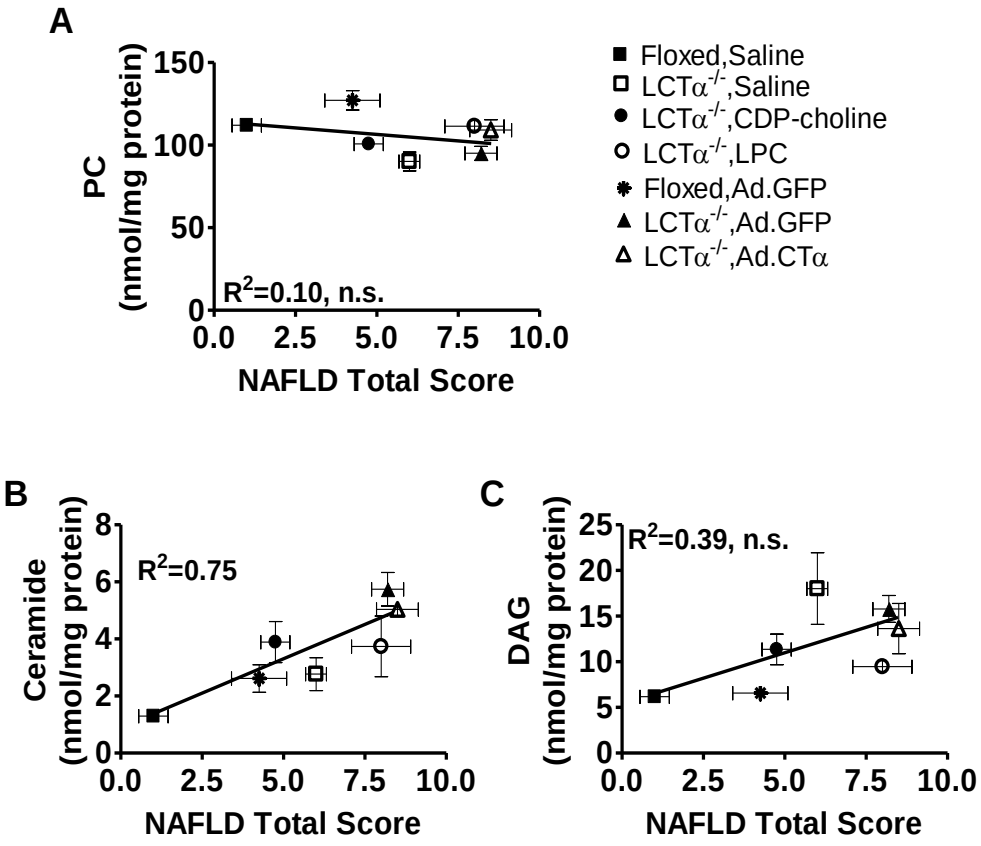

Figure 3.12 Hepatic levels of ceramide, correlate with the development of non-alcoholic steatohepatitis. Correlation data comparing levels of hepatic ceramide, diacylglycerol (DAG) or phosphatidylcholine (PC) with the total score of non-alcoholic fatty liver disease (NAFLD). Correlations include data from:floxed and LCTα$^{-/-}$ mice administered saline, CDP-choline, or LPC during the HF diet; and floxed and LCTα$^{-/-}$ mice fed the HF diet after delivery of adenoviruses expressing GFP, or expressing GFP together with HA-tagged CTα. (A) Correlation between levels of hepatic PC and the total score of NAFLD. R^2=0.10, n.s. (B) Correlation between levels of hepatic ceramide and the total score of NAFLD. R^2=0.75, $p < 0.05$. (C) Correlation between levels of hepatic DAG and the total score of NAFLD. R^2=0.39,n.s. (n.s. denotes no significance). Figure legends depicted in (A) is representative for all graphs.

3.5 References

1. Angulo, P. (2002) *N Engl J Med* **346**, 1221-1231

2. Browning, J. D., and Horton, J. D. (2004) *J Clin Invest* **114**, 147-152

3. Yeh, M. M., and Brunt, E. M. (2007) *Am J Clin Pathol* **128**, 837-847

4. Day, C. P., and James, O. F. (1998) *Gastroenterology* **114**, 842-845

5. Yao, Z. M., and Vance, D. E. (1990) *Biochem Cell Biol* **68**, 552-558

6. Vetelainen, R., van Vliet, A., and van Gulik, T. M. (2007) *J Gastroenterol Hepatol* **22**, 1526-1533

7. Caballero, F., Fernandez, A., Matias, N., Martinez, L., Fucho, R., Elena, M., Caballeria, J., Morales, A., Fernandez-Checa, J. C., and Garcia-Ruiz, C. (2010) *J Biol Chem* **285**, 18528-18536

8. Rinella, M. E., Elias, M. S., Smolak, R. R., Fu, T., Borensztajn, J., and Green, R. M. (2008) *J Lipid Res* **49**, 1068-1076

9. Rinella, M. E., and Green, R. M. (2004) *J Hepatol* **40**, 47-51

10. Vance DE and Vance JE (2008) Phospholipid biosynthesis in eukaryotes. in *Biochemistry of Lipids, Lipoproteins, and Membranes, 5th Edition* (Vance DE and Vance JE ed.), Elsevier, Amsterdam. pp 213-244

11. Kennedy, E. P., and Weiss, S. B. (1956) *J Biol Chem* **222**, 193-214

12. Karim, M., Jackson, P., and Jackowski, S. (2003) *Biochim Biophys Acta* **1633**, 1-12

13. Vance, D. E., and Ridgway, N. D. (1988) *Prog Lipid Res* **27**, 61-79

14. Noga, A. A., and Vance, D. E. (2003) *J Biol Chem* **278**, 21851-21859

15. Noga, A. A., Zhao, Y., and Vance, D. E. (2002) *J Biol Chem* **277**, 42358-42365

16. Jacobs, R. L., Devlin, C., Tabas, I., and Vance, D. E. (2004) *J Biol Chem* **279**, 47402-47410

17. Puri, P., Baillie, R. A., Wiest, M. M., Mirshahi, F., Choudhury, J., Cheung, O., Sargeant, C., Contos, M. J., and Sanyal, A. J. (2007) *Hepatology* **46**, 1081-1090

18. Song, J., da Costa, K. A., Fischer, L. M., Kohlmeier, M., Kwock, L., Wang, S., and Zeisel, S. H. (2005) *FASEB J* **19**, 1266-1271

19. Saibara, T., and Ono, M. (2007) *J Hepatol* **47**, 869-870

20. Jacobs, R. L., Lingrell, S., Zhao, Y., Francis, G. A., and Vance, D. E. (2008) *J Biol Chem* **283**, 2147-2155

21. Schneider, W. J., and Vance, D. E. (1978) *J Neurochem* **30**, 1599-1601

22. Stead, L. M., Brosnan, J. T., Brosnan, M. E., Vance, D. E., and Jacobs, R. L. (2006) *Am J Clin Nutr* **83**, 5-10

23. Jacobs, R. L., Zhao, Y., Koonen, D. P., Sletten, T., Su, B., Lingrell, S., Cao, G., Peake, D. A., Kuo, M. S., Proctor, S. D., Kennedy, B. P., Dyck, J. R., and Vance, D. E. (2010) *J Biol Chem* **285**, 22403-22413

24. Craig, S. A. (2004) *Am J Clin Nutr* **80**, 539-549

25. Jacobs, R. L., Stead, L. M., Devlin, C., Tabas, I., Brosnan, M. E., Brosnan, J. T., and Vance, D. E. (2005) *J Biol Chem* **280**, 28299-28305

26. Sparks, J. D., Collins, H. L., Chirieac, D. V., Cianci, J., Jokinen, J., Sowden, M. P., Galloway, C. A., and Sparks, C. E. (2006) *Biochem J* **395**, 363-371

27. Song, Z., Deaciuc, I., Zhou, Z., Song, M., Chen, T., Hill, D., and McClain, C. J. (2007) *Am J Physiol Gastrointest Liver Physiol* **293**, G894-902

28. Wang, Z., Yao, T., Pini, M., Zhou, Z., Fantuzzi, G., and Song, Z. (2010) *Am J Physiol Gastrointest Liver Physiol* **298**, G634-642

29. Ji, C., and Kaplowitz, N. (2003) *Gastroenterology* **124**, 1488-1499

30. Kharbanda, K. K., Mailliard, M. E., Baldwin, C. R., Beckenhauer, H. C., Sorrell, M. F., and Tuma, D. J. (2007) *J Hepatol* **46**, 314-321

31. Abdelmalek, M. F., Sanderson, S. O., Angulo, P., Soldevila-Pico, C., Liu, C., Peter, J., Keach, J., Cave, M., Chen, T., McClain, C. J., and Lindor, K. D. (2009) *Hepatology* **50**, 1818-1826

32. Wu, G., Sher, R. B., Cox, G. A., and Vance, D. E. (2009) *Biochim Biophys Acta* **1791**, 347-356

33. Adibhatla, R. M., Hatcher, J. F., and Dempsey, R. J. (2004) *J Neurosci Res* **76**, 390-396

34. Adibhatla, R. M., Hatcher, J. F., Larsen, E. C., Chen, X., Sun, D., and Tsao, F. H. (2006) *J Biol Chem* **281**, 6718-6725

35. Reo, N. V., Adinehzadeh, M., and Foy, B. D. (2002) *Biochim Biophys Acta* **1580**, 171-188

36. Sundler, R., and Akesson, B. (1975) *J Biol Chem* **250**, 3359-3367

37. Wang, Y., MacDonald, J. I., and Kent, C. (1995) *J Biol Chem* **270**, 354-360

38. Wang, Y., Sweitzer, T. D., Weinhold, P. A., and Kent, C. (1993) *J Biol Chem* **268**, 5899-5904

39. Guo, Y., Walther, T. C., Rao, M., Stuurman, N., Goshima, G., Terayama, K., Wong, J. S., Vale, R. D., Walter, P., and Farese, R. V. (2008) *Nature* **453**, 657-661

40. Turpin, S. M., Hoy, A. J., Brown, R. D., Rudaz, C. G., Honeyman, J., Matzaris, M., and Watt, M. J. (2011) *Diabetologia* **54**, 146-156

41. Mas, E., Danjoux, M., Garcia, V., Carpentier, S., Segui, B., and Levade, T. (2009) *PLoS One* **4**, e7929

42. Brown, J. M., Betters, J. L., Lord, C., Ma, Y., Han, X., Yang, K., Alger, H. M., Melchior, J., Sawyer, J., Shah, R., Wilson, M. D., Liu, X., Graham, M. J., Lee, R., Crooke, R., Shulman, G. I., Xue, B., Shi, H., and Yu, L. (2010) *J Lipid Res* **51**, 3306-3315

43. Jana, A., and Pahan, K. (2004) *J Biol Chem* **279**, 51451-51459

44. Reinehr, R., Becker, S., Keitel, V., Eberle, A., Grether-Beck, S., and Haussinger, D. (2005) *Gastroenterology* **129**, 2009-2031

45. Zhang, D. X., Zou, A. P., and Li, P. L. (2003) *Am J Physiol Heart Circ Physiol* **284**, H605-612

46. Yi, F., Zhang, A. Y., Janscha, J. L., Li, P. L., and Zou, A. P. (2004) *Kidney Int* **66**, 1977-1987

CHAPTER 4

The Ratio of Phosphatidylcholine to Phosphatidylethanolamine Does Not Predict Integrity of MT58 Chinese Hamster Ovary Cells

4.1 Introduction

Phosphatidylcholine (PC) is the most abundant phospholipid in mammalian cellular membranes, comprising approximately 50% of the total phospholipid mass (1). In all nucleated cells, PC is made via the CDP-choline pathway and flux through the pathway is regulated by the activity of CTP:phosphocholine cytidylyltransferase (CT) (2,3). There are two isoforms of CT, CTα, encoded by *Pcyt*1a, and CTβ, encoded by *Pcyt*1b (4). CTα is believed to be the predominant isoform and is ubiquitously expressed (4). The phosphatidylethanolamine *N*-methyltransferase (PEMT) pathway, which is primarily in the liver, synthesizes PC via sequential methylation reactions of phosphatidylethanolamine (PE) (5).

PE is the second most abundant phospholipid within mammalian membranes. PE is synthesized from the CDP-ethanolamine pathway, and flux through the pathway is regulated by CTP:phosphoethanolamine cytidylyltransferase (ET) (2,3). A second PE biosynthetic enzyme, phosphatidylserine decarboxylase (PSD),catalyzes the decarboxylation of phosphatidylserine (PS) to PE (6). In the Chinese hamster ovary (Cho) cell line, the PSD pathway is responsible for synthesizing ~80% of cellular PE (7).

The MT58 cell line, which is a chemically mutated Cho cell line, contains a thermo-sensitive mutation in CTα (8-10). When maintained at the permissive temperature of 33ºC, cell growth and viability of MT58 cells is comparable to ChoK1 controls (10). However, shifting MT58 cells to the restrictive temperature of 40ºC results in a complete abolishment of CT activity, followed by a 2-fold reduction in the amount of cellular PC compared to that of ChoK1 cells (9,10). The deficiency of cellular PC in MT58 cells inhibits cellular growth and induces apoptosis as indicated by

the presence of fragmented DNA, decreased progression into the cell cycle, and cellular condensation (11). Addition of lysophosphatidylcholine (LPC) to the growth medium stimulates cellular growth and rescues MT58 cells from apoptosis (12). These studies illustrate that cellular PC-deficiency is sufficient to induce apoptosis.

Other studies have demonstrated that inhibition of PC biosynthesis induces cellular apoptosis (13-16). For example, PC12 cells show a 50% reduction in the amount of total PC resulting in apoptosis when the cells are cultured in choline-deficient medium (17). Furthermore, the induction of apoptosis in HeLa cells by the anticancer drug, 1-*O*-octadecyl-2-*O*-methyl-*rac*-glycerol-3-phosphocholine (edelfosine), can be prevented by either increased CT expression or treating the cells with LPC. This study suggests that edelfosine impairs PC biosynthesis resulting in cellular apoptosis (18). In addition, targeted deletion of the CTα gene in mice is embryonic lethal at embryonic day 3.5 (19). Clearly, PC homeostasis is critical for cellular growth and survival.

A reduction in cellular PC content ultimately results in an imbalance of the PC:PE molar ratio. A previous study has demonstrated a role for the PC:PE ratio in maintaining membrane integrity of hepatic cells. This study demonstrated that a drastic reduction in the PC:PE ratio plays an underlining role in the development of hepatic steatohepatitis (20). A reduced PC:PE ratio has been reported in other models of steatohepatitis (21-23), as well as within brain microsomal membranes of apolipoprotein E-deficient mice (24). Furthermore, a recent study has demonstrated that the PC:PE ratio may be important for maintaining mitochondrial membrane fluidity as a reduced mitochondrial PC:PE ratio in a mouse model of steatohepatitis resulted in depletion of mitochondrial glutathione (25). These studies suggest that the PC:PE ratio influences membrane integrity.

Therefore, a reduced PC:PE ratio, rather than the reduction of cellular PC, may play a pivotal role in the induction of apoptosis due to compromised cellular membranes. Thus, to investigate whether a reduced PC:PE ratio is involved in the induction of apoptosis, we utilized the MT58 cell line which has a natural deficiency of cellular PC due to impaired PC biosynthesis. We hypothesized that if the PC:PE ratio does influence membrane stability, then normalization of the PC:PE ratio should stabilize cellular membranes and rescue MT58 cells from apoptosis. Here, we report that the PC:PE ratio does not play a role in the induction of apoptosis and rather, cellular growth and survival is regulated by the amount of PC and PE within cellular membranes.

4.2 Experimental Procedures

4.2.1 Cell culture

ChoK1 and MT58 cell lines were cultured in Ham's F-12 medium (Invitrogen) supplemented with 10% fetal bovine serum (Invitrogen). Both cell lines were maintained in 10 mm culture dishes at 5% CO_2, 90% relative humidity at 37ºC. Since cell growth of MT58 was comparable to ChoK1 controls at 37ºC, this temperature was used as the permissive temperature. Both ChoK1 and MT58 cells were shifted to 41ºC for analysis at the restrictive temperature.

4.2.2 Silencing of phosphatidylserine decarboxylase and CTP:phosphoethanolamine cytidylyltransferase

Chok1 and MT58 cells were plated at a density of 1.5 x 10^5 cells per well in 6 well culture dishes. The cells were co-transfected with 0.1 µM dicer-substrate silencing RNAs targeting PSD or ET (siPSD/ET). For control experiments, MT58 and ChoK1 cells were transfected with a scrambled silencing RNA sequence (siScrambled). Lipofectamine2000 (Invitrogen) was used as the transfection reagent in a ratio of 1:3

(siRNA:lipofectamine2000). Knockdown of PSD and ET were verified via real-time quantitative PCR using a Rotor-Gene 3000 instrument (Montreal Biotech). Cellular gene expression was normalized to cyclophilin mRNA. For preparation of cDNA, cellular RNA was isolated using TRIzol reagent (Invitrogen) according to the manufacturer's instructions. Total RNA was treated with DNaseI (Invitrogen), and reverse-transcribed using an oligo(dT)12-18 primer and Superscript II reverse transcriptase (Invitrogen) according to the manufacturer's instructions.

Primer sequences for PSD: forward primer, 5'-GTGCTGAGTGGGGACTGGA3'; reverse primer, 5'-CGTTATCTGGGACTGTTTGTG-3'. Primer sequences for ET: forward primer, 5'-AGCTAGCCAAGAGGCCCTAC-3'; reverse primer, 5'-CACCAGGTCCACCTTGAAGT-3'. Primer sequences for cyclophilin: forward primer, 5'-TTCAAAGACAGCAGAAAACTTTCG-3'; reverse primer, 5'-TCTTCTTGCTGGTCTTGCCATTCC-3'.

4.2.3 Determination of cellular phospholipid content

MT58 cells were cultured at 37ºC to 80% confluency after which the temperature was shifted to 41ºC for 24 h. LPC was added to the culture medium in a final concentration of 5, 10 or 30 µM immediately before shifting the cells to 41ºC. Cells were collected in PBS, pelleted by low-speed centrifugation, re-suspended in buffer A (50 mM Tris-HCl, pH 7.4, 150 mM NaCl, and 1.0 mM EDTA) and sonicated. Lipids were extracted by the method of Folch *et al.* (26). Briefly, total lipids were extracted from cellular homogenate (1 mg of protein) with chloroform:methanol (2:1). Phospholipids were separated by thin-layer chromatography in chloroform:methanol:acetic acid:water (25:15:4:2, v/v). Bands corresponding to PC and PE were scraped and the mass of PC and PE was quantified by a phosphorus assay (27).

For silencing RNA experiments, MT58 and ChoK1 cells were transfected with either siPSD/ET or siScrambled as described above. 48 h post-transfection, the cells were shifted to 41ºC and incubated for 24 h. Cells were harvested and phospholipids analyzed.

4.2.4 Apoptosis and cytotoxicity assays

To measure apoptosis, MT58 cells were first plated at a density of 1.5 x 10^5 cells per well in 6 well culture dishes in the absence or presence of 30 µM LPC and incubated at 41ºC for 24, 48 or 72 h. At each time point, the culture medium was removed, cells were washed with PBS, fixed in buffered formalin, and incubated with Hoechst 33258 stain (Invitrogen) in PBS (1 in 100 dilution). Stained cells were observed using a fluorescence microscope. Cell number was established by counting the total number of cells per field. Apoptotic cells were distinguished by their small, punctuated morphology. Three random fields were counted per dish. For some experiments, MT58 and ChoK1 cells were first transfected with either siPSD/ET or siScrambled, as described above. 24 h post-transfection, the cells were shifted to 41ºC and apoptotic cells were analyzed.

To measure cellular cytotoxicity, MT58 and ChoK1 cells were plated at a density of 1.5 x 10^5 cells per well in 6-well culture dishes in the absence or presence of 30 µM LPC. Cells were incubated at 37ºC or 41ºC for 48 h. To measure cellular cytotoxicity, lactate dehydrogenase (LDH) released into the culture medium was analyzed using a commercially available kit (Cayman Chemical).

For some experiments, MT58 and ChoK1 cells were first transfected with either siPSD/ET or siScrambled, as described above. 24 h post-transfection, cells were either shifted to 41ºC or maintained at 37ºC for 48 h. LDH was measured as described.

4.2.5 Cell growth and proliferation assay

ChoK1 and MT58 cell lines were plated at 1.5 x 10^5 in 6-well culture dishes. Cells were incubated at either 37ºC or 41ºC for 24, 48 or 72 h. At the indicated times, culture medium was removed, the adherent cells were harvested with trypsin and viable cells that excluded trypan blue were counted. Cell proliferation was measured by labelling with [^{3}H]thymidine as previously described (28). Briefly, ChoK1 and MT58 cells were plated at 1.0 X 10^5 in 6-well culture dishes. After synchronizing cells in culture medium containing 0.5% fetal bovine serum, cell proliferation was stimulated with addition of culture medium containing 10% fetal bovine serum. Cells were incubated with [^{3}H]thymidine (1µCi/1.5 ml of culture medium) for 4 hours after which [^{3}H]thymidine incorporation into cellular DNA was determined.

4.2.5 Statistical analysis

Data are presented as means ± standard error mean (S.E) of three independent experiments. Comparisons between two groups were performed using a two-way *t* test. Comparisons among multiple groups were performed via one-way ANOVA. For cell growth experiments, a repeated measures one-way ANOVA was performed. In all cases, $p < 0.05$ was considered significant.

4.3 Results

4.3.1 The PC:PE ratio is reduced in MT58 cells after incubation at 37^{o}C or 41^{o}C

To determine if the PC:PE ratio influences cellular growth of MT58 cells, we quantified the cellular PC:PE ratio after incubation at either the permissive or restrictive temperatures. After incubation at the permissive temperature of 37ºC, MT58 cells showed a 25% reduction in the PC:PE ratio compared to ChoK1 cells (Figure 4.1A). However, cell growth of

MT58 cells was comparable to that of ChoK1 cells after incubation at 37ºC despite the lower phospholipid ratio (Figure 4.1B). After incubation at the restrictive temperature of 41ºC, the PC:PE ratio decreased to below 1.0 in MT58 cells (Figure 4.1A). The change in temperature resulted in complete growth arrest of MT58 cells (Figure 4.1B). That MT58 cells show a reduction in the PC:PE ratio after incubation at either temperature suggests that cell growth is not influenced by a reduction within the PC:PE ratio.

4.3.2 Silencing of PSD and ET reduces cellular phosphatidylethanolamine mass, but does not stimulate cellular growth in MT58 cells

We hypothesized if the PC:PE ratio influences membrane integrity, then increasing the ratio, by decreasing PE mass, will stabilize cellular membranes and prevent apoptosis of MT58 cells. To reduce PE mass, silencing RNA was utilized to knockdown the two key enzymes involved in PE biosynthesis, PSD and ET. Although the majority of PE is synthesized via the PSD pathway (7), we chose to knockdown both PSD and ET together to prevent utilization of recycled ethanolamine and to avoid increased utilization of ethanolamine present in the fetal bovine serum in the culture medium. Knockdown of PSD together with ET resulted in an 83% reduction of cellular PSD mRNA, and a 67% decrease in cellular ET mRNA (Figure 4.2A). Furthermore, silencing of PSD and ET resulted in 30% lower PE content in both MT58 cells and ChoK1 controls at 41^{o}C (Figure 4.2B, C). Curiously, unlike in ChoK1 cells, knockdown of PSD and ET resulted in 20% lower PC content in MT58 cells (Figure 4.2B, C). The reduction in PE mass resulted in a 1.5-fold increase of the PC:PE ratio in ChoK1 cells (Figure 4.2C) whereas the PC:PE ratio was not changed in MT58 cells (Figure 4.2B).

Interestingly, knockdown of PSD and ET in ChoK1 cells resulted in a dramatic reduction in [^{3}H]thymidine incorporation into DNA (Figure 4.3A). Incorporation of [^{3}H]thymidine into DNA was further reduced in MT58 cells expressing silencing RNA for PSD and ET compared to the scrambled controls (Figure 4.3A). This data suggests that cellular PE levels may influence cellular proliferation. However, ChoK1 cells showed unimpeded cellular growth with knockdown of PE biosynthetic enzymes (Figure 4.3B) suggesting that PC is sufficient to overcome the defect in PE biosynthesis and maintain cellular growth over a 72 h period. Cell growth arrest was observed in MT58 cells expressing either the scrambled control or the silencing RNA for PSD and ET (Figure 4.3B). All together, these data show that reduction in PE mass, in an attempt to increase the PC:PE ratio, does not stimulate cellular growth of MT58 cells.

4.3.3 Silencing of PSD and ET does not stabilize cellular membranes in MT58 cells

To assess whether a reduction of PE mass will stabilize cellular membranes and rescue cells from apoptosis, we measured the release of lactate dehydrogenase (LDH). Knockdown of PSD and ET in MT58 cells resulted in a 2-fold increase in the release of LDH compared to the scrambled control cells (Figure 4.3C). To further address whether or not decreased PE content influences membrane integrity of MT58 cells, apoptosis was measured. We found that a reduction in both membrane PC and PE in MT58 cells resulted in an increase in the percentage of apoptotic cells after incubation at the restrictive temperature (Figure 4.4A, B). However, lower PE mass in ChoK1 cells did not induce apoptosis after 24 or 48 h of incubation at the restrictive temperature (Figure 4.5A, B). Only after 72 h of incubation at the restrictive temperature did we observe a 2-fold increase in the percentage of apoptotic ChoK1 cells (Figure 4.5B).

All together, these data provide further evidence that the membrane composition of PC and PE, not the PC:PE ratio, influences cellular integrity of MT58 cells.

4.3.4 Lysophosphatidylcholine restores cellular phosphatidylcholine and phosphatidylethanolamine, but does not normalize the PC:PE ratio

In a further attempt to increase the PC:PE ratio, MT58 cells were treated with 5, 10 or 30 μM LPC. Since LPC incorporation into PC is independent of CT activity, LPC should increase the PC:PE ratio. Addition of 10 μM and 30 μM LPC resulted in a 25% and 30% increase in PC mass compared to untreated MT58 cells (Figure 4.6A) while 5 μM LPC did not affect the cellular content of PC (Fig. 4.6A). While 5 μM LPC did not change the content of cellular PE (Figure 4.6B), the addition of 10 μM and 30 μM LPC normalized PE mass in MT58 after incubation at the restrictive temperature (Figure 4.6B). Surprisingly, none of the LPC treatments restored the PC:PE ratio (Figure 4.6C). Although it was unexpected that LPC treatment did not restore the PC:PE ratio, the increase in PC (Figure 4.6A) as well as PE (Figure 4.6B) was sufficient to prevent normalization of the PC:PE ratio. Despite the lower PC:PE ratio, 30 μM LPC increased cellular proliferation as indicated by incorporation of [^{3}H]thymidine into DNA (Figure 4.6D). However, cellular proliferation was not restored to the levels observed after incubation of MT58 cells at the permissive temperature (Figure 4.6D).

4.3.5 The PC:PE ratio does not influence cellular integrity of MT58 cells.

As a measure of cellular cytotoxicity, we quantified LDH activity in the growth medium from MT58 cells incubated at the permissive and restrictive temperature. After incubation at the restrictive temperature, the medium of MT58 had 3-fold higher LDH activity than MT58 cells after

incubation at the permissive temperature (Figure 4.7). Treatment with 30 μM LPC abolished cellular cytotoxicity of MT58 cells after incubation at the restrictive temperature (Figure 4.7). That LPC treatment abolished cellular cytotoxicity to below that observed in MT58 cells incubated at the permissive temperature suggests that the composition of membrane PC and PE, not the PC:PE ratio, influences membrane integrity of MT58 cells. Furthermore, incubation of MT58 cells at the restrictive temperature with 30 μM LPC prevented the induction of apoptosis in MT58 cells (Figure 4.8A, B) suggesting that the reduced PC:PE ratio is not a contributing factor to the induction of apoptosis of MT58 cells.

4.3.6 The PC:PE ratio does not correlate with cell growth.

Correlation graphs further illustrate the relationship between cellular PC and PE content, the PC:PE ratio and cell growth and apoptosis after incubation at the restrictive temperature. We found a positive correlation between cellular PC mass and cell growth after 72 h of incubation at the restrictive temperature (R^2=0.6) (Figure 4.9A) and a strong positive correlation between the total amount of cellular PC and PE and cellular growth (R^2=0.76) (Figure 4.9B). There was no relationship found between either the PC:PE ratio, or PE content and cellular growth (Figure 4.9C, D). Furthermore, there is a strong negative correlation (R^2=0.85) between cellular PC content and the percentage of apoptotic cells after 72 h of incubation at the restrictive temperature (Figure 4.10A), as well as a strong negative correlation (R^2=0.97) between the total amount of PC and PE and apoptosis (Figure 4.10B). However, there was no relationship found between either the PC:PE ratio, or PE content and apoptosis (Figure 4.10C,D). This data confirms that cellular integrity of MT58 cells is influenced by total cellular PC and PE content.

4.4 Discussion

PC content is important for maintaining the growth and integrity of cells, and several studies have clearly demonstrated that PC-deficiency is sufficient to induce apoptosis (11,13-16). However, a low PC:PE ratio is associated with reduced membrane integrity of hepatic plasma and mitochondrial membranes in mouse models of steatohepatitis (20,25). Therefore, along with an insufficient amount of cellular PC, a reduced PC:PE molar ratio may result in loss of membrane integrity, resulting in cellular apoptosis. Thus, we utilized the MT58 cell line to study whether a lower ratio of PC to PE influences membrane integrity and apoptosis of MT58 cells. We predicted that if the PC:PE ratio were important for maintaining membrane integrity, then increasing the ratio would stabilize cellular membranes, and prevent apoptosis. The data present indicate that the main contributor of cell growth arrest and apoptosis in MT58 cells is a deficiency in membrane content of PC and PE. Correlation studies further confirmed that the total amount of PC and PE, not the PC:PE ratio, influences cellular growth and apoptosis of MT58 cells.

4.4.1 Cellular phospholipids, not the PC:PE ratio regulates cellular growth

The data outlined in this study indicates that membrane composition of PC and PE in MT58 cells, as opposed to the ratio of the two abundant phospholipids, influences cellular growth of MT58 cells. This is supported by two lines of evidence. First, MT58 cells have comparable cellular growth after incubation at the permissive temperature compared to control cells, despite a lower PC:PE ratio. Growth arrest and apoptosis of MT58 cells does not occur until after incubation at the restrictive temperature, when the concentrations of PC and PE are both reduced. Second, treatment of MT58 cells with LPC stimulated cell growth, without normalizing the PC:PE ratio indicating that the

phospholipid ratio does not influence cellular growth. A previous study has shown that depriving immortalized CWSV-1 rat hepatocytes of choline induces apoptosis [29]. CWSV-1 hepatocytes cultured in choline-deficient media showed a 50% reduction of both cellular PC mass and the PC:PE ratio (29). However, after adaptation to the choline-deficient medium, the PC:PE ratio remained reduced by 50% even though CWSV-1 cells maintained normal cellular growth and escaped apoptosis (29). This study supports that the PC:PE ratio does not influence cellular growth. In addition, the PC:PE ratio is reduced (due to increased PE mass) in rat hepatocyte cancer nodules (30), and is reduced by 50% (due to changes in both PC and PE) in normal regenerating liver (30).

A previous study from our lab demonstrated that expression of PEMT in MT58 cells (which do not express PEMT) does not stimulate cellular growth or rescue the cells from apoptosis after incubation at the restrictive temperature even though the PEMT pathway actively synthesized and normalized cellular PC (31). MT58 cells have an imbalance of PC biosynthesis and PC degradation (32). Treatment of PEMT expressing MT58 cells with a phospholipase A_2 inhibitor stimulated cellular growth showing that PEMT was unable to maintain the cellular demand for PC (33). Therefore, these studies verify that cellular proliferation is not dependent on a pre-determined PC:PE ratio, but rather is dependent on the composition of membrane phospholipids.

4.4.2 Cellular apoptosis is not regulated by changes within the PC:PE ratio

We hypothesized that if a lower PC:PE ratio caused a loss of membrane integrity resulting in cellular death of MT58 cells, normalization of the PC:PE ratio would stabilize cellular membranes and prevent apoptosis. We found that knockdown of PSD and ET did not normalize the PC:PE ratio in MT58 cells due to reduced PE and PC masses.

The reduction of both PC and PE caused a further loss of membrane integrity resulting in an enhanced onset of apoptosis. Therefore, reducing PE mass, in an attempt to increase the PC:PE ratio, did not stabilize cellular membranes of MT58 cells. Treatment of MT58 cells with LPC did not normalize the PC:PE ratio due to increased cellular content of both PC and PE. However, despite the lower PC:PE ratio, LPC treatment prevented cellular apoptosis. These results indicate that changes in the total amount of membrane phospholipids, not the PC:PE ratio, regulates cellular survival. Previous studies support this conclusion as treatment of fibroblast cell lines with short-chain ceramides have been shown to inhibit PC biosynthesis (34,35), as well as PE biosynthesis (35) leading to the induction of apoptosis. In addition, enforced expression of CTα in HeLa cells leads to increased PC biosynthesis without an increase in the total amount of cellular PC as a result of increased PC catabolism (36). Membrane PE mass is also regulated by a balance between synthesis and degradation suggesting that cells maintain a specific phospholipid profile to maintain cellular integrity (36). Furthermore, a recent study has shown that the PC:PE ratio decreases by 50% during differentiation of 3T3-L1 cells, without affecting cellular viability (37). Moreover, the change in cellular PC and PE was important for the lipid droplet formation during differentiation of the 3T3-L1 cells into adipocytes (37). This study gives further evidence that the cellular phospholipid composition, not the PC:PE ratio, is important for cellular integrity.

Curiously, knockdown of PSD and ET did not normalize the PC:PE ratio in MT58 cells due to a decrease in cellular PC mass. Silencing of the two PE biosynthetic enzymes in ChoK1 cells did not decrease cellular PC mass, and as a result, we observed the expected increase in the PC:PE ratio. It is unknown why silencing of PSD and ET would cause a reduction of cellular PC content in MT58 cells, but not in ChoK1 cells. As MT58 cells show increased PC degradation even after incubation at the restrictive temperature (32), knockdown of PSD and ET may have lead to a further imbalance of PC metabolism, which was not observed in the ChoK1 control cells.

Deletion of either the PSD or ET gene in mice is embryonic lethal (38,39). Therefore, it may be expected that knockdown of both enzymes in ChoK1 or MT58 cells would be detrimental. However, knockdown of both PSD and ET in Chok1 cells over 72 h resulted in a 30% loss of cellular PE without having an effect on membrane stability as analyzed by LDH release. ChoK1 cells expressing PSD and ET silencing RNA showed a 2-fold increase in the percentage of apoptotic cells after 72 h of incubation at 41ºC compared to ChoK1 cells expressing the scrambled control. However, the percentage of apoptotic ChoK1 cells at the restrictive temperature was minimal (4% of ChoK1 cells were apoptotic) compared to MT58 cells expressing the PSD and ET silencing RNA (80% of MT58 cells were apoptotic). Since knockdown of PSD and ET caused minimal effects in the ChoK1 cells suggests that the enhanced apoptosis and cytotoxicity observed in MT58 cells expressing PSD and ET silencing RNA was due to the loss of membrane phospholipids, and not from other detrimental effects of knocking down PSD and ET.

4.4.3 Knockdown of phosphatidylethanolamine biosynthesis does not prevent apoptosis in MT58 cells

When *Pemt*$^{-/-}$ mice are fed a choline-deficient diet, they develop rapid liver failure due to a large reduction in the PC:PE molar ratio (20). Knockdown of hepatic ET increased the PC:PE ratio from 1.0 to 1.2 and attenuated liver disease in *Pemt*$^{-/-}$ mice fed the choline-deficient diet (20). Moreover, *Pemt*$^{-/-}$ mice which lack the Mdr2 gene, which is responsible for secretion of PC into bile, did not develop severe liver failure when fed the choline-deficient diet. *Pemt*$^{-/-}$/*Mdr2*$^{-/-}$ mice were able to maintain their PC:PE ratio via increased PE degradation, and decreased PC secretion into bile and thus, these mice escaped severe liver failure (20). This study demonstrated that the PC:PE ratio influences membrane integrity and that the ratio may be a marker for cellular viability. However, the results in the current study have demonstrated that in CHO and MT-58 cells membrane stability, growth and survival are influenced by the concentrations of PC and PE, not by the PC:PE ratio. These appear to be confounding results. However, the liver cell results show only a correlation between the PC:PE ratio and plasma membrane integrity of hepatic cells. The *Pemt*$^{-/-}$/*Mdr2*$^{-/-}$ mice adjust PE metabolism to compensate for changes in the membrane phospholipid environment. The *Pemt*$^{-/-}$ mice do not adjust PE metabolism, resulting in a large increase in plasma membrane PE content (20). Therefore, knockdown of ET in *Pemt*$^{-/-}$ mice may have attenuated steatohepatitis due to the normalization of PE metabolism within the plasma membrane, as opposed to the normalization of the PC:PE ratio. In the current study, incubation of MT58 cells at the restrictive temperature reduces PE content. Therefore, impairing PE biosynthesis in MT58 cells may not stabilize cellular membranes because PE metabolism is already adjusted to accommodate the changes occurring within the membrane phospholipid environment after incubation at the restrictive temperature.

4.4.4 Conclusion

In summary, we show that incubation of MT58 cells at both the permissive and restrictive temperature results in a reduction in the PC:PE ratio. Treatment with LPC normalized cellular PC and PE content, stimulated cellular growth and rescued cells from apoptosis. Knockdown of PSD together with ET decreased PE mass and caused a further loss of cellular integrity of MT58 cells. Neither treatment normalized the PC:PE ratio. Finally, correlation studies clearly showed that the cellular amount of both PC and PE, and not the PC:PE ratio, is the main predictor of cellular growth and apoptosis of MT58 cells after incubation at the restrictive temperature. Thus, the cellular growth and survival of MT58 cells are regulated by cellular maintenance of PC and PE metabolism.

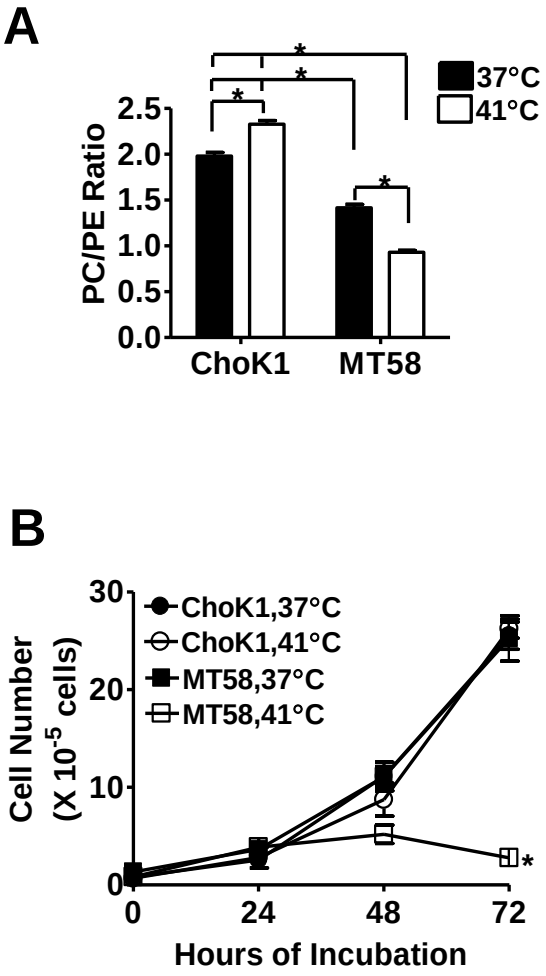

Figure 4.1 The PC:PE ratio in MT58 cells is reduced after incubation at both the restrictive and permissive temperatures. MT58 and ChoK1 control cells were incubated at either the permissive (37ºC) or restrictive (41ºC) temperatures for 24 h after which lipids were extracted. (A) The PC:PE ratio was calculated from the PC and PE masses. (B) MT58 and ChoK1 control cells were incubated at either the permissive or restrictive temperature for 24, 48 or 72 h. Cell growth was analyzed by trypan blue exclusion. All data are means ± S.E. of three independent experiments. *, $p < 0.05$

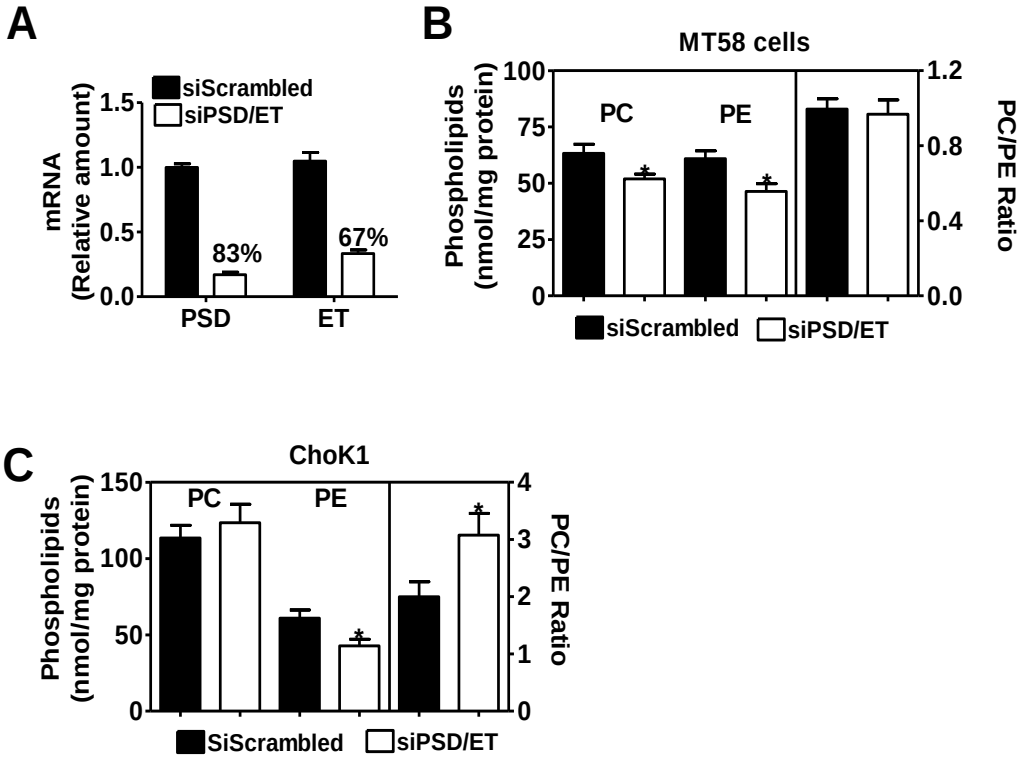

Figure 4.2 Knockdown of PSD and ET decreased the amount of cellular phosphatidylethanolamine. MT58 and ChoK1 control cells were co-transfected with silencing RNA sequences targeting phosphatidylserine decarboxylase and CTP: phosphoethanolamine cytidylyltransferase (siPSD/ET), or with scrambled silencing RNA sequence (siScrambled). (A) 48 h post-transfection, total RNA was isolated from the MT58 cells. Relative amounts of PSD and ET mRNA were determined by real-time qPCR. Data are relative to cyclophilin mRNA. (B) 48 h post-transfection, MT58 cells were shifted to the restrictive temperature (41ºC). After 24 h incubation, phosphatidylcholine (PC) and phosphatidylethanolamine (PE) concentrations were quantified. The PC:PE ratio was calculated from the PC and PE mass. (C) 48 h post transfection, ChoK1 cells were shifted to the restrictive temperature. After 24 h incubation, PC and PE concentrations were quantified. The PC:PE ratio was calculated from PC and PE mass. All data are means ± S.E. of three independent experiments. *, $p < 0.05$

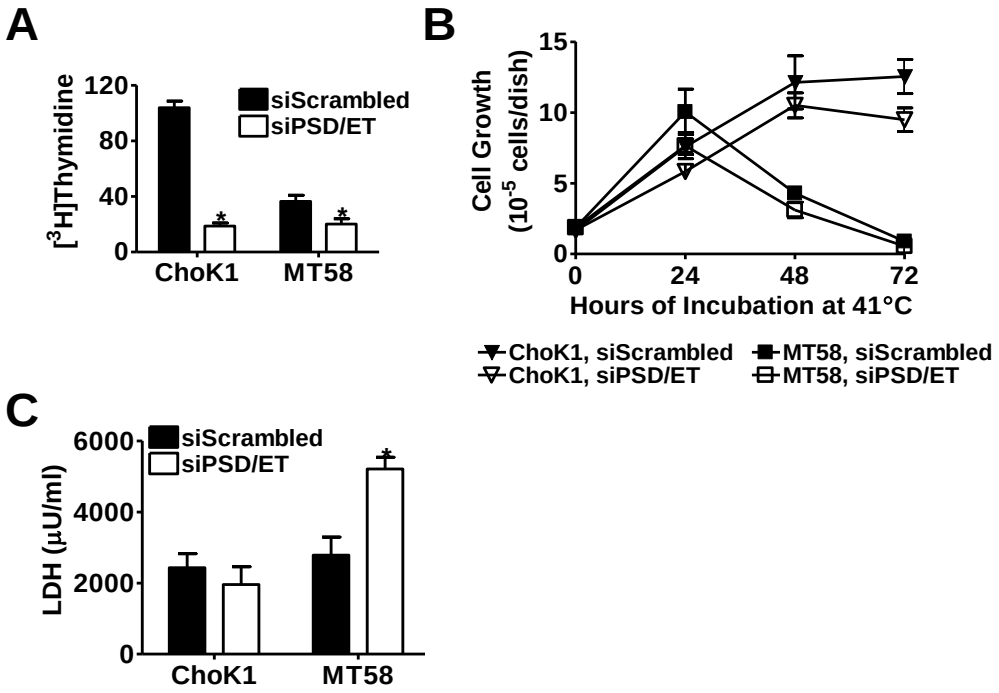

Figure 4.3 Reduction of cellular phosphatidylethanolamine does not restore cellular growth or prevent cytotoxicity in MT58 cells. MT58 and ChoK1 control cells were co-transfected with silencing RNA sequences targeting phosphatidylserine decarboxylase and CTP: phosphoethanolamine cytidylyltransferase (siPSD/ET), or with a scrambled silencing RNA sequence (siScrambled). (A) ChoK1 and MT58 were incubated at the restrictive temperature (41ºC) for 24 h. Cell proliferation was determined by incubating the cells with 1 µCi of [^{3}H] thymidine for 4 h. [^{3}H]thymidine incorporation into DNA was measured. [^{3}H]thymidine incorporation is expressed as a percentage of ChoK1 cells expressing siScrambled. (B) MT58 and ChoK1 control cells were incubated at the restrictive temperature for 24, 48 or 72 h. Cell growth was analyzed by trypan blue exclusion. (C) MT58 and ChoK1 cells were shifted to the restrictive temperature 24 h post-transfection. After 48 h of incubation at the restrictive temperature, lactate dehydrogenase (LDH) activity in the growth medium was quantified. All data are means ± S.E. of three independent experiments. *, $p < 0.05$

Figure 4.4 A reduction of cellular phosphatidylethanolamine mass does not rescue MT58 cells from apoptosis. MT58 cells were co-transfected with silencing RNA sequences targeting phosphatidylserine decarboxylase and CTP:phosphoethanolamine cytidylyltransferase (siPSD/ET), or were transfected with a scrambled silencing RNA sequence (siScrambled). MT58 cells were shifted to the restrictive (41ºC) temperature 24 h post-transfection and were incubated at the restrictive temperature for 24, 48 or 72 h. After each time point, MT58 cells were fixed and stained with Hoechst 33258 and cells were visualized by fluorescence. Apoptotic bodies were counted and expressed as a percentage of total cells. (A) Typical pictures of MT58 cells stained with Hoechst 33258 at each time point is displayed in the top panel. (B) The graph represents the percentage of MT58 apoptotic cells at each time point. All data are means ± S.E. of three independent experiments. *, $p < 0.05$

Figure 4.4 A

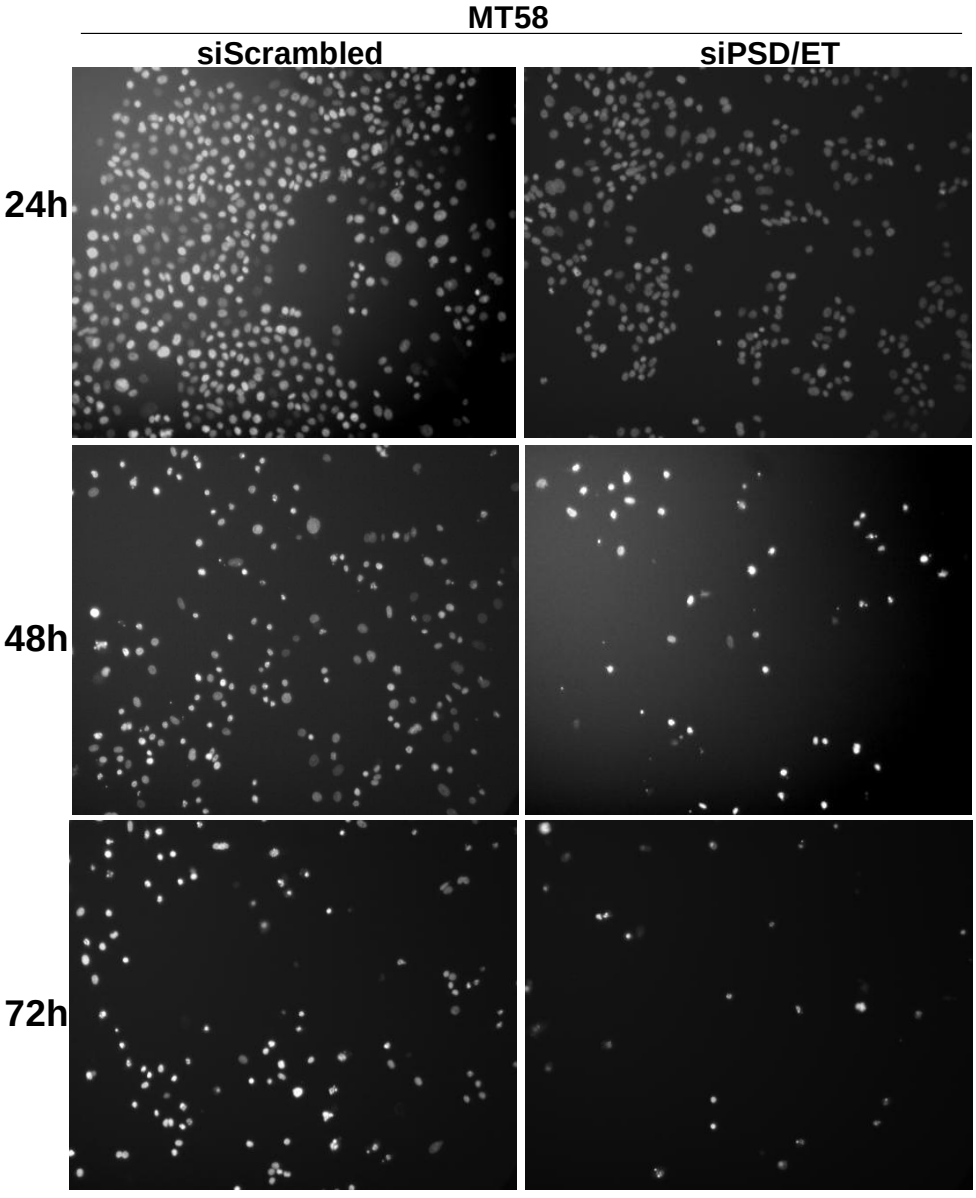

Figure 4.4 B

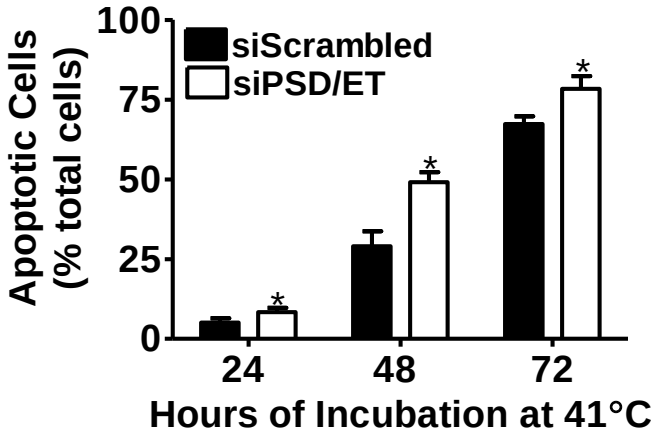
Apoptotic Cells
(% total cells)
100
75
50
25
0
siScrambled
siPSD/ET
*
*
*
24
48
72
Hours of Incubation at 41°C

Figure 4.5 A reduction of cellular phosphatidylethanolamine mass does not induce apoptosis in ChoK1 cells. ChoK1 cells were co-transfected with silencing RNA sequences targeting phosphatidylserine decarboxylase and CTP:phosphoethanolamine cytidylyltransferase (siPSD/ET), or were transfected with a scrambled silencing RNA sequence (siScrambled). ChoK1 cells were shifted to the restrictive (41ºC) temperature 24 h post-transfection and were incubated at the restrictive temperature for 24, 48 or 72 h. After each time point, ChoK1 cells were fixed and stained with Hoechst 33258 and cells were visualized by fluorescence. Apoptotic bodies were counted and expressed as a percentage of total cells. (A) Typical pictures of ChoK1 cells stained with Hoechst 33258 at each time point is displayed in the top panel. (B) The graph represents the percentage of ChoK1 apoptotic cells at each time point. All data are means ± S.E. of three independent experiments. *, $p < 0.05$

Figure 4.5 A

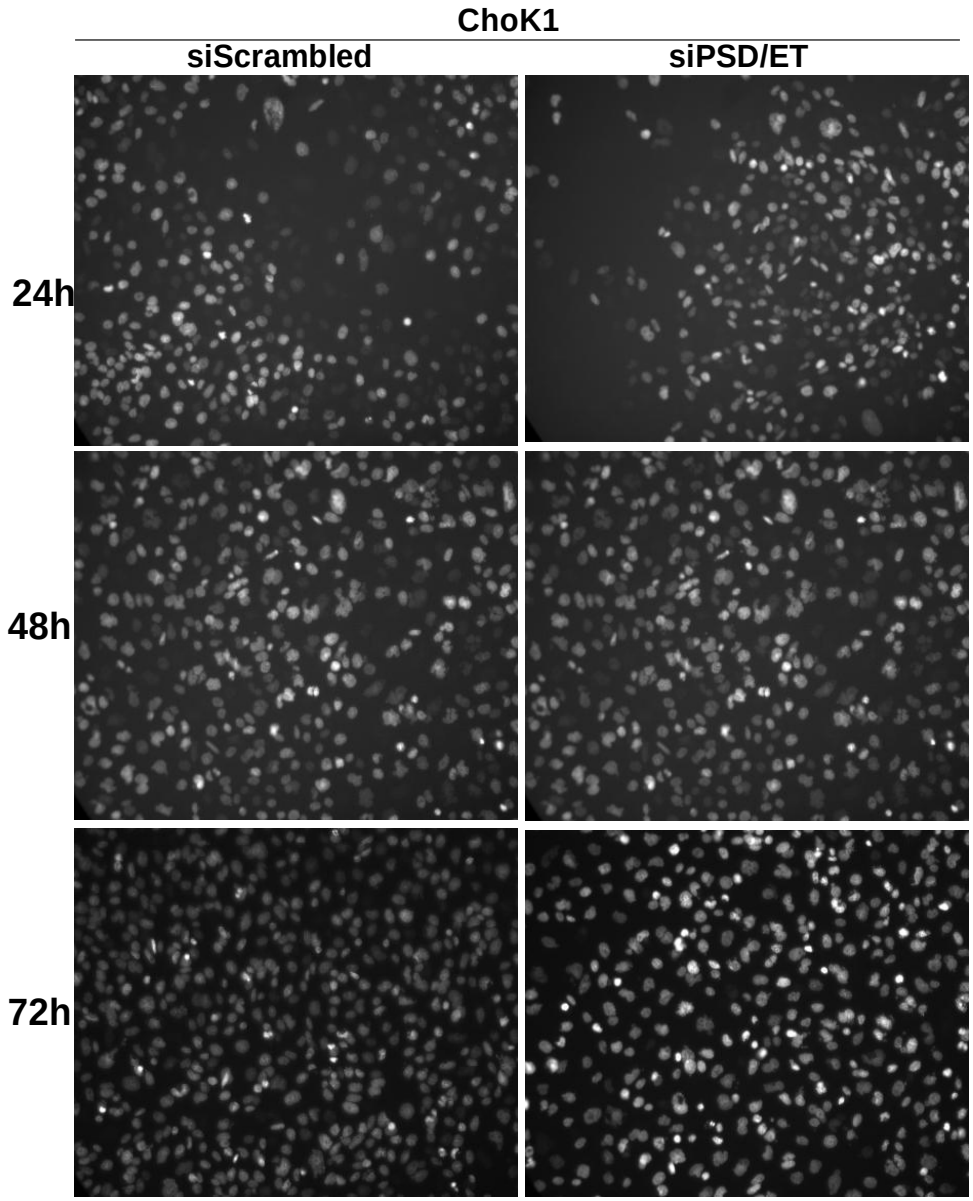

Figure 4.5 B

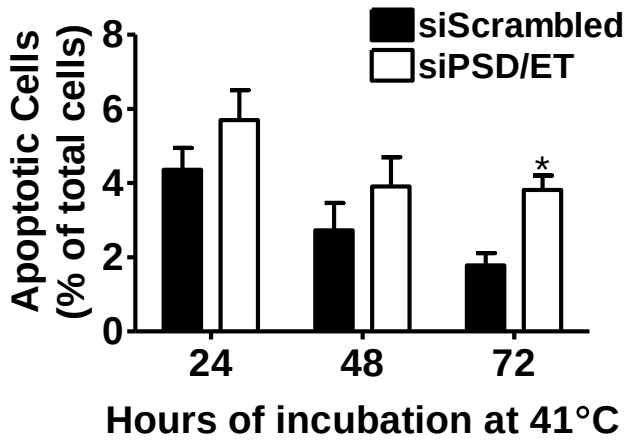
siScrambled
siPSD/ET
Apoptotic Cells
(% of total cells)
0
2
4
6
8
*
24
48
72
Hours of incubation at 41°C

Figure 4.6 Lysophosphatidylcholine normalizes the amount of cellular phosphatidylcholine, and stimulates cell growth without normalizing the PC:PE ratio. MT58 cells were incubated for 24 h at either the permissive (37ºC) or restrictive (41ºC) temperatures. For some experiments, MT58 cells were treated with 5, 10, or 30 µM lysophosphatidylcholine (LPC) and immediately incubated at the restrictive temperature for 24 h. (A, B) Total phosphatidylcholine (PC) and phosphatidylethanolamine (PE) mass was quantified. (C) The PC:PE ratio was calculated from the PC and PE masses. (D) MT58 cells were incubated at either the permissive (37ºC) or restrictive temperature (41ºC). For some experiments, 30 µM lysophosphatidylcholine (LPC) was added to MT58 cells immediately before incubation at the restrictive temperature for 24 h. After 24 h incubation at either temperature, cells were labelled with 1 µCi of [^{3}H]thymidine for 4 h after which [^{3}H]thymidine incorporation into DNA was measured. [^{3}H]thymidine incorporation is expressed as a percentage of MT58 cells after incubation at the permissive temperature. All data are means ± S.E. of three independent experiments. *, $p < 0.05$ compared to MT58 cells incubated at 37ºC. ^, $p < 0.05$ compared to untreated MT58 cells incubated at 41ºC.

Figure 4.6

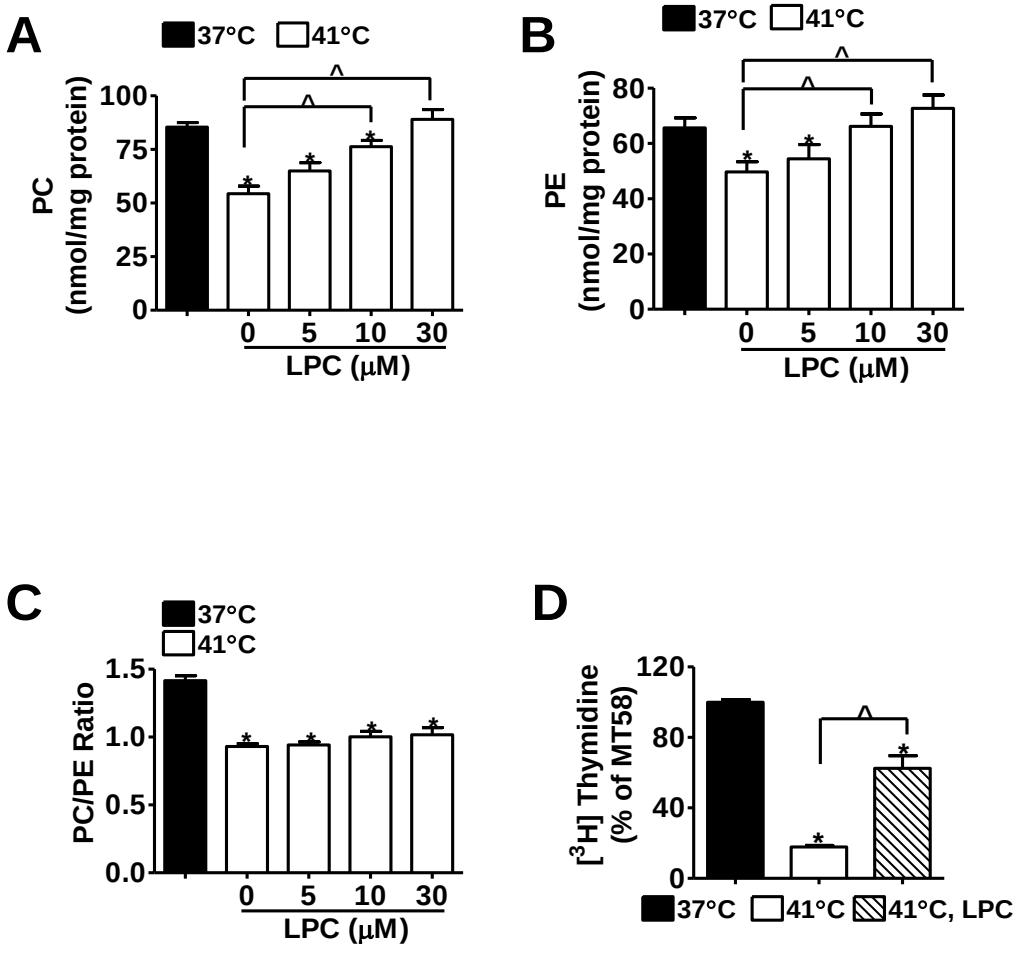
A
37°C
41°C
PC
(nmol/mg protein)
100
75
50
25
0
0
5
10
30
LPC (μM)
B
37°C
41°C
PE
(nmol/mg protein)
80
60
40
20
0
0
5
10
30
LPC (μM)
C
37°C
41°C
PC/PE Ratio
1.5
1.0
0.5
0.0
0
5
10
30
LPC (μM)
D
[3H] Thymidine
(% of MT58)
120
80
40
0
37°C
41°C
41°C, LPC

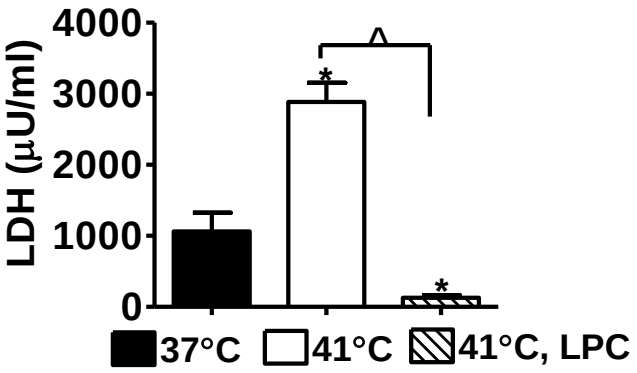

Figure 4.7 Despite the lower PC:PE ratio, lysophosphatidylcholine prevents cellular cytotoxicity of MT58 cells. MT58 cells were incubated at either the permissive (37ºC) or restrictive temperature (41ºC) for 48 h. Immediately before incubation at the restrictive temperature, 30 µM lysophosphatidylcholine (LPC) was added to the MT58 cells. Lactate dehydrogenase (LDH) activity in the growth medium was quantified as a measure of cellular cytotoxicity. All data are means ± S.E. of three independent experiments. *, $p < 0.05$ compared to MT58 cells incubated at 37ºC. ^, $p < 0.05$ compared to untreated MT58 cells incubated at 41ºC.

Figure 4.8 Despite the lower PC:PE ratio, lysophosphatidylcholine rescues MT58 cells from apoptosis. MT58 cells were incubated at the restrictive temperature for 24, 48, or 72 h in the absence or presence of 30 μM LPC. (A) MT58 cells were fixed and stained with Hoechst 33258 stain and visualized by fluorescent microscopy. A typical picture of each time point is displayed. (B) Apoptotic bodies stained with Hoechst 33258 were counted and expressed as percentage of total cells. All data are means ± S.E. of three independent experiments. ^, $p < 0.05$ compared to untreated MT58 cells incubated at 41ºC.

Figure 4.8 A

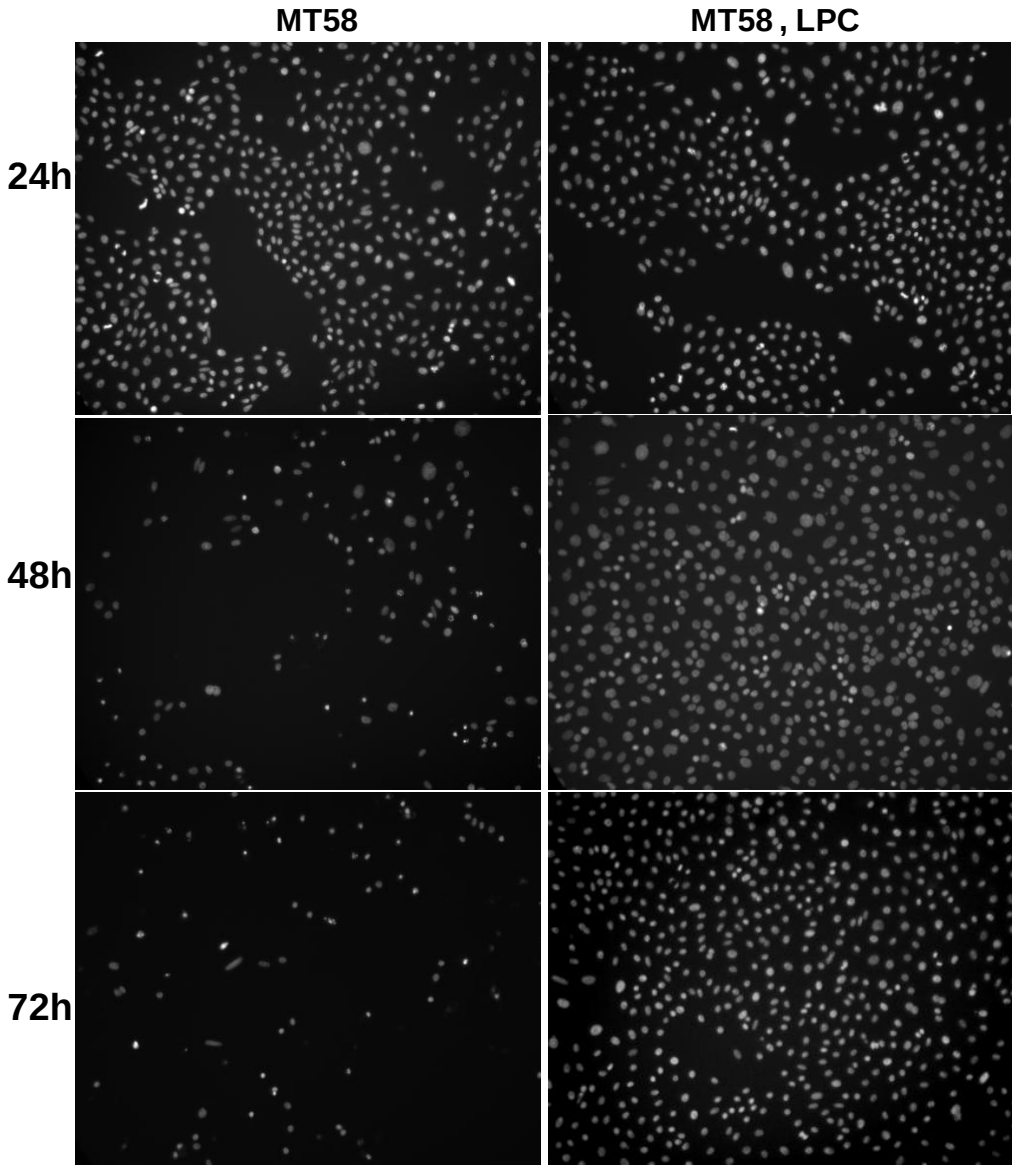

Figure 4.8 B

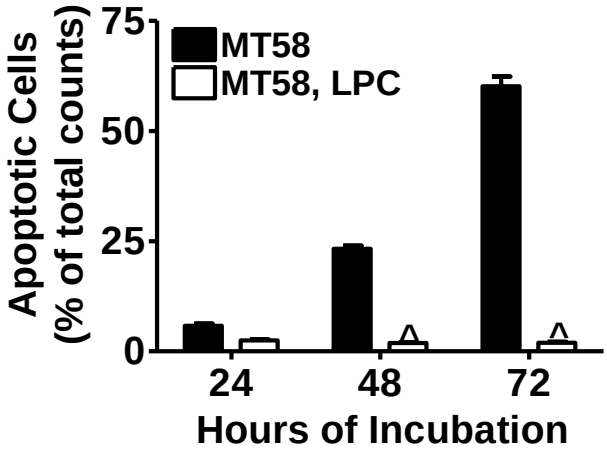
Apoptotic Cells
(% of total counts)
75
50
25
0
MT58
MT58, LPC
24
48
72
Hours of Incubation

Figure 4.9 Total amount of cellular phosphatidylcholine and phosphatidylethanolamine correlates with cell growth after incubation at the restrictive temperature. Correlation curves include data values from: untreated MT58 cells; MT58 cells treated with 30 μM lysophosphatidylcholine (LPC); and MT58 cells which were co-transfected with silencing RNA sequences targeting both phosphatidylserine decarboxylase and CTP:phosphoethanolamine cytidylyltransferase (siPSD/ET); MT58 cells transfected with a scrambled silencing RNA sequence (siScrambled); untreated ChoK1 controls; and ChoK1 cells transfected with siPSD/ET or siScrambled. (A) Correlation between cellular phosphatidylcholine (PC) mass and cell growth after 72 h incubation at the restrictive temperature. R^2=0.60, $p < 0.05$. (B) Correlation between the total cellular mass of both PC and PE and cell growth after 72 h incubation at the restrictive temperature. R^2=0.76, $p < 0.05$. (C) Correlation between the PC:PE ratio and cell growth after 72 h incubation at the restrictive temperature. R^2=0.42, n.s. (D) Correlation between cellular PE mass and cellular growth after incubation at the restrictive temperature for 72 h. R^2=0.27, n.s. (n.s. denotes no significance). Figures legends in (A) are representative for all graphs.

Figure 4.9

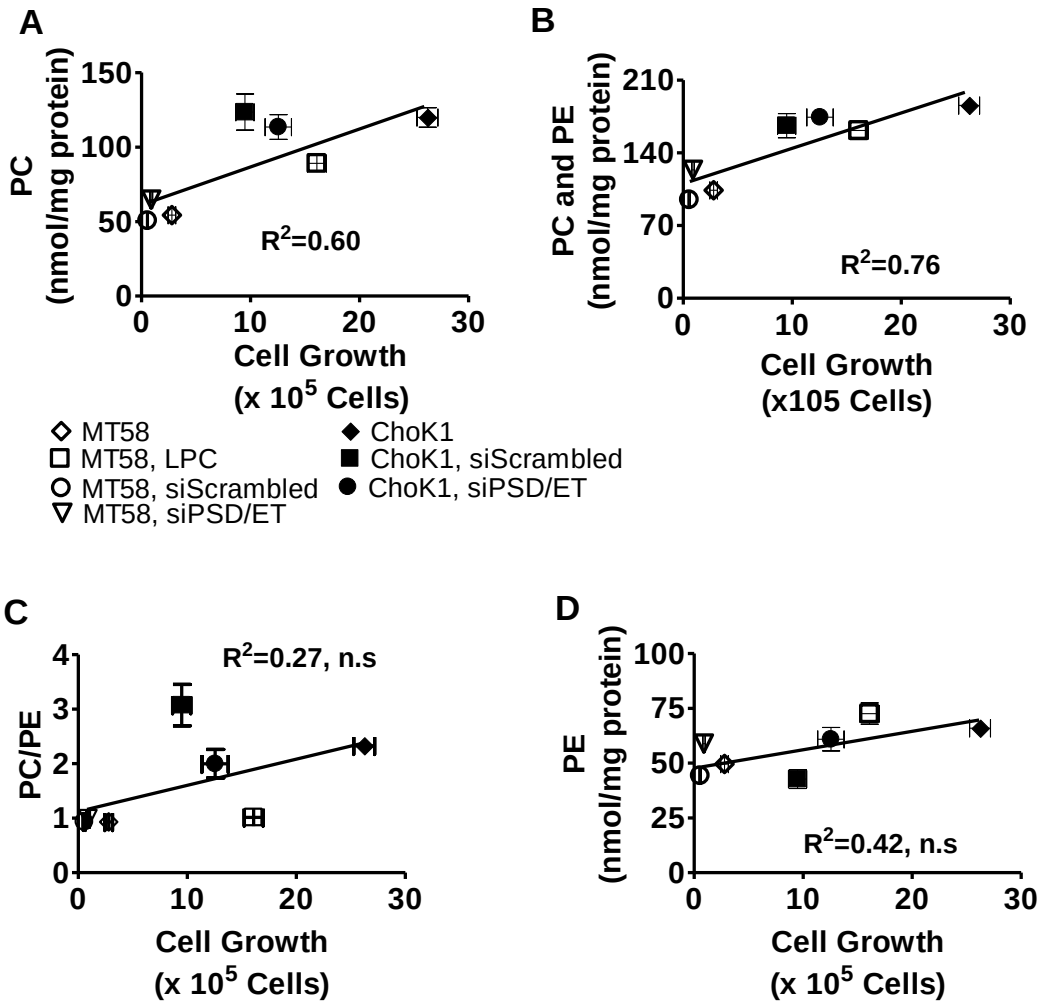
A
PC (nmol/mg protein)
150
100
50
0
0
10
20
30
Cell Growth (x 10^5 Cells)
R^2=0.60
B
PC and PE (nmol/mg protein)
210
140
70
0
0
10
20
30
Cell Growth (x105 Cells)
R^2=0.76
MT58
MT58, LPC
MT58, siScrambled
MT58, siPSD/ET
ChoK1
ChoK1, siScrambled
ChoK1, siPSD/ET
C
PC/PE
4
3
2
1
0
0
10
20
30
Cell Growth (x 10^5 Cells)
R^2=0.27, n.s
D
PE (nmol/mg protein)
100
75
50
25
0
0
10
20
30
Cell Growth (x 10^5 Cells)
R^2=0.42, n.s

Figure 4.10 Total amount of cellular phosphatidylcholine and phosphatidylethanolamine correlates with cellular apoptosis after incubation at the restrictive temperature. Correlation curves include data values from: untreated MT58 cells; MT58 cells treated with 30 μM lysophosphatidylcholine (LPC); and MT58 cells which were co-transfected with silencing RNA sequences targeting both phosphatidylserine decarboxylase and CTP:phosphoethanolamine cytidylyltransferase (siPSD/ET); MT58 cells transfected with a scrambled silencing RNA sequence (siScrambled); and ChoK1 cells transfected with siPSD/ET or siScrambled. (A) Correlation between cellular PC mass and the percentage of apoptotic cells after 72 h incubation at the restrictive temperature. R^2=0.85, $p < 0.05$. (B) Correlation between the total cellular mass of both PC and PE and the percentage of apoptotic cells after 72 h incubation at the restrictive temperature. R^2=0 .97, $p < 0.05$. (C) Correlation between the PC:PE ratio and the percentage of apoptotic cells after 72 h incubation at the restrictive temperature. R^2=0.45, n.s. (D) Correlation between cellular PE mass and the percentage of apoptotic cells after 72 h incubation at the restrictive temperature. R^2=0.23, n.s. (n.s. denotes no significance). Figure legends in (A) are representative for all graphs.

Figure 4.10

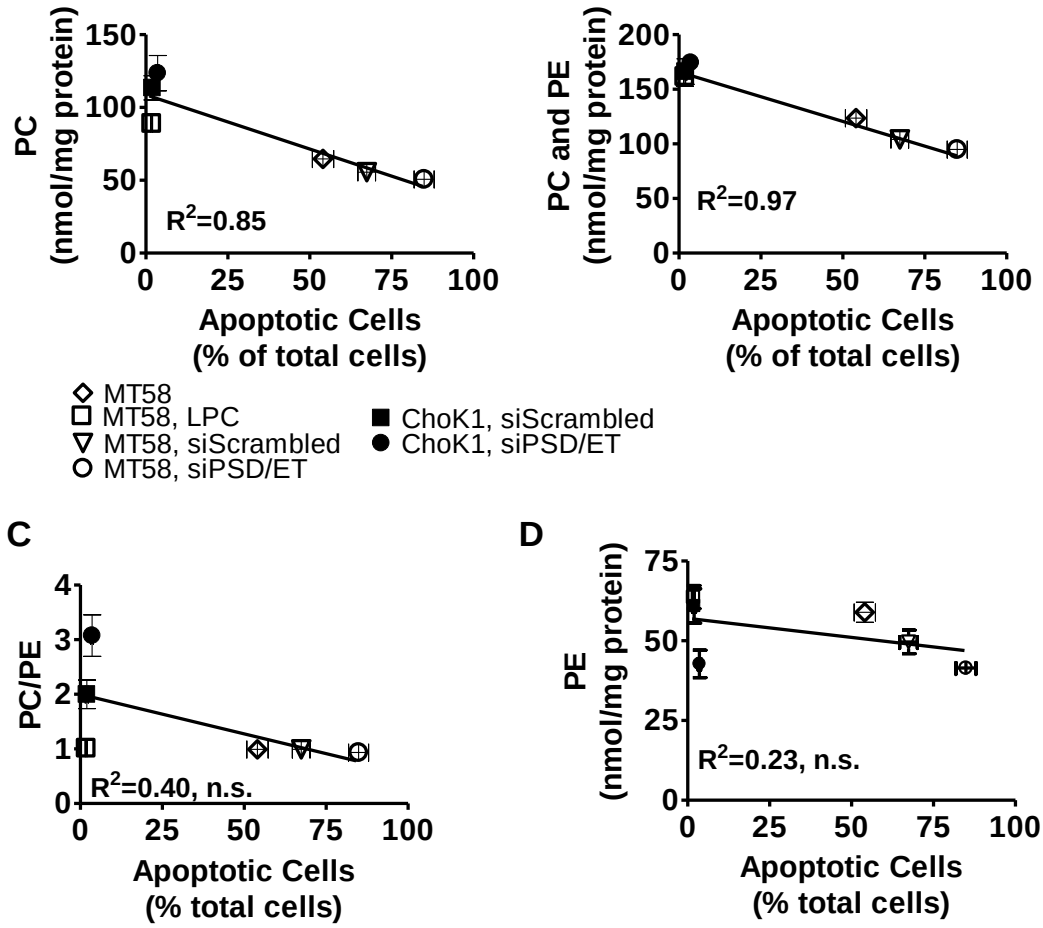
PC
(nmol/mg protein)
150
100
50
0
R2=0.85
0
25
50
75
100
Apoptotic Cells
(% of total cells)
PC and PE
(nmol/mg protein)
200
150
100
50
0
R2=0.97
0
25
50
75
100
Apoptotic Cells
(% of total cells)
MT58
MT58, LPC
MT58, siScrambled
MT58, siPSD/ET
ChoK1, siScrambled
ChoK1, siPSD/ET
C
PC/PE
4
3
2
1
0
R2=0.40, n.s.
0
25
50
75
100
Apoptotic Cells
(% total cells)
D
PE
(nmol/mg protein)
75
50
25
0
R2=0.23, n.s.
0
25
50
75
100
Apoptotic Cells
(% total cells)

4.5 References

1. Kent, C. (1995) *Annu Rev Biochem* **64**, 315-343

2. Kennedy, E. P., and Weiss, S. B. (1956) *J Biol Chem* **222**, 193-214

3. Vance DE and Vance JE (2008) Phospholipid biosynthesis in eukaryotes. in *Biochemistry of Lipids, Lipoproteins, and Membranes, 5th Edition* (Vance DE and Vance JE ed.), Elsevier, Amsterdam. pp 213-244

4. Karim, M., Jackson, P., and Jackowski, S. (2003) *Biochim Biophys Acta* **1633**, 1-12

5. Vance, D. E., and Ridgway, N. D. (1988) *Prog Lipid Res* **27**, 61-79

6. Schuiki, I., and Daum, G. (2009) *IUBMB Life* **61**, 151-162

7. Miller, M. A., and Kent, C. (1986) *J Biol Chem* **261**, 9753-9761

8. Esko, J. D., Nishijima, M., and Raetz, C. R. (1982) *Proc Natl Acad Sci U S A* **79**, 1698-1702

9. Esko, J. D., Wermuth, M. M., and Raetz, C. R. (1981) *J Biol Chem* **256**, 7388-7393

10. Esko, J. D., and Raetz, C. R. (1980) *Proc Natl Acad Sci U S A* **77**, 5192-5196

11. Cui, Z., Houweling, M., Chen, M. H., Record, M., Chap, H., Vance, D. E., and Terce, F. (1996) *J Biol Chem* **271**, 14668-14671

12. van der Sanden, M. H., Houweling, M., van Golde, L. M., and Vaandrager, A. B. (2003) *The Biochemical journal* **369**, 643-650

13. Zweigner, J., Jackowski, S., Smith, S. H., Van Der Merwe, M., Weber, J. R., and Tuomanen, E. I. (2004) *J Exp Med* **200**, 99-106

14. van der Luit, A. H., Budde, M., Ruurs, P., Verheij, M., and van Blitterswijk, W. J. (2002) *J Biol Chem* **277**, 39541-39547

15. Boggs, K., Rock, C. O., and Jackowski, S. (1998) *Biochim Biophys Acta* **1389**, 1-12

16. Anthony, M. L., Zhao, M., and Brindle, K. M. (1999) *J Biol Chem* **274**, 19686-19692

17. Yen, C. L., Mar, M. H., and Zeisel, S. H. (1999) *FASEB J* **13**, 135-142

18. Baburina, I., and Jackowski, S. (1998) *J Biol Chem* **273**, 2169-2173

19. Wang, L., Magdaleno, S., Tabas, I., and Jackowski, S. (2005) *Mol Cell Biol* **25**, 3357-3363

20. Li, Z., Agellon, L. B., Allen, T. M., Umeda, M., Jewell, L., Mason, A., and Vance, D. E. (2006) *Cell Metab* **3**, 321-331

21. Ji, C., Shinohara, M., Vance, D., Than, T. A., Ookhtens, M., Chan, C., and Kaplowitz, N. (2008) *Alcohol Clin Exp Res* **32**, 1049-1058

22. Mas, E., Danjoux, M., Garcia, V., Carpentier, S., Segui, B., and Levade, T. (2009) *PLoS One* **4**, e7929

23. Fast, D. G., and Vance, D. E. (1995) *Biochim Biophys Acta* **1258**, 159-168

24. Lomnitski, L., Oron, L., Sklan, D., and Michaelson, D. M. (1999) *J Neurosci Res* **58**, 586-592

25. Caballero, F., Fernandez, A., Matias, N., Martinez, L., Fucho, R., Elena, M., Caballeria, J., Morales, A., Fernandez-Checa, J. C., and Garcia-Ruiz, C. (2010) *J Biol Chem* **285**, 18528-18536

26. Folch, J., Lees, M., and Sloane Stanley, G. H. (1957) *J Biol Chem* **226**, 497-509

27. Zhou, X., and Arthur, G. (1992) *J Lipid Res* **33**, 1233-1236

28. Banchio, C., Schang, L. M., and Vance, D. E. (2003) *J Biol Chem* **278**, 32457-32464

29. Zeisel, S. H., Albright, C. D., Shin, O. H., Mar, M. H., Salganik, R. I., and da Costa, K. A. (1997) *Carcinogenesis* **18**, 731-738

30. Abel, S., Smuts, C. M., de Villiers, C., and Gelderblom, W. C. (2001) *Carcinogenesis* **22**, 795-804

31. Houweling, M., Cui, Z., and Vance, D. E. (1995) *J Biol Chem* **270**, 16277-16282

32. Testerink, N., van der Sanden, M. H., Houweling, M., Helms, J. B., and Vaandrager, A. B. (2009) *J Lipid Res* **50**, 2182-2192

33. Waite, K. A., and Vance, D. E. (2000) *J Biol Chem* **275**, 21197-21202

34. Allan, D. (2000) *The Biochemical journal* **345 Pt 3**, 603-610

35. Bladergroen, B. A., Bussiere, M., Klein, W., Geelen, M. J., Van Golde, L. M., and Houweling, M. (1999) *Eur J Biochem* **264**, 152-160

36. Baburina, I., and Jackowski, S. (1999) *J Biol Chem* **274**, 9400-9408

37. Horl, G., Wagner, A., Cole, L. K., Malli, R., Reicher, H., Kotzbeck, P., Kofeler, H., Hofler, G., Frank, S., Bogner-Strauss, J. G., Sattler, W., Vance, D. E., and Steyrer, E. (2011) *J Biol Chem* **286**, 17338-17350

38. Steenbergen, R., Nanowski, T. S., Beigneux, A., Kulinski, A., Young, S. G., and Vance, J. E. (2005) *J Biol Chem* **280**, 40032-40040

39. Fullerton, M. D., Hakimuddin, F., and Bakovic, M. (2007) *Mol Cell Biol* **27**, 3327-3336

CHAPTER 5

Summary and Future Directions

5.1 Conclusions

Recent studies have suggested that a deficiency in hepatic PC, and/or the enzymes involved in PC biosynthesis could play an important role in the pathogenesis of non-alcoholic steatohepatitis (NASH) (1-3). The generation of liver-specific CTα knockout (LCTα$^{-/-}$) mice have outlined the importance of CTα in controlling secretion of very-low-density lipoproteins (VLDL) (4) and impaired VLDL secretion is associated with the pathogenesis of NASH (5-7). Therefore, in chapters 2 and 3, we utilized LCTα$^{-/-}$ mice to investigate the relationship between impaired hepatic PC biosynthesis and NASH.

Before investigating the relationship between impaired hepatic PC homeostasis and NASH, it was necessary to determine whether LCTα$^{-/-}$ mice developed NASH. Surprisingly, within one week of HF feeding, CTα-deficient livers developed moderate NASH as determined by elevated levels of plasma alanine aminotransferase, increased hepatic gene expression of inflammation markers, and clinical assessment of liver histology which revealed the presence of histological markers associated with NASH (steatosis, inflammation and hepatocyte ballooning degeneration).

Hepatic triacylglycerol (TG) accumulation contributes to the “first hit” of NASH development. To elucidate the mechanisms responsible for hepatic steatosis in CTα-deficient livers, we utilized *in vivo* radiolabelling, analyzed hepatic gene and protein expression, and measured various plasma parameters. Our data indicated that the development of hepatic steatosis in CTα-deficient livers was largely attributed to impaired TG secretion, as *de novo* lipogenesis was unchanged by LCTα deficiency. These data support earlier findings that CTα is important for controlling VLDL secretion (4,8). Additionally, LCTα$^{-/-}$ mice showed reduced fatty acid uptake and enhanced fatty acid oxidation, possibly as an attempt to eliminate excess hepatic TG. Recent studies have demonstrated that

LDL- and HDL-associated PC is converted to TG in hepatocytes via the combined action of PC-PLC and diacylglycerol acyltransferase 2 (9,10). The conversion of LDL- and HDL-associated PC to hepatic TG may also be a major contributor in the development of hepatic steatosis in LCTα$^{-/-}$ mice. The physiological importance of LDL- and HDL-associated PC in maintaining hepatic TG is being investigated (van der Veen, J., personal communication).

Along with increased levels of hepatic TG, LCTα$^{-/-}$ mice showed a 2-fold increase in hepatic diacylglycerol (DAG) and ceramide. Hepatic steatosis is strongly associated with insulin resistance in both animals and humans (11-13). Furthermore, both elevated levels of hepatic DAG and ceramide have been implicated in impaired insulin signalling (reviewed in (14,15)). However, despite the development of hepatic steatosis in response to LCTα deficiency, LCTα$^{-/-}$ mice were not insulin resistant as indicated by the insulin and glucose tolerance tests. In addition, the pyruvate tolerance test indicated that LCTα$^{-/-}$ livers were not insulin resistant after one week of HF feeding. This result is not surprising since one week of HF feeding may not be sufficient to induce insulin resistance. Furthermore, hepatic steatosis and insulin resistance may develop independently of each other as mice which over-express DGAT in the liver develop hepatic steatosis without developing insulin resistance (16). It would be interesting to determine whether the DAG and ceramide species which accumulate in CTα-deficient livers are active and involved in hepatic signalling pathways.

The transition of hepatic steatosis to NASH occurs from a “second hit” which involves cellular stresses, such as ER stress, leading to hepatocellular injury. Hepatic genes involved in inflammation were increased by LCTα deficiency indicating that CTα-deficient livers are susceptible to systemic inflammation, resulting in NASH. Oxidative stress and ER stress were not detected after one week of HF feeding suggesting

that these cellular stresses are not involved in the development of NASH in CTα-deficient livers. Previous studies have demonstrated that a reduced ratio of PC to phosphatidylethanolamine (PE) compromises hepatic membranes leading to the transition of hepatic steatosis to NASH (17). However, the hepatic PC:PE ratio is comparable between LCTα$^{-/-}$ mice and floxed mice indicating that a reduced PC:PE ratio does not contribute to the pathogenesis of NASH in CTα-deficient livers. Since this study has focused on the pathogenesis of NASH after only 7 days of HF feeding, it may be interesting to prolong the feeding study to elucidate possible mechanisms involved in the development of NASH which may not have developed during the first week of HF feeding. For instance, fatty acid oxidation is an important source of reactive oxygen species (18,19). Reactive oxygen species deplete cells of ATP, stimulates the release of proinflammatory cytokines, and promotes hepatic membrane destruction by lipid peroxidation (18,20). CTα-deficient livers have increased fatty acid oxidation as indicated by elevated levels of plasma ketone bodies. Therefore, it is surprising that CTα-deficient livers do not show signs of oxidative stress after one week of HF feeding. However, oxidative stress may be a more prominent contributor to the pathogenesis of NASH in CTα-deficient livers after 10 weeks of HF feeding.

As LCTα$^{-/-}$ mice developed NASH within one week of HF feeding, we were interested to investigate whether impaired PC biosynthesis played a direct role in the pathogenesis of NASH. In an attempt to improve hepatic PC and attenuate NASH, LCTα$^{-/-}$ mice were treated with various metabolites of PC (lysophosphatidylcholine (LPC), CDP-choline, choline and betaine), all of which may be incorporated into hepatic PC independently of CTα. LCTα$^{-/-}$ mice were also treated with adenoviruses expressing CTα which should stimulate active hepatic PC biosynthesis and prevent NASH. Surprisingly, despite normalization of hepatic PC, neither CDP-choline nor LPC prevented NASH. Furthermore, although ectopic expression of CTα prevented hepatic steatosis in CTα-deficient

livers, the development of NASH was not prevented. These results indicated that impaired PC biosynthesis reduced hepatic TG secretion which increased the susceptibility of CTα-deficient livers to develop NASH. However, impaired PC biosynthesis does not play a direct role in the pathogenesis of NASH in LCTα$^{-/-}$ mice.

Betaine supplementation prevented hepatic steatosis, partially reduced the levels of plasma alanine aminotransferase and prevented portal inflammation (as determined by clinical assessment of liver histology) in LCTα$^{-/-}$ mice, without normalization of hepatic PC content. Previous studies have shown that betaine is beneficial for prevention of NASH and alcoholic steatohepatitis (21-23). Furthermore, betaine has been shown to prevent hepatic steatosis in human patients with NASH (24). Therefore, it is not surprising that betaine improved hepatic steatosis, and partially improved NASH in CTα-deficient livers. Betaine has been shown to decrease hepatic protein and mRNA levels of sterol regulatory element binding protein 1c in models of NASH and alcoholic steatohepatitis suggesting that dietary betaine may decrease lipogenesis (21,23). LCTα$^{-/-}$ mice showed improved hepatic TG and DAG with betaine treatment indicating that betaine may have reduced hepatic lipogenesis in CTα-deficient livers. The mechanism involved in the regulation of hepatic mRNA and protein levels of sterol regulatory element binding protein 1c by betaine remain to be elucidated.

Interestingly, the hepatic mass of ceramide in LCTα$^{-/-}$ mice was double that in floxed controls. None of the treatments we used in this study normalized hepatic ceramide levels or fully prevented the development of NASH. In addition, our results show a positive correlation between hepatic levels of ceramide and the pathology score of NAFLD. Other studies in murine models of NASH also reported an accumulation of hepatic ceramide (25-27); however, a cause-effect relationship between the hepatic ceramide content and the progression to NASH remains

unknown. Future work should elucidate the mechanisms involved in ceramide accumulation, and should clarify the importance of ceramide accumulation in CTα-deficient livers.

In chapter 4, we utilized the mutant 58 (MT58) Chinese hamster ovary cell line to investigate whether cellular growth and integrity is influenced by a reduced PC:PE ratio. We first determined whether the PC:PE ratio is reduced in MT58 cells after incubation at the restrictive temperature. Interestingly, the PC:PE ratio was significantly reduced after incubation at both the permissive and restrictive temperatures. That the PC:PE ratio was reduced after incubation at the permissive temperature suggests the PC:PE ratio does not influence cellular growth or integrity of MT58 cells. Nevertheless, we hypothesized that if a reduced PC:PE ratio does influence cellular integrity of MT58 cells, then increasing the PC:PE ratio should stabilize cellular membranes and rescue MT58 cells from cellular death. In an attempt to increase the cellular PC:PE ratio, the MT58 cells were treated with silencing RNA to knockdown the two key enzymes involved in PE biosynthesis (phosphatidylserine decarboxylase and CTP:phosphoethanolamine cytidylyltransferase). Knockdown of both PE biosynthetic enzymes did not increase the PC:PE ratio in MT58 cells due to a reduction in cellular levels of both PE and PC. Furthermore, the reduction in both membrane phospholipids resulted in a further loss of membrane integrity and enhanced apoptosis in MT58 cells after incubation at the restrictive temperature. In a further attempt to increase the PC:PE ratio, MT58 cells were treated with LPC. LPC normalized cellular PC mass, stimulated cellular growth and rescued MT58 cells from apoptosis. However, the PC:PE ratio was not normalized with LPC due to an increase in PE mass. Furthermore, LPC prevented the release of lactate dehydrogenase from MT58 cells indicating that the total amount of membrane PC and PE, not a reduced PC:PE ratio, influences membrane integrity. These data show that manipulation of the PC:PE ratio will not

rescue MT58 cells from apoptosis since cellular growth and integrity is not influenced by the PC:PE ratio.

Although our results show that a reduced PC:PE ratio does not influence cellular integrity, a reduced PC:PE ratio has been demonstrated to compromise hepatic membranes resulting in NASH in choline-deficient mice lacking phosphatidylethanolamine *N*-methyltransferase (PEMT) (17). Interestingly, along with lower levels of membrane PC, plasma membrane PE levels were highly elevated in *Pemt*$^{-/-}$ mice fed a choline-deficient diet (17). Although there is a correlation between the PC:PE ratio and the development of NASH, the transition from hepatic steatosis to NASH in choline-deficient *Pemt*$^{-/-}$ mice may result from changes in the total amount of hepatic PC and PE. Future research should focus on determining the actual role of a reduced PC:PE ratio in the development of NASH. It would be interesting to investigate the role of the PC:PE ratio in HF-fed LCTα$^{-/-}$ mice and *Pemt*$^{-/-}$ mice which are not fed a choline-deficient diet. The PC:PE ratio may be important in organelle membranes and a reduced PC:PE ratio may be associated with organellar dysfunction. For instance, mice fed a methionine and choline deficient diet show a reduced PC:PE ratio within mitochondrial membranes resulting in mitochondrial dysfunction (25).

In summary, this thesis describes a comprehensive study investigating the direct role of impaired PC biosynthesis in the pathogenesis of NASH. We show that impaired PC biosynthesis indirectly contributes to the pathogenesis of NASH via reduced hepatic TG secretion. The development of hepatic steatosis increases the susceptibility of CTα-deficient livers to the pathogenesis of NASH. However, reduced levels of hepatic PC may not play a direct role in the transition from hepatic steatosis to NASH. This thesis has also shown that the cellular integrity of MT58 cells is influenced by the total amount of both cellular PC and PE, not by a reduced PC:PE ratio.

5.2 References

1. Puri, P., Baillie, R. A., Wiest, M. M., Mirshahi, F., Choudhury, J., Cheung, O., Sargeant, C., Contos, M. J., and Sanyal, A. J. (2007) *Hepatology* **46**, 1081-1090

2. Song, J., da Costa, K. A., Fischer, L. M., Kohlmeier, M., Kwock, L., Wang, S., and Zeisel, S. H. (2005) *FASEB J* **19**, 1266-1271

3. Saibara, T., and Ono, M. (2007) *J Hepatol* **47**, 869-870

4. Jacobs, R. L., Devlin, C., Tabas, I., and Vance, D. E. (2004) *J Biol Chem* **279**, 47402-47410

5. Mensenkamp, A. R., Havekes, L. M., Romijn, J. A., and Kuipers, F. (2001) *J Hepatol* **35**, 816-822

6. Minehira, K., Young, S. G., Villanueva, C. J., Yetukuri, L., Oresic, M., Hellerstein, M. K., Farese, R. V., Jr., Horton, J. D., Preitner, F., Thorens, B., and Tappy, L. (2008) *J Lipid Res* **49**, 2038-2044

7. Raabe, M., Veniant, M. M., Sullivan, M. A., Zlot, C. H., Bjorkegren, J., Nielsen, L. B., Wong, J. S., Hamilton, R. L., and Young, S. G. (1999) *J Clin Invest* **103**, 1287-1298

8. Jacobs, R. L., Lingrell, S., Zhao, Y., Francis, G. A., and Vance, D. E. (2008) *J Biol Chem* **283**, 2147-2155

9. Minahk, C., Kim, K. W., Nelson, R., Trigatti, B., Lehner, R., and Vance, D. E. (2008) *J Biol Chem* **283**, 6449-6458

10. Robichaud, J. C., van der Veen, J. N., Yao, Z., Trigatti, B., and Vance, D. E. (2009) *Biochim Biophys Acta* **1790**, 538-551

11. Shimomura, I., Bashmakov, Y., and Horton, J. D. (1999) *J Biol Chem* **274**, 30028-30032

12. Seppala-Lindroos, A., Vehkavaara, S., Hakkinen, A. M., Goto, T., Westerbacka, J., Sovijarvi, A., Halavaara, J., and Yki-Jarvinen, H. (2002) *J Clin Endocrinol Metab* **87**, 3023-3028

13. Marchesini, G., Brizi, M., Morselli-Labate, A. M., Bianchi, G., Bugianesi, E., McCullough, A. J., Forlani, G., and Melchionda, N. (1999) *Am J Med* **107**, 450-455

14. Erion, D. M., and Shulman, G. I. (2010) *Nat Med* **16**, 400-402

15. Summers, S. A. (2006) *Prog Lipid Res* **45**, 42-72

16. Monetti, M., Levin, M. C., Watt, M. J., Sajan, M. P., Marmor, S., Hubbard, B. K., Stevens, R. D., Bain, J. R., Newgard, C. B., Farese, R. V., Sr., Hevener, A. L., and Farese, R. V., Jr. (2007) *Cell Metab* **6**, 69-78

17. Li, Z., Agellon, L. B., Allen, T. M., Umeda, M., Jewell, L., Mason, A., and Vance, D. E. (2006) *Cell Metab* **3**, 321-331

18. Garcia-Ruiz, C., Colell, A., Morales, A., Kaplowitz, N., and Fernandez-Checa, J. C. (1995) *Mol Pharmacol* **48**, 825-834

19. Mannaerts, G. P., Van Veldhoven, P. P., and Casteels, M. (2000) *Cell Biochem Biophys* **32 Spring**, 73-87

20. Bergamini, C. M., Gambetti, S., Dondi, A., and Cervellati, C. (2004) *Curr Pharm Des* **10**, 1611-1626

21. Song, Z., Deaciuc, I., Zhou, Z., Song, M., Chen, T., Hill, D., and McClain, C. J. (2007) *Am J Physiol Gastrointest Liver Physiol* **293**, G894-902

22. Wang, Z., Yao, T., Pini, M., Zhou, Z., Fantuzzi, G., and Song, Z. (2010) *Am J Physiol Gastrointest Liver Physiol* **298**, G634-642

23. Ji, C., and Kaplowitz, N. (2003) *Gastroenterology* **124**, 1488-1499

24. Abdelmalek, M. F., Sanderson, S. O., Angulo, P., Soldevila-Pico, C., Liu, C., Peter, J., Keach, J., Cave, M., Chen, T., McClain, C. J., and Lindor, K. D. (2009) *Hepatology* **50**, 1818-1826

25. Caballero, F., Fernandez, A., Matias, N., Martinez, L., Fucho, R., Elena, M., Caballeria, J., Morales, A., Fernandez-Checa, J. C., and Garcia-Ruiz, C. (2010) *J Biol Chem* **285**, 18528-18536

26. Brown, J. M., Betters, J. L., Lord, C., Ma, Y., Han, X., Yang, K., Alger, H. M., Melchior, J., Sawyer, J., Shah, R., Wilson, M. D., Liu, X., Graham, M. J., Lee, R., Crooke, R., Shulman, G. I., Xue, B., Shi, H., and Yu, L. (2010) *J Lipid Res* **51**, 3306-3315

27. Turpin, S. M., Hoy, A. J., Brown, R. D., Rudaz, C. G., Honeyman, J., Matzaris, M., and Watt, M. J. (2011) *Diabetologia* **54**, 146-156

APPENDIX I

Does CTP:phosphocholine cytidylyltransferase-α play a role in regulation of gene expression?

Introduction

CTP:phosphocholine cytidylyltransferase (CT) is the rate-limiting enzyme of phosphatidylcholine biosynthesis via the CDP-choline pathway (1,2). Two isoforms of CT exist, CTα and CTβ, each encoded by their own gene (3). CTα is believed to be the predominant isoform and is ubiquitously expressed (3). Interestingly, a nuclear localization signal was identified within the N-terminal region of CTα, while CTβ lacks this N-terminal signal (4). Therefore, in the majority of cell types, CTα is a nuclear protein which translocates to the nuclear envelope when activated, whereas CTβ is a cytosolic protein which localizes to ER membranes upon activation (3,5). Thus, it is unclear why CTα is a nuclear protein, especially when the other enzymes involved in the CDP-choline pathway (choline kinase, CK, and CDP-choline: 1,2-diacylglycerol cholinephopshotransferase, CPT) reside outside the nucleus (2). The possibility that CTα serves a specific nuclear function, other than its requirement for PC biosynthesis, is intriguing. Enzymes involved in glucose metabolism have been identified to act in the nucleus to regulate histone gene expression and histone acetylation (6-8). Furthermore, other enzymes involved in lipid metabolism and transport, such as Lipin1 and sterol carrier protein 2, have shown to hold additional functions as transcriptional co-activators (9-11).

Lipin1 is a phosphatidate phosphatase enzyme which has a key role in glycerolipid synthesis as it catalyzes the conversion of phosphatidate to diacylglycerol (12,13). This enzyme provides the diacylglycerol required for triacylglycerol and phospholipid biosynthesis (13-15). Lipin1 is a cytosolic protein, and similar to CTα, associates with biological membranes, specifically the endoplasmic reticulum membrane, in response to fatty acids (16). Furthermore, similar to CTα, immunocytochemistry studies revealed that lipin1 resides in the nucleus suggesting that lipin1 may have a specific nuclear function (17).

Indeed, lipin1 has been found to co-activate the nuclear receptors peroxisome proliferator activated receptor-α (PPARα) and PPARγ (11,18). In addition, lipin1 acts as a transcriptional repressor of nuclear factor of activated T-cells c4 (NFATc4) by enhancing the recruitment of histone deacetylases (19). Moreover, before lipin1 was identified as a transcriptional co-activator, the yeast homologue, Smp2, was found to associate with promoters of phospholipid biosynthetic enzymes. As Smp2 is a key regulator of nuclear membrane growth during cell cycle, its role in regulating the transcription of phospholipid biosynthetic enzymes is important for coordinating nuclear growth during the cell cycle (20).

Based on the similarities between lipin1 and CTα, we hypothesized that CTα is important for transcriptional regulation, either by directly binding DNA to act as a transcription factor, or by co-activating other transcription factor complexes. Transcriptional regulation of CTα occurs during the S phase of the cell cycle, possibly in preparation for increased PC biosynthesis during the cell cycle (21,22). Therefore, we hypothesized that CTα may regulate genes involved in cell cycle progression, matching its own regulation during the cell cycle.

Experimental Procedures

Preparation of mouse CTα cDNA.

Hepatic RNA was isolated using TRIzol reagent (Invitrogen) according to the manufacturer's instructions. Total RNA was treated with DNaseI (Invitrogen) and reverse-transcribed using an oligo(dT)12-18 primer and Superscript II reverse transcriptase (Invitrogen) according to manufacturer's instructions. Amplification of CTα cDNA was performed by PCR using Pfu Hotstart DNA polymerase (Stratagene) together with the following primer set: forward primer, 5' - ACACACACGTCGACGATGCACAGAGTTCAGCTAAAGT - 3'; reverse primer, 5' – GTGTGTGTGTCGGCCGCTTAGTCCTCTTCATCCTCGCT – 3'.

Preparation of GST-CTα fusion protein.

Mouse CTα cDNA was cloned into pGex-6P-3 vector (Amersham Biosciences) using NotI and SalI restriction enzymes. The GST (glutathione S-transferase) tag or GST-CTα fusion protein was expressed in *Escherichia coli*, and affinity purified on glutathione-Sepharose 4B (Amersham Biosciences). Expression of the purified GST-CTα fusion protein was assessed via immunoblotting. Total CT activity was measured from *E. coli* expressing either GST or GST-CTα (25μg) by monitoring conversion of [^{3}H]phosphocholine into CDP-choline as previously described (23).

Genomic binding site cloning.

Mouse CpG-island rich library (Geneservice) in *E. Coli* was isolated and purified by a spin column (Qiagen). Isolated genomic DNA (average insert ~600bp) was amplified by PCR for 30 cycles (denaturing for 30 s at 94ºC, annealing for 30 s at 55ºC, and extension for 1 min at 72ºC) using Advantage Taq Polymerase (Clontech) with the following primer sequences supplied by the manufacturer: forward primer, 5'-CGGCCGCCTGCAGGTCGACCTTAA-3'; reverse primer, 5'-AACGCGTTGGGAGCTCTCCCTTAA - 3'.

Genomic binding site cloning (GBSC) was performed as previously described (10). Briefly, amplified CpG island rich library genomic DNA was precleaned by incubation of 25µg of DNA with GST immobilized on glutathione-Sepharose 4B, and 400µl binding buffer (40 mM Tris, pH 7.5, 100 mM KCl, 10% glycerol, 5mM EDTA, 1mMDTT, 0.1mg/ml BSA, 0.1% TritonX-100, protease inhibitor cocktail mixture) for 1 h at 4ºC. Precleaned DNA was incubated with 10µg of either GST or the GST-CTα fusion protein for 1 h at 4ºC with agitation. The beads were washed 5 times with 200µl binding buffer. Bound genomic DNA was amplified by PCR for 25 cycles (denaturing for 30 s at 94ºC, annealing for 30 s at 55ºC, and extension for 35 s at 72ºC) with Advantage Taq Polymerase, and the above noted primers. After three rounds of GBSC, bound genomic DNA was separated by 2% agarose gel, and cloned into pCR2.1-TOPO using TOPO TA cloning (invitrogen). Positive clones containing the genomic DNA inserts were sequenced.

Immunoprecipitation.

Recombinant adenoviruses encoding HA (hemagglutinin)-tagged CTα were propagated as described (24). The McArdle RH7777cell line were grown as previously described (25). McArdle RH7777 cells were infected with adenoviruses expressing either GFP alone or GFP with HA-CTα (6 plaque-forming units/cell) for 24 h before the start of the experiment. The cells were washed 3 times with PBS, and collected and lysed in RIPA buffer. Protein G sepharose beads were precleaned with 1 ml of cell lysate for 10 min at 4ºC. Cell lysate was preincubated with 8 µl of mouse HA antibody (Novus) for 1 h at 4ºC before the addition of protein G Sepharose beads. Incubations continued for an additional 16 h at 4ºC. Protein complexes were washed 3 times with 0.1% SDS, and re-suspended in 2x SDS-PAGE sample. Immunoprecipitated proteins were separated by SDS-PAGE and visualized with Coomasie brilliant blue stain.

For some experiments, the cells were incubated with cross-linking reagents (1% formaldehyde and 1.5 mM ethylene glycolbis) before harvesting and immunoprecipitation with mouse HA antibody. Immunoprecipitated protein complexes were separated by SDS-PAGE before immunobloting with mouse HA antibody.

Results

Purification and expression of GST-CTα fusion protein.

As CTα is largely a nuclear protein, we sought to investigate whether the nuclear role of CTα includes regulation of gene expression. Before attempting to identify promoter regions which may be regulated by CTα, we constructed a GST-CTα fusion protein. Purification of the GST tag and GST-CTα fusion protein was verified by immunoblotting using an antibody detecting GST (Figure 1A, lanes 4 and 8). In addition, CT activity assay was performed in total cell lysate from E. coli expressing either GST or the GST-CTα fusion protein to assess the functionality of the GST-CTα fusion protein. While GST did not show CT activity (Figure 1B), we found a large amount of CT activity associated with the GST-CTα fusion protein verifying the functionality of the fusion protein (Figure 1B). As a positive control, we determined CT activity in hepatocyte microsomes, which contains active CT (Figure 1B).

Attempt to identify potential genes regulated by CTα.

To identify if CTα is a potential transcription factor, we utilized the GBSC technique to identify candidate gene promoters which may be regulated by CTα. As depicted in Figure 2, GBSC entails incubation of a mouse CpG- island rich library with the GST-CTα fusion protein. GST-CTα may be immuonprecipitated and immobilized with glutathione-Sepharose 4B. The bound genomic DNA is amplified via PCR and the amplified genomic DNA is used as the substrate for subsequent rounds of GBSC. PCR amplification of the CpG-island rich library was required before proceeding with GBSC (Figure 3A). Approximately 60% of genes are associated with CpG islands, including all housekeeper genes (26). The CpG islands contain the promoter region, and usually one or more exons of the associated gene (26). As shown in Figure 3A, the majority of

genomic DNA within the CpG-island rich library is ~600 bp. Unfortunately, there was no way to determine whether all genes within the library were equally amplified. The amplified CpG-island rich library was utilized for the first round of GBSC. After three rounds of GBSC, we identified 2 DNA bands by agarose gel which were bound to the GST-CTα fusion protein, but were not associated with GST (Figure 3B). The two genomic DNA bands associated with the GST-CTα fusion protein were isolated, cloned and sequenced to identify potential promoter regions which may have bound to CTα. The sequenced genomic DNA was aligned with mouse transcripts using Ensemble. As shown in Table 1, the majority of isolated genomic DNA clones aligned with random areas of the mouse genome which were not in close proximity to potential candidate genes. The potential transcripts which aligned with the clones isolated from the GBSC assay aligned with *Rn18s*, 18s ribosomal RNA, which is a housekeeper gene (Table 1). This is not surprising considering the CpG-island rich library includes all housekeeper genes (26).

In a second attempt to identify potential promoter regions regulated by CTα, we performed chromatin immunoprecipitation assays. However, this technique produced several false positives, and was unsuccessful at identifying potential genes which may be regulated by CTα.

Attempt to identify potential proteins which bound to CTα.

The GBSC assay is a technique used to assess if CTα directly binds to DNA. However, CTα may act as a co-activator and may not directly bind DNA. Therefore, we performed immunoprecipitation assays in an attempt to identify transcription factors which may bind to CTα. Since a suitable antibody detecting CTα was unavailable, we infected McArdle RH7777 cells with adenoviruses expressing either GFP, or GFP with HA-tagged CTα. Exogenous CTα localizes to the nucleus showing

that the HA tag does not affect the cellular localization of CTα (24). To detect proteins which may associate with CTα, we performed an immunoprecipitation assay with an antibody detecting HA. Immunoprecipitated proteins were visualized with Coomasie brilliant blue stain (Figure 4). The proteins which associated with HA-CTα were identical to those which bound to GFP. As the GFP samples do not contain the HA tag, the proteins bound to HA-CTα resulted from non-specific binding (Figure 4).

Since non-specific binding was associated with CTα, we took advantage of cross-linking reagents in an attempt to cross-link CTα to proteins which may be in close proximity. Formaldehyde was one cross-linking reagent used, which has the ability to cross-link protein-protein, along with protein-DNA and protein-RNA. Since formaldehyde generate cross-links spanning approximately 2Å, we also utilized ethylene glycolbis as a cross-linking reagent as it generates cross-links spanning 16.1Å (27). The cross-linking reagents were used in combination. CTα-protein complexes were identified by immunoblotting (Figure 5). Protein complexes were detected in the cell lysates (Figure 5) as well as in samples after immunoprecipitation with HA antibody (Figure 5). The 49 kDa band visualized in the immunoblot represents HA-CTα. The protein bands visualized at 99kDa and 117kDa kDa represent unknown CTα-protein complexes (Figure 5). Unfortunately, we were unable to identify the protein-complexes which were visualized by immunoblotting.

Discussion

That CTα resides in the nucleus indicates that CTα serves a specific role in the nucleus apart from PC biosynthesis. A similar protein, lipin1 which is involved in the biosynthesis of TG, has recently been identified as a co-activator and a repressor (11,18,19). Therefore, we hypothesized that CTα may be important in the regulation of gene expression, either as a transcription factor, or as a co-activator. Previous studies have shown that transcriptional regulation of CTα occurs during the S phase of the cell cycle, possibly in preparation for PC biosynthesis which occurs during progression in the cell cycle (21,22). Therefore, we predicted that CTα may regulate genes involved in cell cycle progression.

In an attempt to identify potential promoter regions which may be regulated by CTα, we utilized GBSC. The GBSC technique has previously been used for screening potential estrogen-responsive genes (28,29), as well as for identifying potential gene targets for phospholipid scramblase 1 (10). However, the only genes found associated with GST-CTα were *Rn18s*, 18s ribosomal RNA, and *Nolc1*, nucleolar and coiled body phosphoprotein. The association of *Rn18s* with GST-CTα is likely non-specific since *Rn18s* is a housekeeper gene. In addition, we were unable to reproduce the association of *Nolc1* with GST-CTα suggesting that this association was also due to non-specific binding. Therefore, we were unable to detect candidate genes which may be regulated by CTα.

Could CTα act as a co-activator?

CTα has the potential to serve as a regulator of gene expression without directly binding to DNA. In an attempt to identify transcription factors in which CTα may co-activate, we took advantage of cross-linking reagents together with an immunoprecipitation assay. The use of cross-linking reagents allowed us to visualize -CTα-protein complexes.

Unfortunately, we were unsuccessful in identifying the proteins which bound to CTα. Two CTα-protein complexes were visualized with the approximate molecular weights of 99 kDa, and 117 kDa. Previous studies have identified calmodulin as a protein which binds and stabilizes CTα (30). However, the molecular weight of calmodulin is 18 kDa and the combined molecular weight of HA-CTα with calmodulin (~68 kDa) suggests that it would not be the band detected at 99 kDa. The 14-3-3ζ protein, which has a molecular weight of ~29 kDa also associates with CTα in murine lung epithelial cells (31). Furthermore, 14-3-3ζ is important for the nuclear import of CTα in murine lung epithelial cells (31). A protein complex of 14-3-3ζ and HA-CTα would also be too small to account for the 99 kDa protein band visualized by the immunoblotting assay. However, we cannot rule out that the 99 kDa protein band does not contain either calmodulin or 14-3-3ζ as a multi-protein complex which may associate with CTα.

Previous studies have demonstrated that CTα, in coordination with nuclear lamins A/C and B, plays a role in the proliferation of the nucleoplasmic reticulum (32,33). Although direct binding of CTα with either of the nuclear lamins was not studied, it is possible that CTα may associate with either of the lamins. Lamin A/C has a molecular weight of 70 kDa, as does lamin B. Association of either of the nuclear lamins with HA-CTα could account for protein complex visualized at 117 kDa.

Other potential nuclear roles of CTα.

If CTα is not a transcription factor or a co-activator, why does CTα reside in the nucleus? The nuclear localization of CTα may serve as a strategy to protect the enzyme from protease degradation within the cytosol. Indeed, CTα has been shown to be a target of both caspase-directed and calpain-mediated degradation (34-36). Furthermore, recent

evidence has clearly demonstrated that CTα exports the nucleus despite the lack of a nuclear export signal (33,37). Therefore, CTα may reside in the nucleus in preparation for high rates of PC biosynthesis. However, if the nucleus serves as merely a storage site for CTα, it is curious why CTβ does not reside in the nucleus when both isoforms may serve the same biological function.

As mentioned above, previous studies have identified a role for CTα, in coordination with lamin A/C and B, in proliferation of the nucleoplasmic reticulum suggesting that CTα may be important for maintaining the membrane curvature of the nucleoplasmic reticulum (32,38). Furthermore, nuclear CTα may be important to maintain a supply of endonuclear PC (39). It cannot be excluded that CTα may serve multiple functions within the nucleus as other nuclear proteins have shown to be multi-faceted. For instance, glyceraldehydes-3-phosphate dehydrogenase, which localizes in the cytosol as well as in the nucleus, is a multifunction nuclear protein which is involved in regulation of histone gene expression (40), telomere structure (41), nuclear membrane fusion (42), and DNA repair (43,44).

In summary, we have attempted to characterize the nuclear role of CTα. In particular, we hypothesized that CTα is important for regulation of gene expression. We utilized GBSC, chromatin immunoprecipitation and cross-linking techniques in an attempt to identify potential candidate genes which CTα may regulate, along with potential transcription factors which CTα may co-activate. Unfortunately, this study was inconclusive, and the nuclear role of CTα still remains relatively uncharacterized.

Clone	Gene
Clone 1	Random, not close to potential genes
Clone 2	Rn18s – 18s ribosomal RNA
Clone 3	Nolc1 – nucleolar and coiled body phosphoprotein
Clone 4	Rn18s – 18s ribosomal RNA
Clone 5	Random, not close to potential genes
Clone 6	Rn18s – 18s ribosomal RNA
Clone 7	Random, not close to potential genes
Clone 8	Random, not close to potential genes
Clone 9	Random, not close to potential genes
Clone 10	Rn18s – 18s ribosomal RNA
Clone 11	Random, not close to potential genes
Clone 12	Random, not close to potential genes
Clone 13	Rn18s – 18s ribosomal RNA

Table 1: Genes found associated with GST- CTα after genomic binding site cloning. Genomic DNA which bound to GST-CTα after genomic binding site cloning was isolated, cloned and sequenced. Sequenced genomic DNA was aligned with mouse transcripts using Ensembl.

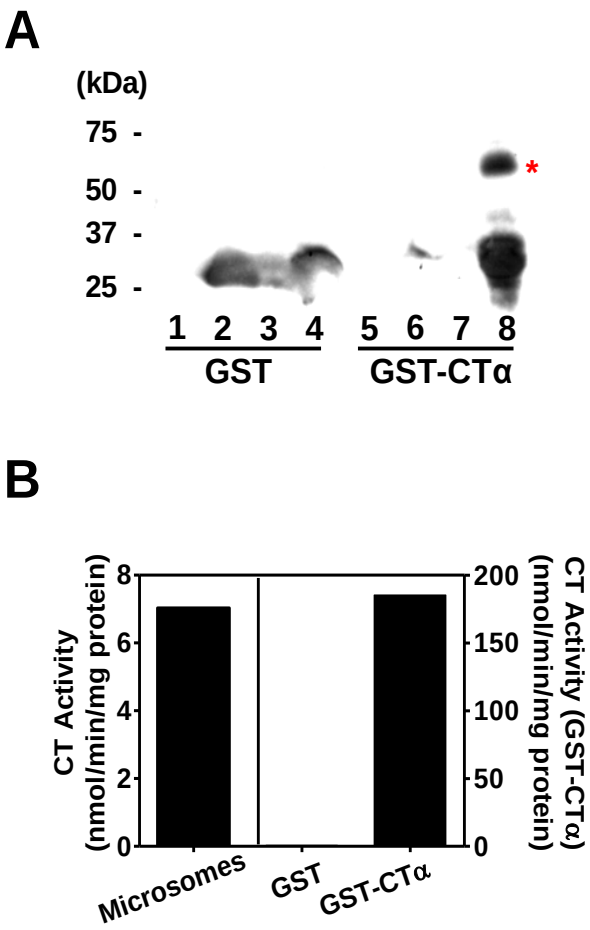

Figure 1: Expression of GST-CTα fusion protein. Mouse CTα cDNA was cloned into pGex-6P-3 vector (Ambersham Biosciences) using NotI and SalI restriction enzymes. GST-CTα fusion protein was expressed in *Escherichia coli*, and affinity purified on glutathione-sepharose 4B (Amersham Biosciences). (A) Expression of purified GST or GST-CTα fusion protein was assessed via an immunoblot assay using an antibody detecting GST. Lanes 1, 5: insoluble material. Lanes 2, 6: *E. coli* expressing GST or GST-CTα. Lanes 3, 7: GST or GST-CTα not attached to glutathione-Sepharose 4B. Lanes 4, 8: GST or GST-CTα immobilized on glutathione-Sepharose 4B. The star represents GST-CTα. A typical immunoblot is displayed. (B) Total CT activity recovered from *E. coli* expressing either GST or GST-CTα. CT activity was measured in microsomes prepared from mouse hepatocytes.

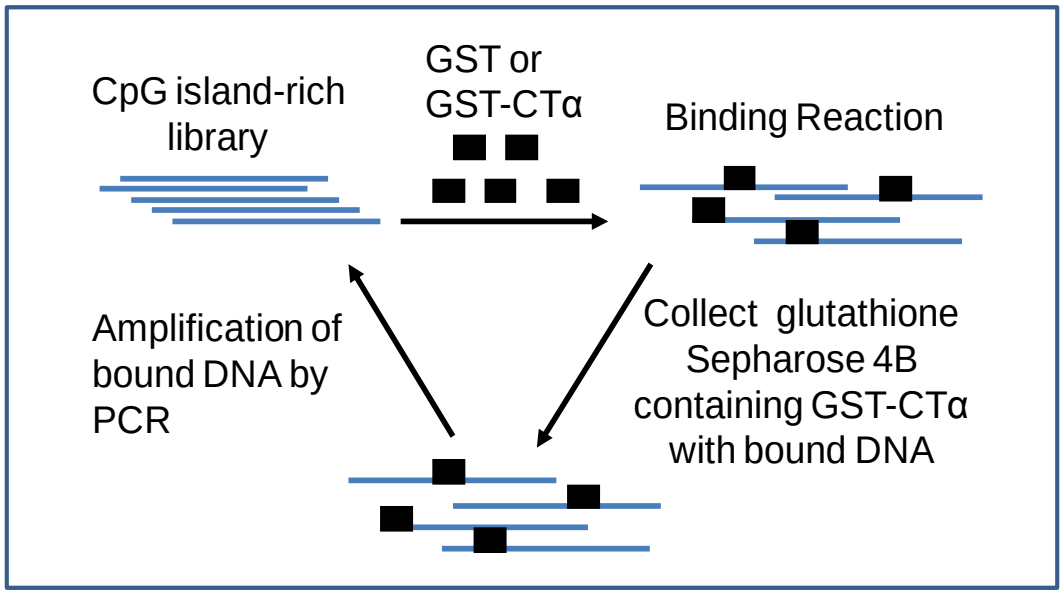

Figure 2: Schematic representation of genomic binding site cloning. Genomic binding site cloning (GBSC) involves binding of a mouse CpG-island rich library with either GST or GST-CTα fusion protein immobilized on glutathione-Sepharose 4B. Bound genomic DNA is immunoprecipitated with glutathione-Sepharose 4B and amplified with PCR. The amplified genomic DNA is utilized for subsequent rounds of GBSC.

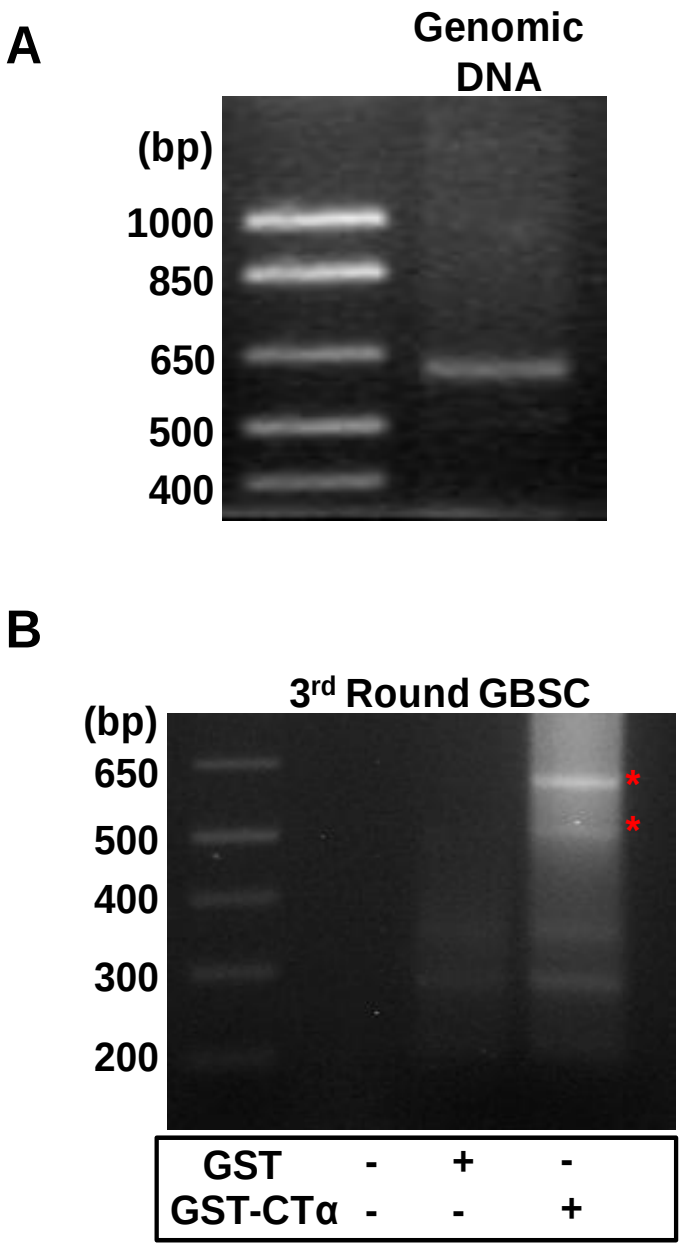

Figure 3: Genomic binding site cloning. (A) Amplification of the mouse CpG-island rich library by PCR. (B) Amplified genomic DNA bound to either purified GST or GST-CTα after three rounds of genomic binding site cloning. The red stars indicate the genomic DNA bands which were isolated, cloned and sequenced.

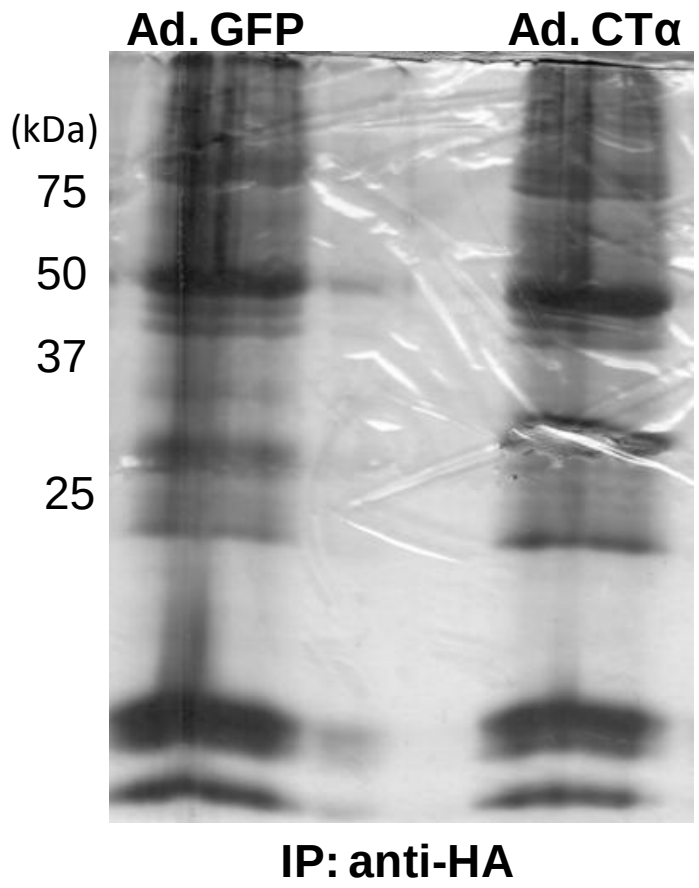

Figure 4: Immunoprecipitation assay to detect proteins which associate with CTα. McArdle RH7777 cells were infected with adenoviruses expressing either GFP alone or GFP with HA-CTα for 24 h before the start of the experiment. Total cell lysates were incubated with a mouse HA antibody and protein G Sepharose beads for 16 h at 4ºC. Immunoprecipitated HA proteins were separated by SDS-PAGE and visualized by Coomasie brilliant blue stain.

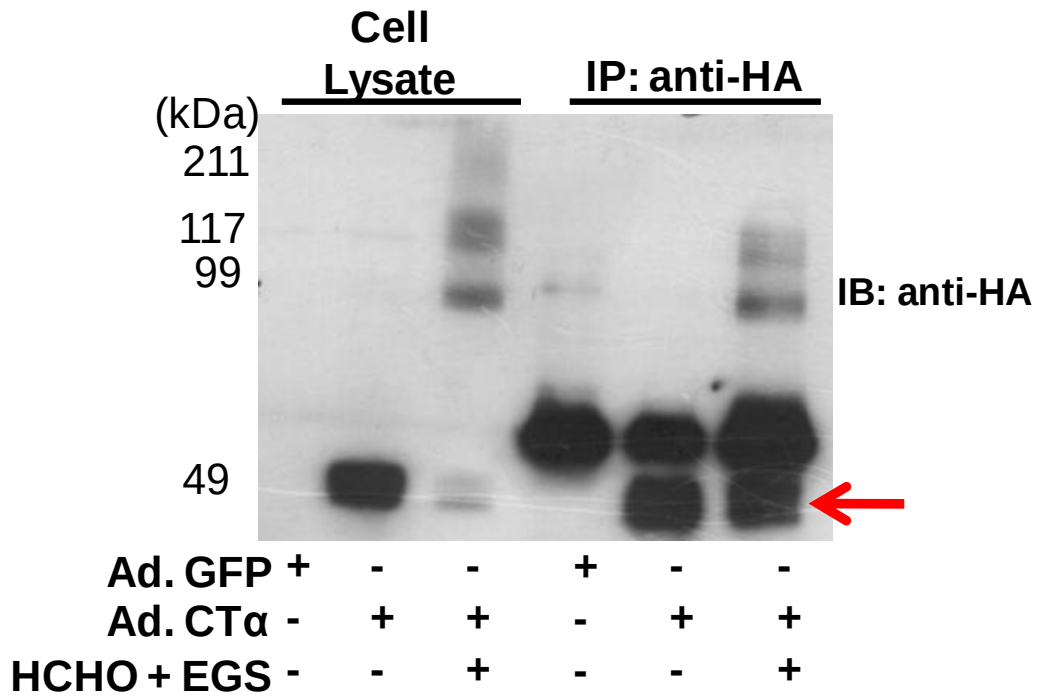

Figure 5: Detection of proteins which associate with CTα. McArdle RH7777 cells were infected with adenoviruses expressing either GFP alone or GFP with HA-CTα for 24 h before the start of the experiment. The cells were incubated with cross-linking reagents (1% formaldehyde and ethylene glycolbis) before harvesting. Total cell lysates were incubated with a mouse HA antibody and protein G Sepharose beads for 16 h at 4ºC. Total cell lysates or immunoprecipitated protein complexes were separated by SDS-PAGE. HA-CTα was detected via an immunoblot assay using an antibody detecting HA. The red arrow represents HA-CTα. A typical immunoblot is presented.

References

1. Kennedy, E. P., and Weiss, S. B. (1956) *J Biol Chem* **222**, 193-214

2. Vance DE and Vance JE (2008) Phospholipid biosynthesis in eukaryotes. in *Biochemistry of Lipids, Lipoproteins, and Membranes, 5th Edition* (Vance DE and Vance JE ed.), Elsevier, Amsterdam. pp 213-244

3. Karim, M., Jackson, P., and Jackowski, S. (2003) *Biochim Biophys Acta* **1633**, 1-12

4. Wang, Y., MacDonald, J. I., and Kent, C. (1995) *J Biol Chem* **270**, 354-360

5. Wang, Y., Sweitzer, T. D., Weinhold, P. A., and Kent, C. (1993) *J Biol Chem* **268**, 5899-5904

6. Sirover, M. A. (2005) *J Cell Biochem* **95**, 45-52

7. Wellen, K. E., Hatzivassiliou, G., Sachdeva, U. M., Bui, T. V., Cross, J. R., and Thompson, C. B. (2009) *Science* **324**, 1076-1080

8. Takahashi, H., McCaffery, J. M., Irizarry, R. A., and Boeke, J. D. (2006) *Mol Cell* **23**, 207-217

9. Ko, M. H., and Puglielli, L. (2007) *J Biol Chem* **282**, 19742-19752

10. Zhou, Q., Ben-Efraim, I., Bigcas, J. L., Junqueira, D., Wiedmer, T., and Sims, P. J. (2005) *J Biol Chem* **280**, 35062-35068

11. Finck, B. N., Gropler, M. C., Chen, Z., Leone, T. C., Croce, M. A., Harris, T. E., Lawrence, J. C., Jr., and Kelly, D. P. (2006) *Cell Metab* **4**, 199-210

12. Donkor, J., Sariahmetoglu, M., Dewald, J., Brindley, D. N., and Reue, K. (2007) *J Biol Chem* **282**, 3450-3457

13. Han, G. S., Wu, W. I., and Carman, G. M. (2006) *J Biol Chem* **281**, 9210-9218

14. Kennedy, E. P. (1957) *Fed Proc* **16**, 847-853

15. Kennedy, E. P. (1953) *J Biol Chem* **201**, 399-412

16. Cascales, C., Mangiapane, E. H., and Brindley, D. N. (1984) *Biochem J* **219**, 911-916

17. Peterfy, M., Phan, J., and Reue, K. (2005) *J Biol Chem* **280**, 32883-32889

18. Koh, Y. K., Lee, M. Y., Kim, J. W., Kim, M., Moon, J. S., Lee, Y. J., Ahn, Y. H., and Kim, K. S. (2008) *J Biol Chem* **283**, 34896-34906

19. Kim, H. B., Kumar, A., Wang, L., Liu, G. H., Keller, S. R., Lawrence, J. C., Jr., Finck, B. N., and Harris, T. E. (2010) *Mol Cell Biol* **30**, 3126-3139

20. Santos-Rosa, H., Leung, J., Grimsey, N., Peak-Chew, S., and Siniossoglou, S. (2005) *EMBO J* **24**, 1931-1941

21. Banchio, C., Schang, L. M., and Vance, D. E. (2004) *J Biol Chem* **279**, 40220-40226

22. Golfman, L. S., Bakovic, M., and Vance, D. E. (2001) *J Biol Chem* **276**, 43688-43692

23. Schneider, W. J., and Vance, D. E. (1978) *J Neurochem* **30**, 1599-1601

24. Jacobs, R. L., Lingrell, S., Zhao, Y., Francis, G. A., and Vance, D. E. (2008) *J Biol Chem* **283**, 2147-2155

25. Cui, Z., Houweling, M., and Vance, D. E. (1995) *Biochem J* **312 (Pt 3)**, 939-945

26. Cross, S. H., Charlton, J. A., Nan, X., and Bird, A. P. (1994) *Nat Genet* **6**, 236-244

27. Zeng, P. Y., Vakoc, C. R., Chen, Z. C., Blobel, G. A., and Berger, S. L. (2006) *Biotechniques* **41**, 694, 696, 698

28. Watanabe, T., Inoue, S., Hiroi, H., Orimo, A., Kawashima, H., and Muramatsu, M. (1998) *Mol Cell Biol* **18**, 442-449

29. Inoue, S., Kondo, S., Hashimoto, M., Kondo, T., and Muramatsu, M. (1991) *Nucleic Acids Res* **19**, 4091-4096

30. Chen, B. B., and Mallampalli, R. K. (2007) *J Biol Chem* **282**, 33494-33506

31. Agassandian, M., Chen, B. B., Schuster, C. C., Houtman, J. C., and Mallampalli, R. K. (2010) *FASEB J* **24**, 1271-1283

32. Gehrig, K., Cornell, R. B., and Ridgway, N. D. (2008) *Mol Biol Cell* **19**, 237-247

33. Gehrig, K., Morton, C. C., and Ridgway, N. D. (2009) *J Lipid Res* **50**, 966-976

34. Lagace, T. A., and Ridgway, N. D. (2005) *Biochem J* **392**, 449-456

35. Henderson, F. C., Miakotina, O. L., and Mallampalli, R. K. (2006) *J Lipid Res* **47**, 2314-2324

36. Zhou, J., Ryan, A. J., Medh, J., and Mallampalli, R. K. (2003) *J Biol Chem* **278**, 37032-37040

37. Guo, Y., Walther, T. C., Rao, M., Stuurman, N., Goshima, G., Terayama, K., Wong, J. S., Vale, R. D., Walter, P., and Farese, R. V. (2008) *Nature* **453**, 657-661

38. Lagace, T. A., and Ridgway, N. D. (2005) *Mol Biol Cell* **16**, 1120-1130

39. Hunt, A. N., Clark, G. T., Attard, G. S., and Postle, A. D. (2001) *J Biol Chem* **276**, 8492-8499

40. Zheng, L., Roeder, R. G., and Luo, Y. (2003) *Cell* **114**, 255-266

41. Sundararaj, K. P., Wood, R. E., Ponnusamy, S., Salas, A. M., Szulc, Z., Bielawska, A., Obeid, L. M., Hannun, Y. A., and Ogretmen, B. (2004) *J Biol Chem* **279**, 6152-6162

42. Nakagawa, T., Hirano, Y., Inomata, A., Yokota, S., Miyachi, K., Kaneda, M., Umeda, M., Furukawa, K., Omata, S., and Horigome, T. (2003) *J Biol Chem* **278**, 20395-20404

43. Krynetski, E. Y., Krynetskaia, N. F., Gallo, A. E., Murti, K. G., and Evans, W. E. (2001) *Mol Pharmacol* **59**, 367-374

44. Krynetski, E. Y., Krynetskaia, N. F., Bianchi, M. E., and Evans, W. E. (2003) *Cancer Res* **63**, 100-106